RSC Advances

REVIEW

View Article Online
View Journal | View Issue

Cite this: *RSC Adv.*, 2020, **10**, 41625

Widely used catalysts in biodiesel production: a review

Bishwajit Changmai,[a] Chhangte Vanlalveni,[b] Avinash Prabhakar Ingle,[c] Rahul Bhagat[d] and Samuel Lalthazuala Rokhum *[ae]

An ever-increasing energy demand and environmental problems associated with exhaustible fossil fuels have led to the search for an alternative renewable source of energy. In this context, biodiesel has attracted attention worldwide as an eco-friendly alternative to fossil fuel for being renewable, non-toxic, biodegradable, and carbon-neutral. Although the homogeneous catalyst has its own merits, much attention is currently paid toward the chemical synthesis of heterogeneous catalysts for biodiesel production as it can be tuned as per specific requirement and easily recovered, thus enhancing reusability. Recently, biomass-derived heterogeneous catalysts have risen to the forefront of biodiesel productions because of their sustainable, economical and eco-friendly nature. Furthermore, nano and bifunctional catalysts have emerged as a powerful catalyst largely due to their high surface area, and potential to convert free fatty acids and triglycerides to biodiesel, respectively. This review highlights the latest synthesis routes of various types of catalysts (including acidic, basic, bifunctional and nanocatalysts) derived from different chemicals, as well as biomass. In addition, the impacts of different methods of preparation of catalysts on the yield of biodiesel are also discussed in details.

Received 16th September 2020
Accepted 23rd October 2020

DOI: 10.1039/d0ra07931f

rsc.li/rsc-advances

1. Introduction

The exponential growth of the world's population coupled with the high standard of living has resulted in a steep increase in energy consumption.[1,2] The world's total primary energy consumed (TPEC), which was over 150 000 000 GW h in the year 2015, is estimated to rise by a triggering 57% in 2050.[3] Currently, the transportation of goods and services, which is the major contributor to the global economy, primarily relies on non-renewable fossil fuels. In total primary energy consumption, 80% of the energy consumed is associated with petroleum resources. Amongst these, 54% is consumed in the transportation sector.[4] It has been predicted that the energy consumption in the transportation section will increase with an average rate of 1.1% per year. As a result, the high energy consumption of non-renewable petroleum-based fuel to fulfill the increasing energy demand of human society has led to an ecological imbalance, excess greenhouse gas emission, acid rain, global warming and drastic decline in fossil fuel reserves. These negative factors associated with the excessive consumption and exhaustible nature of fossil fuels compel scientific communities to look for an alternative energy source.[5,6]

Biofuels are an excellent source of energy and widely seen as a potential substitute for fossil fuels. They are prepared from renewable sources, such as plants, municipal wastes, agricultural crops, and agricultural and forestry by-products.[7] Over the last few decades, biofuels such as biodiesel have gained significant attention as an alternative fuel in the research field because of its sustainable and environment-friendly nature. Biodiesel has exhibited properties similar to conventional fossil fuels (petro-diesel), and has some properties that are better than petro-diesel, such as high combustion efficiency, high flash point, high cetane number, lower CO_2 emission, lower sulfur content and better lubrication.[8,9] The high flash point of biodiesel (423 K), as compared to petrodiesel (337 K), makes it non-flammable and non-explosive, resulting in easy and safe handling, storage, and transportation. Additionally, it can be directly used in the automotive engine without any additional alteration.[10] It is estimated that biodiesel demand will increase to double or triple by the year 2020.[11] In light of this, in the last decades, much attention has been paid to research on biodiesel production with an intension make it more sustainable and economical. An increasing interest in biodiesel is validated by the number of research paper publications in this area, as shown in Fig. 1. Statistical data analysis in Fig. 1 depicted the increasing trend of published research papers in the field of

[a]*Department of Chemistry, National Institute of Technology Silchar, Silchar, 788010, India. E-mail: rokhum@che.nits.ac.in*
[b]*Department of Botany, Mizoram University, Tanhril, Aizawl, Mizoram, 796001, India*
[c]*Department of Biotechnology, Engineering School of Lorena, University of Sao Paulo, Lorena, SP, Brazil*
[d]*Department of Biotechnology, Government Institute of Science, Aurangabad, Maharashtra, India*
[e]*Department of Chemistry, University of Cambridge, Lensfield Road, Cambridge CB2 1EW, UK*

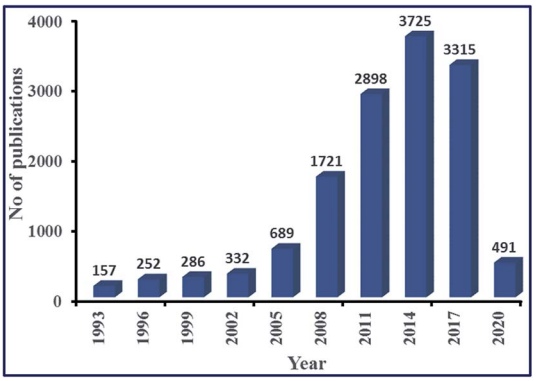

Fig. 1 Publications per year for biodiesel during the period 1993 to Feb 2020 (data collected from SciFinder Database).

biodiesel. These data were collected in February 2020 from "SciFinder Database" using the keyword "biodiesel". From a meager 157 publications in the year 1993, it has exponentially increased to 3725 publications during its peak in 2014.

2. (Trans)esterification

Transesterification or alcoholysis is a process to produce biodiesel in which edible/non-edible oils or triglyceride (TG) and alcohol have undergone nucleophilic reaction to form fatty acid methyl ester (FAME) and glycerol as a byproduct.[12] The transesterification reaction is illustrated in Scheme 1. Three sequential reversible reactions occur in the transesterification process: (i) conversion of triglyceride to diglyceride, (ii) diglyceride conversion to monoglyceride, and finally, (iii) monoglyceride conversion to glycerol. An ester is formed in each conversion step; thus, one TG molecule produces three ester molecules. The transesterification reaction can efficiently convert a triglyceride of vegetable oil into FAME, also called biodiesel, as depicted in Scheme 1. However, the esterification reaction, a reaction between carboxylic acids and alcohols to afford esters,[13–15] is essential to converting all free fatty acids (FFA) of vegetable oil into biodiesel, as shown in Scheme 2. These transesterification and esterification reactions are usually carried out in the two-pots procedure. Usually, the high FFA content of vegetable oil

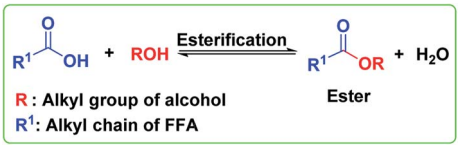

Scheme 2 Acid-catalyzed esterification of FFA content of vegetable oil to biodiesel.

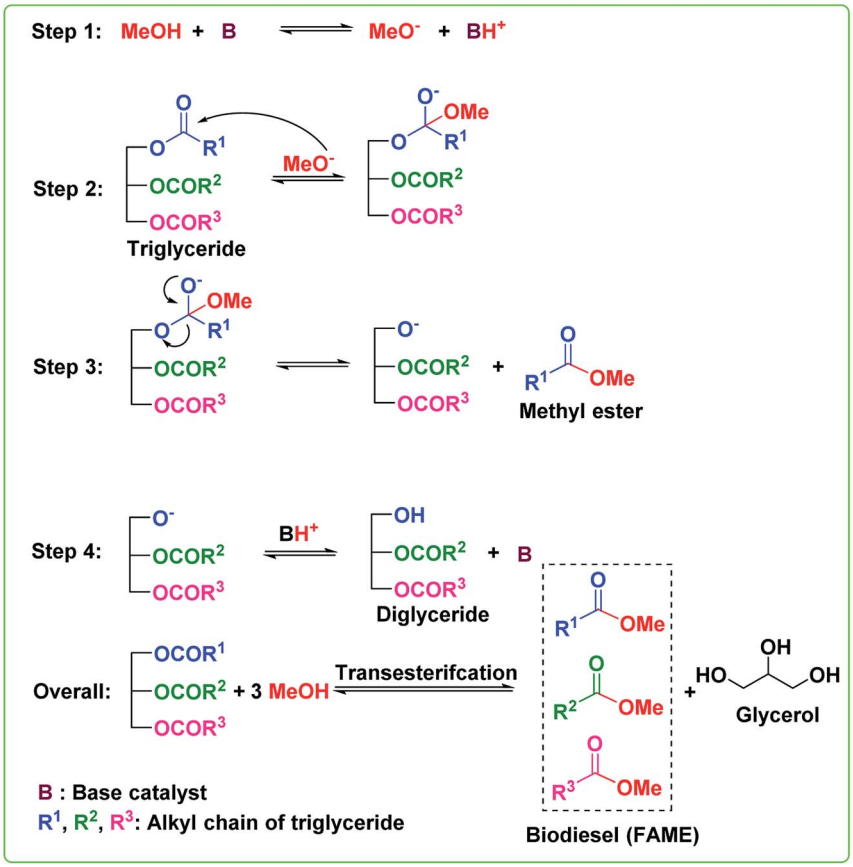

Scheme 1 Base-catalyzed reaction mechanism for the transesterification of TGs of vegetable oil to biodiesel.

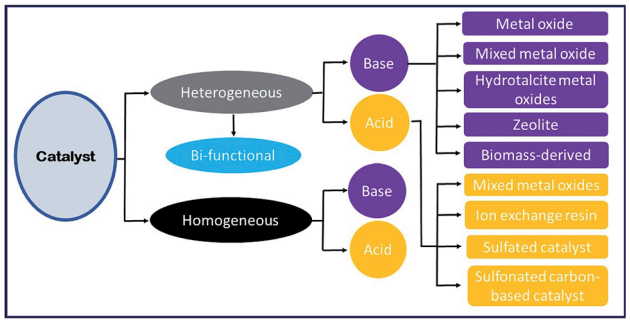

Fig. 2 Catalyst classification for biodiesel synthesis.

is first converted to esters (FAME) *via* esterification reaction by employing an acid catalyst, followed by the trans-esterification reaction using a basic catalyst to convert triglycerides to FAME. However, (trans)esterification reactions (or simultaneous transesterification and esterification) in one-pot is highly desirable to convert both triglycerides and FFA of vegetable oil (with high FFAs) to FAME to reduce the time and cost of biodiesel production. The different routes to synthesize biodiesel are outlined in Fig. 2.

3. Biodiesel

The American Society for Testing and Materials (ASTM) described biodiesel as a mono-alkyl ester produced from edible/non-edible oils or animal fats.[16] Vegetable oils or animal fats comprise mainly triacylglycerol (TAG), which is an ester of fatty acids (FA) and glycerol. The physicochemical properties of vegetable oils and animal fats are greatly influenced by the compositions of the TAG, which further often dictates the quality of biodiesel produced from these resources. FA are classified broadly into two groups: (i) saturated FA, which has carbon–carbon single bonds, and (ii) unsaturated FA, which comprises at least one carbon–carbon double bond. The FA most widely found in vegetable oils are oleic acid (18 : 1), palmitic acid (16 : 0), linoleic acid (18 : 2), linolenic acid (18 : 3), stearic acid (18 : 0), palmitoleic acid (16 : 1), myristic acid (14 : 0), and arachidic acid (20 : 0). Besides these FA, a trace amount of phospholipids, tocopherols, carotenes, sulphur compounds, and water are also found in vegetable oils.[17,18]

4. Feedstocks for biodiesel production

The feedstocks for the production of biodiesel are mainly edible[18–20] and non-edible vegetable oils,[21–23] waste cooking oils[24,25] and animal fats, including tallow,[25] yellow grease,[26] lard,[27] chicken fat[28–30] and by-products from the production of omega-3 fatty acids from fish oil.[31,32] Algae are another promising feedstock for biodiesel, which have a high potential to replace edible oil due to their availability in a pond, sewage water or in shallow ocean water without dislodging land used for food production.[32–34] Worldwide, 31% biodiesel is produced from palm oil, 27% from soybean oil and 20% from rapeseed oil.[35] Different countries use various feedstocks based on their local availability. The major feedstocks used in various countries are listed in Table 1. The feedstock cost alone contributed to 75% of the biodiesel cost.[36] Thus, the proper selection of feedstocks for biodiesel is necessary to reduce the overall cost of biodiesel production. Ironically, the utilization of edible oils (*e.g.*, sunflower, rape, soy) as feedstocks for biodiesel, called the first-generation biofuels, resulted in a food-*versus*-fuel problem, and also disturbed the agricultural farmland allocation.[27,37] In Malaysia, the edible palm oil price has increased by 70% due to its uses as feedstock in the biodiesel industry.[38] In this regard, to mitigate the problem associated with the food-*versus*-fuel nexus and high cost of first-generation biodiesel, non-edible oils are currently largely targeted as a biodiesel feedstock. Another problem associated with first-generation biofuels is their remarkably higher cost than fossil fuels. Hence, to bring down the cost of biodiesel, the utilization of non-edible oil as biodiesel feedstocks is highly relevant. Non-edible oils of more than 300 species are available in South Asia. India has an abundant amount (approximately 1 million tons per year) of such non-edible oils. *Pongamia pinnata* (karanja) and *Jatropha curcas* oils (JCO) were identified as the most promising

Table 1 Countrywise feedstocks used for biodiesel production

Country	Feedstock
India	*Jatropha*/*Pongamia pinnata* (karanja)/soybean/rapeseed/sunflower
Argentina	Soybeans
Brazil	Soybeans/palm oil/castor/cotton oil
France	Rapeseed/sunflower
Peru	Palm/*Jatropha*
Germany	Rapeseed
Spain	Linseed oil/sunflower
Italy	Rapeseed/sunflower
Turkey	Sunflower/rapeseed
Greece	Cottonseed
Sweden	Rapeseed
Norway	Animal fats
China	*Jatropha*/waste cooking oil/rapeseed oil
Indonesia	Palm oil/*Jatropha*/coconut
Japan	Waste cooking oil
Malaysia	Palm oil
Philippines	Coconut/*Jatropha* oil
Bangladesh	Rubber seed/*Pongamia pinnata* oil
Pakistan	*Jatropha* oil
Thailand	Palm/*Jatropha*/coconut oil
Iran	Palm/*Jatropha*/castor/algae oil
Singapore	Palm oil
Ghana	Palm oil
Zimbabwe	*Jatropha* oil
Kenya	Castor oil
Mali	*Jatropha* oil
UK	Rapeseed/waste cooking oil
Ireland	Frying oil/animal fat
Canada	Rapeseed/animal fat/soybean oil
Mexico	Animal fat/waste oil
USA	Soybeans/waste oil/peanut
Cuba	*Jatropha curcas*/*Moringa*/neem oil
Australia	*Jatropha*/*Pongamia*/waste cooking oil/animal tallow
New Zealand	Waste cooking oil/tallow

feedstocks by the Government of India. However, in India's biodiesel program, *Jatropha* has prominence over karanja due to its lower gestation period. If properly managed, non-edible crops planted in different parts of the world have the potential to reduce our dependence on fossil fuels for energy sources and edible oils as biodiesel feedstocks.

Biodiesel has been widely used as biofuels in the European Union (EU), and 49% of biodiesel was produced from rapeseed oil in 2015 in EU.[39] With the increasing uses of waste cooking oil (WCO), recycled vegetable oils and palm oils, the share of rapeseed oil in biodiesel production decreased from 72% in 2008. To reduce our dependency on edible oil and reduce the price of biodiesel, EU has raised the share of WCO to the 2nd position after rapeseed oil in 2015.[40] The top five biodiesel producers in EU are Germany, France, Spain, Netherlands, and Poland. Germany is the largest biodiesel producer in EU, and its production capacity increased from 3.2 billion litres in 2010 to 3.8 billion litres in 2014.[41]

Various types of feedstocks (such as edible plant oils, non-edible oils, waste cooking oils, animal fats, and algal oil) have been considered for the synthesis of biodiesel, and are discussed below.

4.1 Edible plant oils

Soybean oil,[42] sunflower oil,[43] rapeseed oil,[44] and palm oil[45] are widely utilized as a biodiesel feedstock in numerous nations, for example, Argentina, Brazil, Indonesia, Europe, US, and Malaysia. At present, an estimated 95% of the worlds' total biodiesel is produced from sunflower oil, rapeseed oil, and palm oil.[46] Various types of edible oils exploited as feedstocks for the production of biodiesel are recorded in Table 2.

4.2 Non-edible plant oils

Recently, non-edible plant oils have been increasingly considered as another promising potential feedstock for biodiesel, which is attributable to their high oil content and low cost. In addition, unlike edible oils, it does not pose a 'food *versus* fuel' problem as they can be grown in barren and arid regions, which are not suitable for agriculture. Furthermore, non-edible oil plants can grow under harsh conditions and hardly need any attention. Thus, this reduces the cost involved in cultivation, and potentially reduces the cost of biodiesel.[47,48] Some of the commonly investigated non-edible plant oils for biodiesel production include *Jatropha curcas, Pongamia glabra* (Karanja), *Madhuca indica* (Mahua), *Azadirachta indica* (neem), *Moringa oleifera* (moringa seed), *Calophyllum inophyllum, Salvadora oleoides* (Pilu), *Nicotiana tabacum* (tobacco), cottonseed oil, *Eruca sativa Gars*, terebinth, rubber seed oil, desert date, *Acrocomia aculeata* (macaúba), *Crambe abyssinica* (hochst), linseed oil, rubber seed oil, *Sapium sebiferum* (chinese tallow), *Sapindus mukorossi* (soapnut), *Euphorbia tirucalli* (milk bush), *Calophyllum inophyllum* (polanga oil), jojoba, leather pre-fleshings, apricot seed, *Pistacia chinensis* (bunge seed), sal oil and *Croton megalocarpus*. Among all these oil plants, *Jatropha curcas*, *Pongamia glabra* (Karanja), *Madhuca indica* (Mahua), *Azadirachta indica* (neem) are commercially available and most largely used in biodiesel production.[49]

4.3 Waste cooking oil

Biodiesel production from WCO can partially substitute fossil fuels as well as can solve the energy crisis and environmental pollution. Moreover, WCO is cheaper than fresh vegetable oils, consequently, lessening the expense incurred for biodiesel synthesis. WCO can be grouped into two classifications based on their FFA content if the FFA content is >15%. It is then called brown grease; otherwise, it is named 'yellow grease'. Annually, 1 billion tons of WCO is generated throughout the world. In EU, it is estimated that around 0.7–1 MT WCO were collected per year. Among 80 000 tons of WCO, around 65 000 tons were collected from the UK alone, basically originating from commercial restaurants and food processing industries. Therefore, the disposal of WCO is a major concern, which otherwise contaminates water and the environment at large. Although some portions of WCO oil were used in the production of soap, major parts of WCO were usually dumped into the river and landfills. In light of this, the production of biodiesel from WCO not only reduced the cost of biodiesel, but also resolved the disposal problem of WCO and minimized environmental pollution.

4.4 Animal fats

Animal fats are another feedstock for biodiesel production with the potential to reduce the cost of biodiesel. This type of feedstock includes lard, tallow and chicken fat. However, due to the presence of a high quantity of saturated fatty acids, it has some shortcomings both in chemical and physical properties, such as poor cloud point, poor pour point, and so forth. At the same time, its high saturation level has various advantages, such as a high cetane number and high oxidation stability. Moreover,

Table 2 Different forms of edible oils utilized to produce biodiesel

No.	Edible oil for biodiesel production	Plant source	The botanical name of the plant source
1	Sunflower oil	Sunflower	*Helianthus annuus*
2	Rapeseed oil	Rape	*Brassica napus*
3	Soybean oil	Soybean	*Glycine max*
4	Palm oil	Mesocarp of oil palm	*Elaeis guineensis*
5	Coconut oil	Coconut	*Cocos nucifera*

animal fats are more favourable biodiesel feedstocks, as compared to vegetable oils due to their low price.

4.5 Algal oil

Currently, microalgae are viewed as one of the most promising feedstocks for the industrial-scale synthesis of biodiesel. Biodiesel production from algal oil is highly sustainable, as several strains of microalgae can double in size within hours. Thus, they have the capacity to create a large number of litres of biodiesel per hectare every year.[50] Additionally, as several microalgal strains can be grown on non-arable land in a saline water medium, their mass cultivation does not compete with food production.

5. Characterization of catalysts and biodiesel

Several analytical techniques are employed to characterize both catalysts and FAME produced. Each analytical technique will be discussed in the upcoming sections as and when relevant. As a preliminary study, Fourier transform infrared spectroscopy (FT-IR) is usually employed to detect the presence of various functional groups in the catalyst, while X-ray diffraction (XRD) can be employed to investigate the crystallinity and qualitative detection of elements present in the catalyst. The surface morphology, particle size and the structure of the catalysts can be investigated using scanning electron microscopy (SEM) and transmission electron microscopy (TEM). The chemical compositions are investigated using energy-dispersive X-ray spectroscopy (EDX). X-ray fluorescence (XRF) is commonly used for the quantitative detection of metal oxides and X-ray photoelectron spectroscopy (XPS) analyses are routinely performed for the quantitative measurement of the elements present in the catalyst, and also provide the chemical state information of the catalyst. The surface area, pore volume and pore diameter are usually measured by Brunauer–Emmett–Teller (BET) analysis, whereas the thermal stability of the catalysts is analyzed using thermogravimetric analysis (TGA). The acidity and basicity of the catalysts are usually investigated using NH_3 and CO_2 temperature-programmed desorption (TPD) analyses. In addition, the basicity and acidity of the catalyst can be visualized by Hammett indicators tests and acid–base titration methods. Valuable information about the degree of carbonization and/or aromatization of carbonaceous material used as a catalyst can be obtained using solid-state magic-angle spin-nuclear magnetic resonance (MAS NMR). Likewise, the successful conversion of biodiesel feedstocks to FAME is confirmed using different analytical techniques. Usually, NMR analysis is used as a confirmation tool to identify the formation of FAME. Despite not being common, FT-IR analysis can also be used to identify the FAME formation. The chemical components of FAME, along with their respective percentages, are usually identified using gas chromatography-mass spectroscopy (GC-MS) technique. In addition, ^{1}H NMR spectra can be used to give concrete information about the purity of FAME and the percentage conversion of vegetable oil to FAME using the Knothe and Kenar eqn (1).

$$\%\ \text{Conversion} = 100 \times \frac{2A_{\text{Me}}}{3A_{\text{CH}_2}} \quad (1)$$

Here, A_{Me} and A_{CH_2} are the integration values of the methoxy protons and methylene protons of FAME, respectively.

6. Homogeneous catalyst

The homogeneous catalysts utilized for the transesterification reaction are classified into two groups, such as: (i) base catalysts (for example, NaOH and KOH), and (ii) acid catalysts, such as sulphuric, sulphonic, hydrofluoric, and hydrochloric acids.

6.1 Base catalyst

Homogeneous base catalysts are most widely investigated in the transesterification of vegetable oil to FAME, as they are cheap and easily accessible. To date, several homogeneous base catalysts have been utilized for the synthesis of FAME, *e.g.*, KOH, NaOH, and $NaOCH_3$, as shown in Table 3. The uses of NaOH and KOH as catalysts showed excellent catalytic activities towards biodiesel production, such as the minimum reaction time and high biodiesel yield, and occurred at ambient temperature and pressure. However, this process has certain limitations, such as water being formed as a byproduct, which reduces the biodiesel yield. Other than KOH and NaOH, sodium methoxide and potassium methoxide give better biodiesel performance, as water is not formed in these processes. An alkaline catalyst is not suitable for the transesterification of vegetable oils with high FFA content (>2 wt%). However, it is fit for refined vegetable oils with low FFA content (ranging from less than 0.5 wt% to less than 2 wt%).

Dmytryshyn *et al.*[51] examined the transesterification of various vegetable oils, such as canola oil, green seed canola oil from heat-harmed seeds, handled waste fryer oil, and natural waste fryer oil with methanol to afford FAME using the KOH catalyst, and reported a biodiesel yield of 51–87% under the optimum reaction conditions. In another study, KOH was exploited to convert crude rubber oil and palm oil mixture to biodiesel in 98% yield under the optimum reaction conditions. The vegetable oil was esterified using an acid catalyst prior to a base-catalyzed transesterification process, to obtain a low FFA content vegetable oil.[52] Similarly, KOH was utilized as a catalyst for the transformation of soybean oil to FAME in 96% yield.[53] Roselle oil,[34] rapeseed oil,[54] frying oil,[55,56] used olive oil,[57] palm kernel[58] and duck tallow[59] were also successfully transesterified to FAME using the KOH catalyst. Karmee *et al.*[60] reported the transesterification of *Pongamia pinnata* to FAME in 92% conversion using the base catalyst KOH. Interestingly, the utilization of tetrahydrofuran (THF) as a co-solvent increased the conversion to 95%.

Meng *et al.*[23] described an exceptionally high activity of NaOH towards biodiesel production from WCO with high FFA in 89.8% conversion under the optimized reaction settings. The high FFA substance of WCO was reduced by a pre-esterification

Table 3 Distinctive homogeneous base catalysts utilized for biodiesel production

No.	Catalyst	Feedstock	Conditions[a]	Yield (%)	Ref.
1	KOH	Vegetable oil	6 : 1, 1, 25, 40	51–87	51
2	KOH	Crude rubber/palm oil	8 : 1, 2, 55, 300	98	52
3	KOH	Soybean oil	6 : 1, 1, 60, 60	~96	53
4	KOH	Roselle oil	8 : 1, 1.5, 60, 60	99.4	36
5	KOH	Rapeseed	6 : 1, 1, 65, 120	95–96	54
6	KOH	Frying oil	12 : 1, 1, 60, 120	72.5	55
7	KOH	Waste frying oil	6 : 1, 1, 65, 60	96.15	56
8	KOH	Used olive oil	12 : 1, 1.26, 25, 90	94	57
9	KOH	Palm kernel	6 : 1, 1, 60, 60	96	58
10	KOH	Duck tallow	6 : 1, 1, 65, 180	83.6	59
11	KOH	*Pongamia pinnata*	10 : 1, 1, 60, 90	92[b]	60
12	NaOH	Waste cooking oil	6 : 1, 1, 50, 90	89.8[b]	23
13	NaOH	Waste frying oil	4.8 : 1, 0.6, 65, 60	98	61
14	NaOH	Waste frying oil	7.5 : 1, 0.5, 50, 30	96	62
15	NaOH	Canola oil	6 : 1, 1, 45, 15	98	63
16	NaOH	Sunflower	6 : 1, 1, 60, 120	97.1	64
17	NaOH	Refined palm oil	6 : 1, 1, 60, 30	95	65
18	NaOH	Cotton seed oil	6 : 1, 1, 60, 60	97	66
19	$NaOCH_3$	Soybean oil	6 : 1, 0.6, 60, 60	97	53
20	$NaOCH_3$	Rice bran	7.5 : 1, 0.88, 55, 60	83.3	67
21	$NaOCH_3$	Waste cooking oil	6 : 1, 0.75, 65, 90	96.6	68

[a] Methanol-to-oil (M/O) molar ratio, catalyst loading (wt%), temperature (°C), reaction time (min). [b] Conversion.

process with sulphuric acid. Similarly, waste cooking/frying oil,[61,62] canola oil,[63] sunflower oil,[64] palm oil[65] and cotton seed oil[66] were converted to biodiesel using NaOH as a homogeneous catalyst. Furthermore, $NaOCH_3$ (ref. 67 and 68) was evaluated as a catalyst for the transesterification of rice bran oil to FAME by Rashid *et al.*,[67] where 83.3% biodiesel yield was observed in 60 min under the optimum reaction conditions.

6.2 Acid catalyst

Base catalysts are usually preferred over acid catalysts, as they are more reactive and low cost. However, base catalysts may react with the FFA present in the feedstock during transesterification, bringing about soap formation by saponification, which may consume the catalyst and diminish its reactivity. Meanwhile, an acidic catalyst is neutral to the FFA, and thus shows better outcomes for the transesterification or esterification of vegetable oils or fats having a high amount of FFA (≥2 wt%). Generally, acid catalysts are utilized to bring down the FFA content in WCO and animal fats by means of esterification prior to transesterification using a base catalyst.[5] Several acids, such as H_2SO_4, HCl, H_3PO_4 and sulfonated acids, were mostly utilized for the (trans)esterification of vegetable oils.[36] However, acid-catalyzed biodiesel production has some major limitations, such as a slow reaction rate (4000 times slower than the rate of base-catalyzed transesterification), and require a high alcohol-to-oil molar ratio.[69–71] Moreover, it has environmental and corrosive related problems.[69] Because of these demerits, acid-catalyzed biodiesel synthesis is not very popular and is studied less. Some of the reported literature of acid-catalyzed biodiesel production and their results are listed in Table 4.

Wang *et al.*[70] examined the biodiesel synthesis from WCO and reported a 90% yield. Moreover, Miao *et al.*[72] examined the conversion of soybean oil to biodiesel using trifluoroacetic acid catalyst, and reported 98.4% biodiesel yield at optimal reaction conditions. Similarly, various edible/non-edible oils (such as WCO,[73] soybean oil,[71] zanthoxylum bungeanum[74] and tobacco seed oil[75]) were used for biodiesel production using sulfuric acid. Moreover, trifluoroacetic acid was utilized as a homogeneous acid catalyst for the esterification/transesterification of soybean oil to biodiesel.[72] The catalyst brought about a high biodiesel yield of 98.4% under the optimum reaction conditions. From the above discussion, it was observed that acid-catalyzed esterification/transesterification reactions usually require drastic reaction conditions, such as a high M/O molar ratio, catalyst loading, temperature and long reaction time, as compared to base-catalyzed transesterification reactions.

7. Heterogeneous catalysts

Although the homogeneous catalyst has its own advantages, such as high reactivity and low cost, its utilization in the production of biodiesel is accompanied by several shortfalls. These shortfalls include the low quality of glycerol produced, the fact that the catalyst cannot be regenerated, and the lengthy process involved in the purification of biodiesel. Thus, the whole process is labor-intensive and uneconomical. Hence, in recent years, the heterogeneous catalyst has attracted immense attention for biodiesel production, as it can be tailored to match specific requirements, and be easily recovered and reused for several cycles of catalytic reaction, thereby potentially bringing down the labor involved and the cost of biodiesel.

Table 4 Different acidic homogeneous catalysts utilized for biodiesel synthesis

No.	Catalyst	Feedstock	Conditions[a]	Yield (%)	Ref.
1	H_2SO_4	Chicken/mutton tallow	30 : 1, 1.25/2.5, 50/60, 1440	99.01 ± 0.71/93.21 ± 5.07	25
2	H_2SO_4	WCO	20 : 1, 4, 95, 600	90	70
3	H_2SO_4	Used frying oil	3.6 : 1, 0.1, 65, 40	79.3	73
4	H_2SO_4	Soybean oil	6 : 1, 3, 60, 2880	98	71
5	H_2SO_4	*Zanthoxylum bungeanum*	24 : 1, 2, 60, 80	98	74
6	H_2SO_4	Tobacco seed oil	18 : 1, 1, 60, 25	91	75
7	$C_2HF_3O_2$	Soybean oil	20 : 1, 2 M, 120, 300	98.4	72

[a] Methanol-to-oil molar ratio, catalyst loading (wt%), temperature (°C), reaction time (min).

Unlike homogeneous catalysts, heterogeneous catalysts mostly appear in a solid form; thus, the reaction mixture and the catalyst are in a different phase. In the heterogeneous catalyzed reactions, the catalyst surface is the main site for the reaction to occur.[76] The following advantages of utilizing a solid catalyst in transesterification make the process green: (i) the catalyst can be reused, (ii) there is a very minimal amount of wastewater generated during the process, (iii) glycerol separation from the final mixture (glycerol, biodiesel and catalyst) is much easier, and (iv) high purity glycerol is obtained.

Heterogeneous catalysts have several advantages over a homogeneous catalyst, such as simple separation, recyclability and reusability. Moreover, solid catalysts are eco-friendly, less toxic, and have minimum corrosion and reduced energy intake. Thus, solid catalysts provide an efficient and economical pathway for biodiesel production.[12,77,78] Heterogeneous or solid catalysts can be grouped into two categories: (i) basic and (ii) acidic heterogeneous catalysts. Nowadays, researchers have developed several heterogeneous catalysts, which can promote esterification and transesterification reactions simultaneously in one reaction vessel (one-pot). These types of catalysts are mostly utilized for biodiesel synthesis from the vegetable oils or animal fats having a high amount of FFA without the requirement of an additional pretreatment step to reduce the FFA content.[12]

7.1 Base catalysts

In recent years, basic heterogeneous catalysts have been most widely investigated as it can overcome the constraints associated with homogeneous basic catalysts, and shows excellent catalytic activity under mild reaction conditions. However, these catalysts are suitable only for biodiesel feedstock with low FFA content; otherwise, the catalysts will react with the FFA to produce soap by means of the saponification reaction. This makes the separation of biodiesel from glycerol tedious, thereby diminishing the biodiesel yield. Several solid base catalysts reported in the literature, such as the alkaline metal oxides, transition metal oxides, mixed metal oxides, hydrotalcites, zeolites, and biomass-based catalysts, are discussed comprehensively in this section.

7.1.1 Alkaline earth metal oxides. Oxides of alkaline earth metals are one of the most widely studied catalysts for biodiesel synthesis due to their insolubility in methanol and low toxicities. The basicity of the alkaline earth metal oxides follows the order: MgO < CaO < SrO < BaO. MgO is almost inactive towards the transesterification reaction.[79,80] Among all alkaline earth metal oxides, CaO is most widely utilized in FAME production, as it is highly basic, insoluble in alcohol, non-toxic, cheap and easily available.[81] However, it is very sensitive to the FFA content and forms undesirable byproducts *via* saponification, and also loses its activity in the process.[82] Despite its high activity, SrO is less studied in transesterification reactions as it is very sensitive to the atmospheric moisture, and reacts with CO_2 and water to form $SrCO_3$ and $Sr(OH)_2$. Table 5 shows the activity of various alkaline metal oxides towards biodiesel production.

Kouzu *et al.*[82] examined the transesterification of soybean oil using the CaO catalyst, and reported a high biodiesel yield of 95% under the optimized reaction conditions. Granados *et al.*[83] found that CaO calcined at 700 °C showed very high activity towards biodiesel production from sunflower oil, and attained 94% biodiesel yield. Furthermore, the transesterification of rapeseed oil was reported by Kawashima *et al.*,[84] where CaO was pretreated with methanol to form $Ca(OCH_3)$, which acted as an initiator for the transesterification reaction. A high biodiesel yield of 90% was observed using the optimized reaction conditions. In another work, the SrO-catalyzed transesterification of soybean oil has been reported by Liu *et al.*[85] The catalyst showed excellent activity with a high yield of 95% at 70 °C and 30 min time. The catalyst is highly stable and can be reused for 10 successive cycles.

The ultrasonic-assisted biodiesel synthesis from palm oil was reported using diverse metal oxides, such as CaO, BaO and

Table 5 Different alkaline earth metal oxide-catalyzed biodiesel production under various reaction conditions

No.	Catalyst	Feedstock	Conditions[a]	Yield (%)	Ref.
1	CaO	Soybean oil	12 : 1, 8, 65, 180	95	82
2	CaO	Sunflower oil	13 : 1, 3, 60, 120	94	83
3	CaO	Rapeseed oil	3.8 : 1, 0.7, 60, 160	90	84
4	SrO	Soybean oil	6 : 1, 3, 70, 30	95	85
5	BaO	Palm oil	9 : 1, 3, 65, 60	95.2	86

[a] Methanol-to-oil molar ratio, catalyst loading (wt%), temperature (°C), reaction time (min).

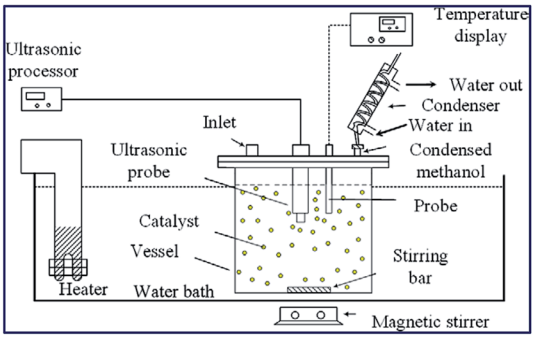

Fig. 3 Schematic portrayal of experimental set up for the ultrasonic-assisted transesterification reaction. Reproduced from ref. 86.

SrO.[86] The activity of the catalyst in ultrasonic-assisted biodiesel synthesis was compared with the traditional magnetic stirring process, and it was found that the ultrasonic process showed 95.2% of yield using BaO within 60 min reaction time, which otherwise take 3–4 h in the conventional stirring process. Similarly, the ultrasonic-assisted transesterification using CaO and SrO resulted in an increase in the biodiesel yield from 5.5% to 77.3% and 48.2% to 95.2%, respectively. These findings show the advantages of using ultrasonication in the field of chemical synthesis, particularly in the field of biodiesel synthesis. The authors also investigated the influence of ultrasonic amplitude on the biodiesel synthesis from palm oil, and observed that 50% ultrasonic amplitude displayed the best result in terms of the biodiesel yield. The catalyst reusability test revealed that the catalytic activity of BaO decreased drastically, especially in the ultrasonic process during the reusability test, which was mainly due to catalyst leaching. The reaction set-up is depicted in Fig. 3.

7.1.2 Transition metal oxides. Despite the high reactivity of alkaline earth metal oxides, they have some serious drawbacks, such as low reusability and high sensitivity towards moisture, that reduced their catalytic efficacy. To overcome these inherent drawbacks, metal oxides of Zn, Ti, Zr and Zn are widely investigated in transesterification reactions, as they are easily available, highly stable and showed excellent catalytic activities.[87–89] To date, numerous transition metal oxide-based catalysts have been reported in the field of biodiesel synthesis from vegetable oils, as depicted in Table 6. da Silva *et al.*[90] reported on Cu(II) and Co(II) impregnated on chitosan catalysts for FAME synthesis from soybean oil. The adsorption process for Cu(II) on chitosan is better than Co(II). However, Co(II)@chitosan showed a higher biodiesel yield (94.01%), as compared to Cu(II)@chitosan (88.82%) using the optimal reaction conditions. In another work, Jitputti *et al.*[87] investigated ZrO_2, ZnO, SO_4^{2-}/SnO_2, SO_4^{2-}/ZrO_2, KNO_3/KL zeolite and KNO_3/ZrO_2 for the FAME synthesis from the crude palm kernel oil and crude coconut oil, and found that the SO_4^{2-}/ZrO_2 catalyst displays the highest reactivity for both oils with a biodiesel yield of 90.30% and 86.30%, respectively. The decreasing order of the catalyst activity towards biodiesel synthesis from crude kernel oil is $SO_4^{2-}/ZrO_2 > SO_4^{2-}/SnO_2 > ZnO > KNO_3/ZrO_2 > KNO_3$/KL zeolite $> ZrO_2$. For the crude coconut oil, it is $SO_4^{2-}/ZrO_2 > SO_4^{2-}/SnO_2 > ZnO > KNO_3$/KL zeolite $> KNO_3/ZrO_2 > ZrO_2$.

Meanwhile, Baskar *et al.*[91] used the Mn-doped ZnO nanomaterial for the conversion of Mahua oil to biodiesel, and observed that the catalyst calcined at 600 °C showed the highest biodiesel yield of 97% under the optimum reaction conditions. The kinetic investigation of the reaction revealed that 181.91 kJ mol^{-1} activation energy is necessary for biodiesel synthesis from Mahua oil utilizing the Mn-doped ZnO catalyst. The prepared Mn-doped ZnO catalyst was seen as a cluster, and is spherical in shape as depicted in Fig. 4 A. FI-TR analysis was performed to confirm the formation of the biodiesel. Absorption bands at 1744 and 1703 cm^{-1} demonstrated the CO stretching of the methyl esters in Mahua oil and biodiesel, respectively. The main spectral region that allows for the chemical discrimination between Mahua oil and the produced biodiesel is in the range of 1500–900 cm^{-1}, and is also called known as the fingerprint region. Fig. 4B reveals the symmetric and asymmetric stretching of the alkyl regions at 1376, 1463, 2852, 2922 cm^{-1}, and the CO group of the lactones and esters at 1735 cm^{-1}. Moreover, the stretching band of the CO group of the typical esters at around 1703 cm^{-1} was observed in Fig. 4C. In light of these FT-IR bands, the product obtained after transesterification of Mahua oil using the Mn-doped ZnO catalyst was confirmed as biodiesel.

Na_2MoO_4 has been synthesized and investigated as a catalyst in the transesterification of soybean oil by Nakagaki *et al.*[92] The catalyst displayed high activity towards the transesterification reaction, and afforded a biodiesel yield of 95.6%. The high reactivity of the catalyst is due to the acid sites of Mo(VI), which can easily polarize the O–H bond. Correspondingly, Serio *et al.*[93] also reported the high reactivity of the vanadyl phosphate-based

Table 6 Various transition metal oxide-catalyzed biodiesel production yields under different reaction conditions

No.	Catalyst	Feedstocks	Conditions[a]	Yield (%)	Ref.
1	Cu(II)@chitosan	Soybean oil	1 : 5[b], 2, 70, 180	88.82	90
2	Co(II)@chitosan	Soybean oil	1 : 5[b], 2, 70, 180	94.01	90
3	SO_4^{2-}/ZrO_2	Crude palm kernel oil	6 : 1, 3, 200, 60	90.30	87
4	SO_4^{2-}/ZrO_2	Crude coconut oil	6 : 1, 3, 200, 60	86.30	87
5	Mn doped ZnO	Mahua oil	7 : 1, 8, 50, 50	97	91
6	Na_2MoO_4	Soybean oil	54 : 1, 3, 120, 180	95.6	92
7	Vanadyl phosphate	Soybean oil	0.88 : 2, 0.5, 180, 60	≥88	93

[a] Methanol-to-oil molar ratio, catalyst loading (wt%), temperature (°C), reaction time (min). [b] w/w.

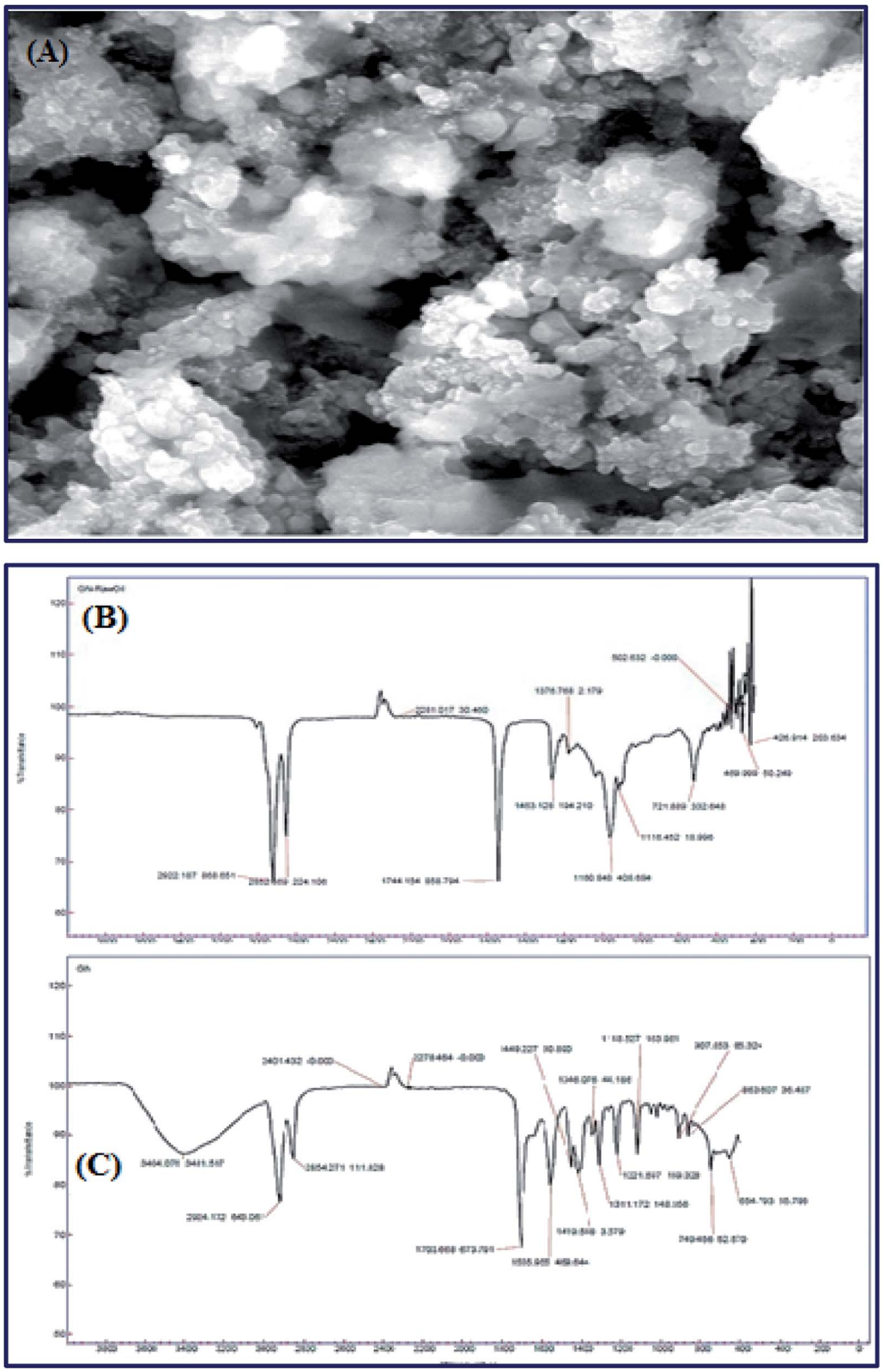

Fig. 4 SEM image (A) and FT-IR spectrum (B and C) of Mn-doped ZnO nanomaterial. Reproduced from ref. 92.

catalyst in the biodiesel synthesis from soybean oil. Regardless of the low surface area, the high reactivity of the catalyst is attributed to the structural/surface morphologies. A biodiesel yield of ≥88% was recorded using the optimal reaction conditions. The dehydrated product of the catalyst $VOPO_4 \cdot 2H_2O$ can be converted to $VOPO_4$ simply by calcination at 400–500 °C.

7.1.3 Zeolites. Zeolites are crystalline aluminosilicates that possess a microporous structure.[94] It can exist in different structural morphologies depending on the synthesis process and reaction conditions, such as the Si/Al molar ratio, pour sizes and proton exchange levels. The wide opportunity for the structural modification of zeolites makes them an excellent catalyst for various acid–base reactions. Recently, zeolites are intensively investigated in the field of biodiesel production due to their shape selectivity and acidic character. Normally, zeolites are moderately active for the esterification reaction. However, by increasing the pore size and varying the Si/Al ratio, the catalytic properties can be improved. Moreover, zeolites can incorporate various metal ions (such as Na^+, K^+, Mg^{2+}), which are mainly responsible for its basic nature.[95] Table 7 shows various reported zeolite catalysts employed in the biodiesel synthesis.

In 2007, a NaX zeolite loaded with various concentrations of KOH was synthesized and reported as a catalyst in FAME production from soybean oil.[96] A catalyst loaded with 10% KOH followed by heating at 393 K for 3 h gave the best result with 85.6% yield under the optimized reaction conditions. Shu *et al.*[97] prepared the La/zeolite beta using $La(NO_3)_3$ as a precursor *via* ion exchange technique, and was exploited in FAME production from soybean oil. They reported that the La/zeolite beta has higher stability and catalytic activity towards FAME production compared to the zeolite beta catalyst. A yield of 48.9% was obtained using the La/zeolite beta under the optimized reaction conditions, such as the 14.5 : 1 M/O molar ratio, 0.011 wt% catalyst loading, 60 °C and 4 h time. In the year 2008, Ramos *et al.*[98] studied three zeolites, such as mordenite, beta and X, for the conversion of sunflower oil biodiesel. They examined the effect of different loaded/stacked metals on such zeolites. Zeolite X showed the best catalytic activity, as it has a higher number of super basic sites, which is absent in other zeolites. The effect of the binder, sodium bentonite, on the catalytic reactivity of such zeolites was tested, where the X zeolite was agglomerated and thus, the catalytic activity was slightly reduced. A high yield of 93.5% and 95.1% of FAME was obtained at 60 °C with and without binder, respectively. In another report, Wu *et al.*[99] synthesized a series of CaO supported on zeolites, such as NaY, KL and NaZSM-5 *via* microwave irradiation, and they were utilized in biodiesel synthesis from soybean oil. They reported that the supported CaO showed a better result compared to the naked CaO, as the supported catalyst has a high surface area, porosity and basic strength. Accordingly, the best result was exhibited by the NaY-supported CaO (30% CaO loaded on NaY) under the optimized reaction conditions.

The strontium nanocatalyst supported on ZSM-5 by the incipient wetness impregnation method was prepared and applied in biodiesel synthesis from sunflower oil.[100] The authors reported the effect of the calcination temperature and Sr/ZSM-5, Ba–Sr/ZSM-5 mass ratios. Ba–Sr/ZSM-5 (Ba 4 wt% to the Sr weight and Sr 6 wt% to the ZSM-5 weight) exhibited the best performance with 87.7% yield under optimal conditions. In the meantime, Narkhede *et al.*[101] synthesized a series of 12-tungstosilicic acid, SiW_{12} (10–40 wt%) impregnated on zeolite Hβ, and applied it in biodiesel synthesis from soybean oil. Interestingly, the SEM image of the 30% SiW_{12}/Hβ (Fig. 5b) is similar to the pure zeolite Hβ (Fig. 5a), and revealed that the framework structure of Hβ was retained even after the impregnation of SiW_{12}. This suggested that SiW_{12} was homogeneously distributed in the framework structure of the Hβ zeolite. They reported a 95% yield of FAME under the optimized reaction conditions.

In 2012, Babajide *et al.*[102] synthesized a zeolite derived from fly ash and then ion-exchanged with K to form the FA/K-X zeolite, which was then applied in biodiesel synthesis from sunflower oil. They reported a high yield of 83.53% under the optimized reaction conditions. Similarly, Manique *et al.*[103] prepared zeolite (sodalite) derived from coal fly ash *via* the hydrothermal process, and utilized in biodiesel synthesis from soybean oil. The developed sodalite has a definite surface area of 10 $m^2\ g^{-1}$. They also reported a maximum conversion of 95.5% soybean oil using the optimized reaction conditions. Recently, Al-Jammal *et al.*[104] prepared zeolite derived from zeolite tuft, followed by the impregnation of a series of KOH solutions (1–6 M), and heated at 80 °C for 4 h to form the KOH/zeolite catalyst. Finally, it was utilized in biodiesel synthesis from waste sunflower oil. The catalyst (1–4 M) KOH/zeolite exhibited a biodiesel yield of 96.7% under the reaction conditions: 11.5 : 1 M/O molar ratio, catalyst amount of 6 wt% w.r.t. oil, 50 °C temperature and reaction time of 2 h.

Table 7 Different zeolite-catalyzed FAME production yields under various reaction conditions

No.	Catalyst	Feedstocks	Conditions[a]	Yield (%)	Ref.
1	KOH@NaX zeolite	Soybean oil	10 : 1, 3, 65, 480	85.6	96
2	La/zeolite beta	Soybean oil	14.5 : 1, 0.011, 60, 240	48.9	97
3	Zeolite X	Sunflower oil	6 : 1, 10, 60, 420	95.1	98
4	CaO@NaY zeolite	Soybean oil	9 : 1, 3, 65, 180	95	99
5	Ba–Sr/ZSM-5	Sunflower oil	9 : 1, 3, 60, 180	87.7	100
6	$H_4[W_{12}SiO_{40}]$@zeolite Hβ	Soybean oil	4 : 1, 0.2, 65, 480	95	101
7	FA/K-X zeolite	Sunflower oil	6 : 1, 3, 60, 480	83.53	102
8	Sodalite	Soybean oil	12 : 1, 4, 65, 120	95.5	103
9	KOH/zeolite	Waste sunflower oil	11.5 : 1, 6, 50, 120	96.7	104
10	La_2O_3/NaY zeolite	Castor oil	15 : 1, 10, 70, 50	84.6	105

[a] Methanol-to-oil molar ratio, catalyst loading (wt%), temperature (°C), reaction time (min).

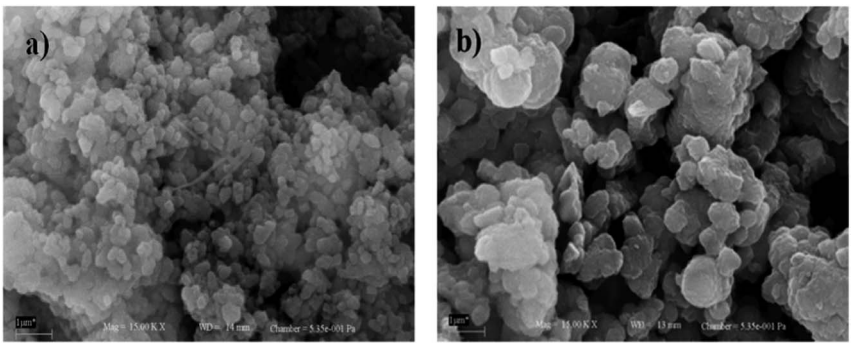

Fig. 5 SEM micrographs of (a) Hβ and (b) 30% SiW_{12}/Hβ. Reproduced from ref. 101.

In the same vein, Du *et al.*[105] developed La_2O_3 impregnated on the NaY zeolite catalyst having a spherical shape of 3–5 mm size, and utilized it in biodiesel synthesis from castor oil. In addition, they explored the impact of the calcination temperature in the range of 600–1000 °C on the biodiesel yield, and observed that the catalyst calcined at 800 °C showed the best result. They also revealed that the incorporation of the surfactant improved the dispersion of La_2O_3 and the pore size of the zeolite. The XRD patterns of the pure zeolite NaY and the catalyst La_2O_3/NaY zeolite calcined in the temperature range of 600–1000 °C are displayed in Fig. 6. The XRD patterns of the pure zeolite (Fig. 6a) and the catalyst calcined at 600 °C (Fig. 6b) and 800 °C (Fig. 6c) are almost the same, and revealed that the crystallinity of the zeolite NaY does not change upon the incorporation of La_2O_3. However, on increasing the temperature to 1000 °C, the XRD pattern (Fig. 6e) showed no characteristic peaks of zeolite, suggesting that at high calcination temperature, the crystallinity of the zeolite is lost.

7.1.4 Supported catalyst. To increase the stability and reusability of the alkaline earth metal oxides, the catalyst support plays an important role as it can reduce the mass transfer limitation and provide a high surface area with high porosity, where the metals are anchored.[106] Until now, several catalyst supports (such as alumina, silica, ZnO and ZrO_2) had been proposed for the production of FAME. Alumina is extensively employed as the catalyst supports for various basic or acidic compounds exploited as a solid catalyst in esterification/transesterification reactions.[107] Several alumina-supported catalysts were employed in the transesterification reaction for biodiesel synthesis, as shown in Table 8. In 2006, Xie *et al.*[108] investigated the potential of KI loaded on an Al_2O_3 support catalyst for biodiesel synthesis from soybean oil. They prepared a series of KI@Al_2O_3 catalysts by changing the KI amount, and investigated their catalytic activities. They observed that the catalyst loaded with 35% KI and calcined at 773 K showed the highest FAME conversion of 96% against all other catalysts under the optimal reaction conditions. In another study, potassium oxide loaded on alumina derived from various potassium salts (such as KNO_3, KOH, KF, KI and K_2CO_3) were compared. It was found that KF@Al_2O_3 showed the best result compared to other catalysts because of the generation of the new phase K_2O on the surface of alumina, and as a result of the increasing basicity of the catalyst.[109] In addition, Ma *et al.*[110] reported the synthesis of FAME *via* transesterification of rapeseed oil using the K@KOH@Al_2O_3 catalyst. The formation of the Al–O–K composite enhanced the basicity of the catalyst and thus, the catalytic efficiency. They investigated the catalytic activity by varying the amount of K and KOH, and found that 7.5 and 20 wt% (w.r.t. alumina) of K and KOH, respectively, displayed the highest activity with 84.52% biodiesel yield. Moreover, Chen *et al.*[111] reported on the biodiesel production from soybean oil using the K@γ-Al_2O_3 catalyst in a rotating packed bed (RPB) reactor. The schematic representation of the RPB model is displayed in Fig. 7. The main advantage of the RPB reactor is that it provides efficient mixing of three immiscible reactants, such as oil, methanol and the catalyst. A high yield of 96.4% was reported using the optimal reaction conditions.

Zhang *et al.*[112] synthesized a KOH-impregnated modified alumina catalyst for biodiesel synthesis from microalgae oil. First, the alumina was modified with lanthanum and barium to increase its surface area, ensure that it possessed the desired pore volume and pore distribution, and finally impregnate KOH on the modified alumina to form the desired catalyst. They

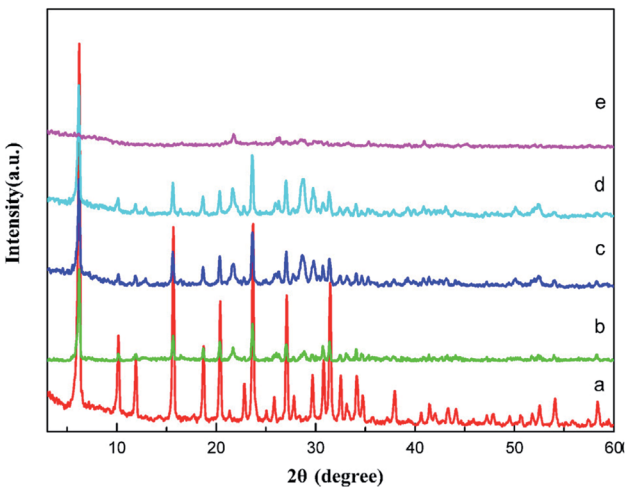

Fig. 6 XRD pattern of pure zeolite (a), La_2O_3/NaY-600 (b), La_2O_3/NaY-800 (c), S–La_2O_3/NaY-800 (d), La_2O_3/NaY-1000 (e). Reproduced from ref. 105.

Table 8 Different aluminium-supported solid catalysts for biodiesel production[c]

No.	Catalyst	Feedstock	Conditions[a]	Yield (%)	Ref.
1	$KI@Al_2O_3$	Soybean oil	15 : 1, 2, 65, 480	96	108
2	$K@KOH@Al_2O_3$	Rapeseed oil	9 : 1, 4, 60, 60	84.52	110
3	$K@\gamma\text{-}Al_2O_3$	Soybean oil	24 : 1, 10.6, 60, 60	96.4	111
4	$KOH/La–Ba–Al_2O_3$	Microalgae	NR, 25, 60, 180	97.7[b]	112
5	$CaO@Al_2O_3$	*Nannochloropsis oculata*	30 : 1, 2, 50, 240	97.5	113
6	$CaO@Al_2O_3$	Palm oil	12 : 1, 6, 65, 300	98.64	114

[a] Methanol-to-oil molar ratio, catalyst loading (wt%), temperature (°C), reaction time (min). [b] Conversion. [c] NR: not reported.

reported that the condition of 25% KOH (w.r.t. modified alumina) impregnated on modified alumina and calcined at 550 °C for 4 h showed the best activity towards the transesterification reaction with 97.7% biodiesel yield under the ideal reaction conditions. Umdu *et al.*[113] synthesized $CaO@Al_2O_3$ *via* the sol–gel method and conducted a transesterification reaction of microalgae (*Nannochloropsis oculata*) oil to produce biodiesel. The catalyst has higher reactivity than the bare CaO, which was almost inactive towards transesterification of the desired microalgae. The alumina was loaded with 80 wt% (w.r.t. Al_2O_3) $Ca(NO_3)_2 \cdot 4H_2O$ and calcined at 500 °C for 6 h to form 80 wt% $CaO@Al_2O_3$ that possessed the highest catalytic activity with 97.5% biodiesel yield. In addition, Zabeti *et al.*[114] synthesized a $CaO@Al_2O_3$ catalyst using calcium acetate *via* calcination at 718 °C for biodiesel synthesis from palm oil. They have used the Response Surface Methodology (RSM) in association with the Central Composite Design (CCD) to determine the optimum reaction conditions, such as the M/O molar ratio, catalyst amount, reaction temperature and reaction time. A biodiesel yield of 98.64% was obtained under the optimum reaction conditions.

Apart from alumina, there are several materials that are used as a catalyst support, such as SiO_2, ZrO_2 and activated carbon (AC) (Table 9). In 2010, Samart *et al.*[115] conducted the transesterification reaction using CaO impregnated on a mesoporous SiO_2 catalyst for FAME production. They also investigated the influence of the CaO amount, and reported that 15 wt% CaO (w.r.t. SiO_2) loading showed the maximum yield of 95.2%. In addition, the synthesis of FAME from palm oil using a CaO impregnated on a bimodal meso–macroporous SiO_2 support catalyst was reported by Witoon *et al.*[116] They investigated the influence of CaO loading and pellet size on the biodiesel conversion, and also compared with the unimodal SiO_2-supported CaO catalyst. CaO in 40 wt% $CaO@SiO_2$ was highly aggregated on the surface of the mesoporous SiO_2, and hence increases the surface basicity. In contrast, CaO in 30 wt% $CaO@SiO_2$ was highly dispersed inside the mesopore of the silica support. Accordingly, 40 wt% $CaO@SiO_2$ showed higher FAME yield compared to 30 wt% $CaO@SiO_2$. They also reported that the catalyst with a pellet size of 335 μm showed a maximum yield of 92.45%. Moreover, Wu *et al.*[117] reported on catalysts consisting of three different potassium compounds (KAc, K_2CO_3 and K_2SiO_3) impregnated on mesoporous SiO_2, such as AlSBA-15 and SBA-15, for the production of FAME from JCO. Three potassium salts with different concentrations were impregnated on AlSBA-15 and SBA-15, and it was found that the basicity lies in the order of 35 wt% K_2SiO_3@AlSBA-15 > 35 wt% K_2CO_3@AlSBA-15 > 35 wt% KAc@AlSBA-15. Thus, 30 wt% K_2SiO_3 showed the highest yield of 95.7% under the optimized reaction conditions.

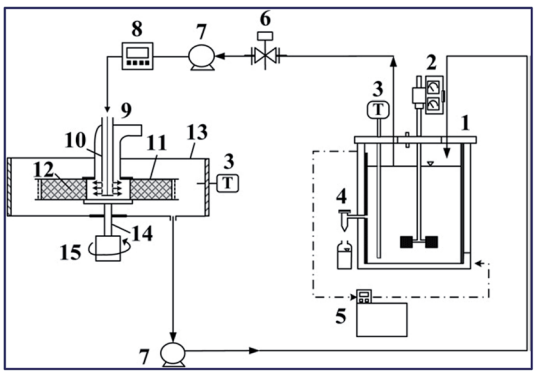

Fig. 7 RPB experimental apparatus utilized for the heterogeneously catalyzed transesterification reaction. Components: (1) CSTR reactor; (2) stirrer; (3) thermocouples; (4) sample port; (5) thermostat; (6) control valve; (7) pumps; (8) flow-meter; (9) RPB reactor; (10) stationary liquid distributor; (11) packed-bed rotator; (12) $K/g\text{-}Al_2O_3$ catalyst; (13) housing case; (14) rotor shaft; (15) motor. Reproduced from ref. 111.

The concept of the AC-based catalyst is an attempt towards the development of a novel alternative to homogeneous alkaline in the form of a heterogeneous catalyst. These kinds of catalysts have pulled in a lot of consideration from the scientific community because the uses of carbon as catalysts not only makes them reusable in the production process, but also greatly reduces the formation of the soap and increases the glycerol purity.[118] To date, different kinds of activated carbon-based catalysts have been developed and successfully exploited in biodiesel production, and some of them are briefly discussed here (Table 18). Narowska *et al.*[118] proposed the development of a novel carbon-based catalyst to replace the alkaline homogeneous catalyst as a solid catalyst, which has the potential to be reused multiple times, eliminating various limitations associated with other traditional catalysts. In this context, the authors demonstrated the preparation of FAME from corn oil *via* transesterification utilizing KOH supported on an activated carbon catalyst. The result showed that the highest yield

Table 9 Different solid supported catalysts for biodiesel synthesis

No.	Catalyst	Feedstocks	Conditions[a]	Yield (%)	Ref.
1	CaO/SiO_2	Soybean oil	16 : 1, 5, 60, 480	95.2	115
2	CaO/SiO_2 (bimodal)	Palm oil	12 : 1, 5, 60, 240	94.15	116
3	K_2SiO_3@AlSBA-	Jatropha oil	9 : 1, 15.30, 60, 180	95.7	117
4	KOH/AC	Corn oil	3 : 1, 0.75, 62.5, 60	92	118
5	CaO/AC	WCO	25 : 1, NR, 60, 480	94	119
6	CaO/AC	Vegetable oil	40 : 111, 120, 420	>90	120
7	KF/AC	WCO	8.85 : 1, 3, 175, 60	83	121
8	KOH/AC	Palm oil	24; 1, 30.3, 64.1, 60	98.03	122
9	K_2CO_3@KFA	Rapeseed oil	15 : 1, 3, 65, 120	99.6	123
10	KOH@AC	WCO	25 : 1, NR, 60, 120	86.3	124
11	CaO@AC	Palm oil	15 : 1, 5.5, 190, 81	80.98	125
12	KAc/AC	Bitter almond oil	9 : 1, 2.50, 65, 150	93.21	126
13	KF/CaO/AC	Soybean oil	12 : 1, 2.1, 65, 20	99.9	127
14	Ag@ZnO	Palm oil	10 : 1, 10, 60, 60	96	128
15	KOH/AC	WCO	12 : 1, 3, 60, 120	96.65	129

[a] Methanol-to-oil molar ratio, catalyst loading (wt%), temperature (°C), reaction time (min).

(92 wt%) of FAME was recorded using optimal reaction conditions. These findings indicated that activated carbon-supported catalysts can be promisingly employed in the transesterification of the waste corn oil using methanol.

Previously, Buasri *et al.*[119] reported on calcium oxide impregnated on the AC catalyst in the synthesis of highly pure FAME from waste cooking palm oil through the continuous transesterification of FFA. After the optimization of various reactions, a maximum FAME yield (94%) was accomplished. In another study, Konwar *et al.*[120] also synthesized AC-supported calcium oxide from the *Turbonilla striatula* shell. Furthermore, their applicability as a catalyst has been investigated in biodiesel synthesis from vegetable oil. It was reported that the catalyst displayed more than 90% oil conversion under the optimized reaction conditions. Moreover, this approached is economically viable due to the easy recoverability of the catalyst. The catalyst was utilized for five progressive reaction cycles with minimum activity loss.

Hameed *et al.*[121] examined a solid catalyst KF supported on AC for biodiesel synthesis from WCO. They designed a composite rotatable reactor to optimize the reaction parameters, and obtained 83% methyl ester yield. In 2010, Baroutian *et al.*[122] studied FAME synthesis in a packed bed membrane reactor (PBMR) from palm oil using a solid catalyst of KOH supported on AC generated from palm shell (Fig. 8). They also investigated the impact of the reaction parameters using RSM. The highest biodiesel yield of 98.03% was reported using the catalyst with optimized reaction conditions. In addition, Li *et al.*[123] reported the *in situ* synthesis of K_2CO_3@KFA *via* mixing of K_2CO_3 and kraft lignin (KF), followed by calcination at 800 °C, and utilized the catalyst in biodiesel synthesis from rapeseed oil. They also investigated the influence of the reaction parameters on the FAME production, and reported a maximum yield of 99.6% under the optimized reaction conditions.

Furthermore, Buasri *et al.*[124] conducted a synthesis process, where a solution of KOH was mixed with activated carbon (AC) originated from coconut shell to form KOH@AC, and used this catalyst in biodiesel synthesis from WCO. The authors claimed that the synthesized catalyst has extraordinary catalytic reactivity, and showed 86% biodiesel yield under the optimized reaction conditions. Similarly, Wan *et al.*[125] examined a solid base catalyst CaO@AC for FAME synthesis from palm oil. RSM was utilized to investigate the impact of the reaction parameters on biodiesel synthesis. A maximum yield of 80.98% was reported under the optimal reaction conditions, and also claimed that the catalyst can retain its activity even after two cycles. Recently, Fadhil *et al.*[126] conducted a transesterification reaction of bitter almond oil to produce biodiesel using KAc impregnated on activated carbon originated from the waste of polyethylene terephthalate. A maximum yield of 93.21% with high purity was reported. The authors claimed that the catalyst

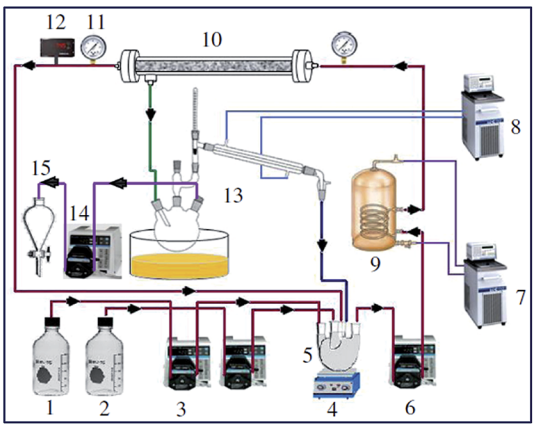

Fig. 8 Schematic diagram of PBMR for FAME synthesis. Components: (1) palm oil; (2) methanol; (3) crude material siphon; (4) magnetic stirrer; (5) blending vessel; (6) flowing siphon; (7) boiling water flowing; (8) water chiller; (9) wound thermal exchanger; (10) ceramic membrane; (11) pressure check; (12) temperature indicator; (13) methanol recuperation unit; (14) siphon; (15) isolating funnel. Reproduced from ref. 122.

showed excellent reactivity towards biodiesel synthesis compared to other reported solid base catalysts, as the catalyst showed a very high yield in very suboptimal reaction conditions. Moreover, according to the authors, the catalyst has great stability as it can be reused for 6 cycles.

Liu *et al.*[127] examined a solid base catalyst KF/CaO/AC calcined at 500 °C for 5 h for the conversion of soybean oil to biodiesel. The authors claimed that the main catalytic role was played by K_2O and $KCaF_3$, which are present in the catalyst. The catalyst demonstrated a high yield of 99.9% in only 20 min. Nonetheless, they reported that the catalyst is highly sensitive towards the water contents in methanol and oleic acid. Therefore, it is necessary to use anhydrous oil and methanol to overcome this problem. In conclusion, from all of these above-mentioned studies, a collective inference can be drawn that the activated carbon-based catalysts will be the next-generation novel alternative to traditionally available catalysts for the efficient transesterification of different oils.

In the meantime, the application of zinc oxide-supported silver nanoparticles (ZnO@Ag NPs) as a solid catalyst for the conversion of palm oil to FAME was reported by Laskar *et al.*[128] The transformation of palm oil to FAME was confirmed using NMR analysis and 10 components of FAME were identified using GC-MS technique, with methyl octadecanoate (C18:0) being the major component. A mixture with different ratios of Ag on ZnO were prepared, where 10 wt% ZnO@Ag was found to be the most active catalyst producing 96% FAME under the optimum reaction conditions. In the recent past, Taslim *et al.*[129] also demonstrated the efficacy of low-cost AC-based catalysts developed from candlenut shells (an agricultural waste) through the impregnation of KOH for biodiesel production from WCO. The results obtained have shown a yield of biodiesel up to 96.65% using the optimized reaction conditions.

7.1.5 Hydrotalcite. Recently, hydrotalcites have attracted interest as a solid catalyst in the transesterification reactions due to their tunable properties and excellent performance. They belong to the layered double hydroxide (LDH) family. The general formula of hydrotalcite is $[M_n^{2+}M_m^{3+}(OH)_{2(n+m)}]^{m+}[A^{x-}]_{m/x}\cdot yH_2O$, where M^{2+} is a divalent metal, *e.g.*, Ca^{2+}, Zn^{2+}, and Mg^{2+}; M^{3+} is a trivalent metal, most frequently Al^{3+}; whereas A^{x-} is an anion with x in the range of 0.1–0.5.[130,131] Table 10 shows various reported hydrotalcite catalysts employed in the biodiesel synthesis from different feedstocks. Navajas *et al.*[132] prepared Mg/Al hydrotalcite with composition within the range of 1.5–5 by co-precipitation method, and applied it in the conversion of sunflower oil to biodiesel. The basicity of the catalyst increased with the increase in the Mg/Al molar ratio and degree of rehydration. They reported a 96% conversion of oil to FAME (92% yield), utilizing the rehydrated hydrotalcite under the optimal reaction conditions.

Zeng *et al.*[133] reported on Mg–Al hydrotalcite with various Mg/Al molar ratios, and used them as a heterogeneous catalyst for the transesterification of soybean oil. The hydrotalcite calcined at 773 K and 3 : 1 Mg-to-Al molar ratio exhibited the highest catalytic activity with 90.5% conversion of oil. Recently, Ma *et al.*[134] investigated a heterogeneous catalyst Mg–Al hydrotalcite in the production of biodiesel from WCO. They mentioned that the catalyst with a Mg/Al molar ratio of 3 : 1 and calcined at 500 °C has a high surface area, excellent crystallinity and mesoporous structure, and subsequently showed excellent activity. They also reported 95.2% FAME yield under the optimized reaction condition. In the same manner, Zeng *et al.*[135] prepared Mg/Al–CO_3 with a Mg/Al molar ratio of 4 : 1 *via* urea method, and compared their structures and catalytic activities with those prepared by co-precipitation for the biodiesel synthesis from microalgae oil. They studied the crystal size and surface basicity of all of the prepared hydrotalcites, and reported that the crystal size of the hydrotalcites prepared using the urea method is greater than the as-synthesized ones. They also reported that the mixed oxide of the hydrotalcite prepared *via* urea method showed the highest catalytic reactivity with the maximum conversion of 90.30%.

Furthermore, the Mg–Al hydrotalcite loaded with 1.5% K was prepared and used as a catalyst for the synthesis of biodiesel from palm oil.[136] A maximum 86.6% yield was reported using the optimized reaction conditions. They also studied the effect of the synthesized biodiesel on six types of elastomers, such as NBR, HNBR, NBR/PVC, acrylic rubber, co-polymer FKM, and terpolymer FKM, which are commonly found in the fuel system. For testing, the elastomers were immersed in B10 (10% biodiesel in diesel) and found that only terpolymer FKM and co-

Table 10 Different hydrotalcite catalyzed FAME production yields under various reaction conditions[b]

No.	Catalyst	Feedstocks	Conditions[a]	Yield (%)	Ref.
1	Mg–Al HT	Sunflower oil	48 : 1, 2, 60, 480	92	132
2	Mg–Al HT	Soybean oil	6 : 1, 1.5, 65, 240	90.5	133
3	Mg–Al HT	WCO	6 : 1, 1.5, 80, 150	95.2	134
4	Mg/Al–CO_3	Microalgae oil	6.4 : 1, 1.7, 66, 240	90.3	135
5	K/Mg–Al HT	Palm oil	30 : 1, 7, 100, 360	86.6	136
6	Zn–Al HT	Soybean oil	26 : 1, NR, 140, 60	76	137
7	KF/Ca–Al	Palm oil	12 : 1, 5, 65, 300	97.98	138
8	Mg–Al HT	Poultry fat	30 : 1, 10, 120, 120	75	139
9	Mg–Al HT	Jatropha oil	30 : 1, 5, 160, 240	93.4	140
10	$Zn_5(OH)_8(NO_3)_2\cdot 2H_2O$	Palm oil	6 : 1, 2, 140, 120	96.5	141

[a] Methanol-to-oil molar ratio, catalyst loading (wt%), temperature (°C), reaction time (min). [b] NR = not reported.

polymer FKM showed a slight change in the properties. Thus, it was concluded that B10 is compatible with the diesel engines without any modification. In another work, Liu *et al.*[137] prepared Zn–Al hydrotalcite within the temperature range of 413–773 K to form dehydrated Zn–Al hydrotalcite and Zn–Al mixed oxides, and used both catalysts in the transesterification reaction in a fixed-bed reactor. The OH groups in the dehydrated Zn–Al are responsible for the high basicity of the catalyst. However, the Mn^{+}–O^{2-} pairs and isolated O^{2-} anions are the main basic sites in the Zn–Al metal oxides. Furthermore, they compared the catalytic activity of both dehydrated Zn–Al HT and Zn–Al oxides, and found that the dehydrated HT calcined at 473 K showed the highest catalytic activity and stability towards biodiesel synthesis with a maximum yield of 76% at 140 °C for 1 h. Similarly, a heterogeneous base catalyst, KF/Ca–Al was developed for the biodiesel production from palm oil.[138] The catalyst was prepared from layered double hydroxides of Ca–Al, where the introduction of KF enhanced the catalytic activity. It was observed that 100 wt% loading of KF decreased the particle size of the catalyst, as shown by the SEM image of KF/Ca–Al (Fig. 9). The authors also reported a biodiesel yield of 97.14% under the optimized reaction conditions. Besides, biodiesel production from poultry fats was reported by using a solid base catalyst, Mg–Al hydrotalcite.[139] The influence of the calcination temperature for the preparation of the catalyst was investigated, and it was disclosed that the catalyst calcined at 550 °C showed the maximum catalytic activity. Moreover, the authors detailed that the rehydration of the catalyst before the transesterification reaction and preferential adsorption of TAGs on the surface of the catalyst reduced the catalytic activity.

Helwani *et al.*[140] synthesized a Mg–Al hydrotalcite *via* combustion method using saccharose for biodiesel synthesis from JCO. The SEM image of the catalyst calcined at 850 °C displays a lamellar microstructure with closely packed flakes (Fig. 10). The catalyst calcined at 850 °C and recrystallized with 20% saccharose fuel showed the best reactivity with 75.2% biodiesel conversion under the optimized reaction conditions. A layered double hydroxide of zinc hydroxide nitrate was also reported for FAME synthesis from palm oil.[141] The catalyst showed excellent reactivity towards the transesterification reaction with 96.5% biodiesel yield.

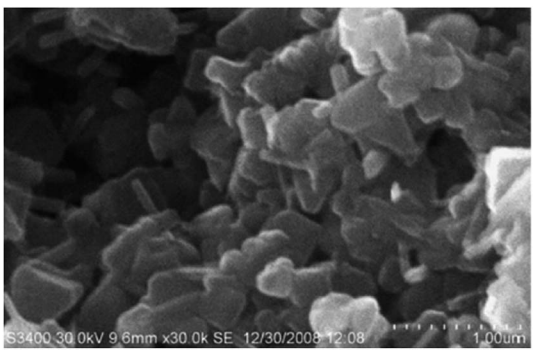

Fig. 9 SEM image of KF/Ca–Al. Reproduced from ref. 138.

7.1.6 Mixed metal oxides. Mixed metal oxides provide exceptionally fascinating properties, especially when each component differs from one another. The basic idea of synthesizing the mixed metal-oxide catalysts is to increase the basic or acid strength, surface area, and stability of these catalysts when compared with the single metal oxides. Henceforth, a series of highly efficient, reusable, and stable solid catalysts were prepared. For example, a combination of two metal oxides can show acid–base properties or some unique properties irrespective of their individual properties.[142] The basicity of the metals increases as it becomes less electronegative down the group. In the meantime, the highly basic metal oxides formed with alkaline and alkaline earth metals are usually carbonated in air, and are thus inert. Hence, the strong basicity can be achieved only after a high temperature treatment to obtain a carbonate-free metal oxide surface, making the process highly energy-demanding.[143] Interestingly, mixed metal oxides with high reactivity can be obtained at a much lower temperature, making it highly demanded in catalysis. To date, several mixed metal oxides have been reported in transesterification reactions, and are listed in Table 11.

Kawashima *et al.*[144] investigated various calcium-containing catalysts ($CaTiO_3$, $CaMnO_3$, $Ca_2Fe_2O_5$, $CaZrO_3$, and CaO–CeO_2) in the biodiesel production from rapeseed oil. Among these, CaO–CeO_2 showed excellent results (approximately 90% yield) with high stability compared to the other calcium-containing heterogeneous catalysts under the optimized reaction conditions. The catalyst can be reused for 7 times with a high yield of >80% each time. Sun *et al.*[145] also prepared a La_2O_3-loaded ZrO_2 catalyst by varying the La_2O_3 amount from 7 to 28 wt%, and investigated for the synthesis of biodiesel. The conditions of 21 wt% La_2O_3 loading on ZrO_2 and calcination at 600 °C demonstrated the highest catalytic activity towards biodiesel production from sunflower oil. The authors proposed a model for the preparation of the catalyst, where $La(NO_3)_3$ was impregnated on the surface of ZrO_2, followed by drying to form

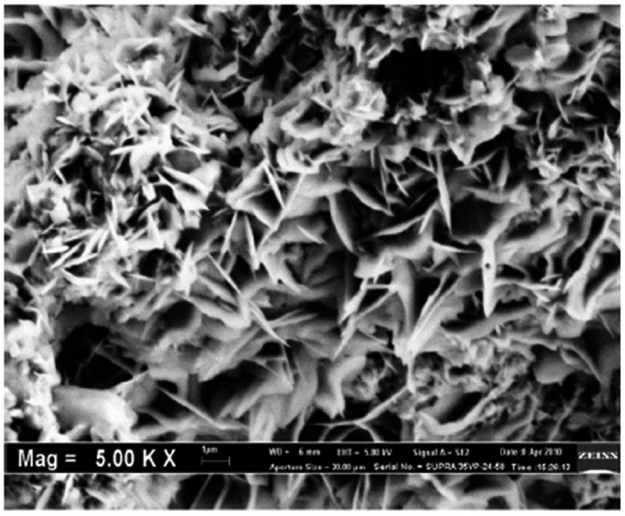

Fig. 10 SEM image of Mg–Al HT calcined at 850 °C. Reproduced from ref. 140.

Table 11 Various mixed metal oxide-catalyzed transesterification yields of vegetable oil

No.	Catalyst	Feedstocks	Conditions[a]	Yield (%)	Ref.
1	$CaO–CeO_2$	Rapeseed oil	6 : 1, 10, 60, 600	90	144
2	La_2O_3/ZrO_2	Sunflower oil	30 : 1, 21, 200, 300	84.9	145
3	TiO_2–MgO	WCO	50 : 1, 10, 160, 360	92.3	146
4	SrO/SiO_2	Olive oil	6 : 1, 5, 65, 10	95	147
5	SrO/CaO	Olive oil	6 : 1, 5, 65, 20	95	147
6	TiO_2–ZnO	Palm oil	6 : 1, 14, 60, 300	92	148
7	$ZnO–La_2O_3$	Waste oil	6 : 1, 2.3, 200, 180	96	149
8	CaO–ZnO	Palm kernel oil	30 : 1, 10, 60, 60	>94	150
9	$MgO–ZrO_2$	Soybean oil	20 : 1, 3, 150, 360	99	151
10	$ZrO_2@SiO_2$	Stearic acid	120 : 1, 10, 120, 180	48.6	152
11	SiO_2/ZrO_2 NP	Soybean oil	6.6 : 1, 2.8 mmol, 50, 180	96.2 ± 1.4	153
12	MgO–CaO	Sunflower oil	12 : 1, 2.5, 60, 60	92	154

[a] Methanol-to-oil molar ratio, Catalyst loading (wt%), temperature (°C), reaction time (min).

a film of $La(NO_3)_3$, which upon calcination forms the La_2O_3/ZrO_2 composite, resulting in a decrease in the particle size due to the *t*/*m* phase transition (Fig. 11). A high oil conversion of 96% and 84.9% FAME yield was observed under optimal reaction conditions. They reported an excellent activity of the catalyst prepared by 21 wt% loaded La_2O_3 and calcined at 600 °C.

Wen *et al.*[146] obtained the TiO_2–MgO catalyst *via* the sol–gel method, and employed it in the FAME synthesis from WCO. Substitution of Ti to the Mg lattice led to defects in the surface of the catalyst, and enhanced both the activity and stability of the catalyst. It was revealed that the catalyst with a 1 : 1 Ti to Mg molar ratio, and calcined at 923 K is the most active one in FAME synthesis. A biodiesel yield of 92.3% was observed when utilizing the catalyst MT-1-923 and the optimal reaction conditions. Similarly, SrO/SiO_2 and SrO/CaO have been synthesized, and their catalytic activity was compared with naked SrO in transesterification of olive oil by Chen *et al.*[147] Although the naked SrO showed very good catalytic activity and afforded 82% yield in just 15 min, the biodiesel yield shrank to 68.9% when the reaction was performed for 3 h. They reported that the reason for the unusual decrease in biodiesel yield was due to a reverse reaction between FAME and glycerol, which showed that the catalyst not only catalyzed the forward reaction, but also catalyzed the reverse reaction. In contrast, modification of SrO with SiO_2 and CaO provided excellent activity, as well as high stability. They observed that around 95% conversion was obtained at 65 °C using SrO/SiO_2 and SrO/CaO in 10 and 20 min, respectively. However, they reported that on decreasing the reaction temperature to 45 °C, SrO/CaO showed only 20.20% conversion as compared to SrO/SiO_2, which showed 76.9% conversion. Thus, SrO/SiO_2 displayed better reactivity towards the transesterification of olive oil than SrO/CaO, and possessed high tolerance to the water content and FFA of the biodiesel feedstocks.

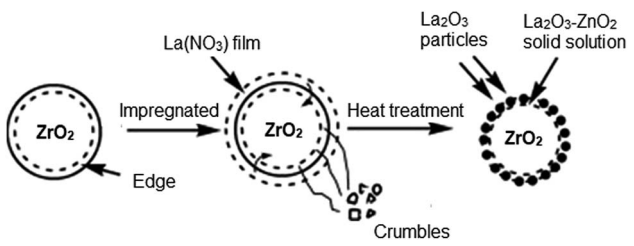

Fig. 11 Proposed model for the solid-state reaction on the catalyst surface. Reproduced from ref. 145.

In the recent past, Madhuvilakku *et al.*[148] developed a TiO_2–ZnO nanocatalyst and utilized it in the FAME synthesis from palm oil. The arrangement of deformities on the catalyst surface as a result of the substitution of Ti on the Zn grid improved the reactivity and stability of the prepared catalyst. They recorded that 92% biodiesel yield was acquired under the optimized reaction conditions. Similarly, a series of $ZnO–La_2O_3$ catalysts have been examined in the biodiesel synthesis from waste oil by Yan *et al.*[149] Incorporation of La promoted the dispersion of ZnO and improved the acidic-basic sites, thereby increasing the catalytic activity towards both transesterification and esterification reactions. The molar ratio of 3 : 1 Zn to La showed the highest activity towards biodiesel production. A high yield of 96% was reported under the optimal reaction conditions. The authors also reported that the catalyst could endure FFA and water contents, and thus allowed for the direct conversion of waste oil to FAME. In another work, the transesterification of palm kernel oil to produce biodiesel was also reported using a mixed metal oxide solid base catalyst CaO–ZnO.[150] Upon incorporation of Zn to the CaO phase, the particle size of the catalyst decreased and reduced the calcination temperature required for the decomposition of carbonates to their oxides. The lowering of the calcination temperature for the decomposition of $CaCO_3$ upon the incorporation of Zn can be explained by the particle size reduction coupled with a loss of H_2O and CO_2 from the zinc carbonate. The schematic representation for the decomposition of $CaCO_3$ and formation of CaO–ZnO mixed metal oxides is displayed in Scheme 3. It is well known that decarbonisation is a reversible process, which mostly depends on atmospheric CO_2, particle size and composition. The dissociation of CO_2 normally occurs in the outer surface (Scheme 3A). Moreover, upon calcination, the evolved CO_2 may

form a layer on the surface of the material during the continuous disjunction of inner particles, generating a possibility for recarbonation of CaO to $CaCO_3$ (Scheme 3B). However, incorporation of $ZnCO_3$ resulted in the formation of voids due to its decomposition to zinc oxide. The resulting voids facilitated heat transfer to the interior particles and evaporation of the gaseous compounds. Moreover, due to the small particle size of CaO–ZnO, the diffusion distance of CO_2 decreased, and thus the calcination temperature also decreased.

Among solid base catalysts, solid ZrO_2 catalysts became popular because of their environmentally benign nature and economic viability for biodiesel production. To date, different types of ZrO_2 catalysts have been developed for use in biodiesel production. In this line, Su *et al.*[151] synthesized microporous solid base MgO–ZrO_2 composites and utilized them as effective heterogeneous catalysts in biodiesel synthesis. They claimed that such microporous catalysts are of great significance as the presence of porous materials in the preparation of these catalysts provided the ability to interact with atoms, ions, and molecules.

Recently, Ibrahim *et al.*[152] examined the influence of different support materials like Al_2O_3, Fe_2O_3, TiO_2 and SiO_2 on the physicochemical properties and efficacy of the ZrO_2 solid catalysts commonly used in biodiesel synthesis. From the results obtained, it was revealed that ZrO_2 supported on SiO_2 showed the highest conversion rate due to a comparatively high surface area and a high number of Lewis acid sites. In another study, Faria *et al.*[153] developed a nanosized catalyst mixed metal oxides SiO_2/ZrO_2 catalyst prepared *via* sol–gel strategy, and examined its reactivity in the synthesis of biodiesel from soybean oil. It was observed that this catalyst displayed promising reactivity and gave 96.2 ± 1.4% biodiesel yield after 3 h of reaction time. In addition, the catalyst can be reused for 6 progressive cycles with little drop in activity. In 2008, Albuquerque *et al.*[154] synthesized MgO–CaO mixed metal oxides with different Mg/M (M = Al or Ca) molar ratios, and used it as a highly active catalyst for the transformation of sunflower oil to biodiesel in 92% yield under the optimized reaction conditions. The highest activity towards the transesterification reaction was found for a bulk Mg : Ca molar ratio of 3.8, whereas bare CaO was found to afford a lower yield of biodiesel under the same reaction conditions. The authors attributed this interesting activity to the higher BET surface area of the MgO–CaO mixed metal oxide (12.8 $m^2\ g^{-1}$), in comparison to CaO (1.2 $m^2\ g^{-1}$).

7.1.7 Biomass-based catalyst. In recent years, the bio-waste derived heterogeneous catalyst has gained significant attention both in the realm of catalysis and biofuel research, and has been reviewed recently by several authors.[155–160] The advantages of using waste materials as a catalyst are largely due to them being cheap, abundant, non-toxic, ecofriendly, economic, renewable, sustainable and easily available. Many researchers utilized waste biomass as a catalyst for low FFA oil (edible oil), as well as high FFA oil (edible and non-edible oils). The biomass includes plant ashes, waste shells, bones, and industrial wastes. Profitably, catalysts derived from waste biomass potentially make biodiesel production highly cost-effective and environmentally benign.

7.1.7.1 Waste shells. Although several of the chemically synthesized heterogeneous catalysts mentioned earlier show promising and comparatively high biodiesel yield, their synthesis routes are sometimes complicated, expensive, chemically wasteful, time consuming and non-economical.

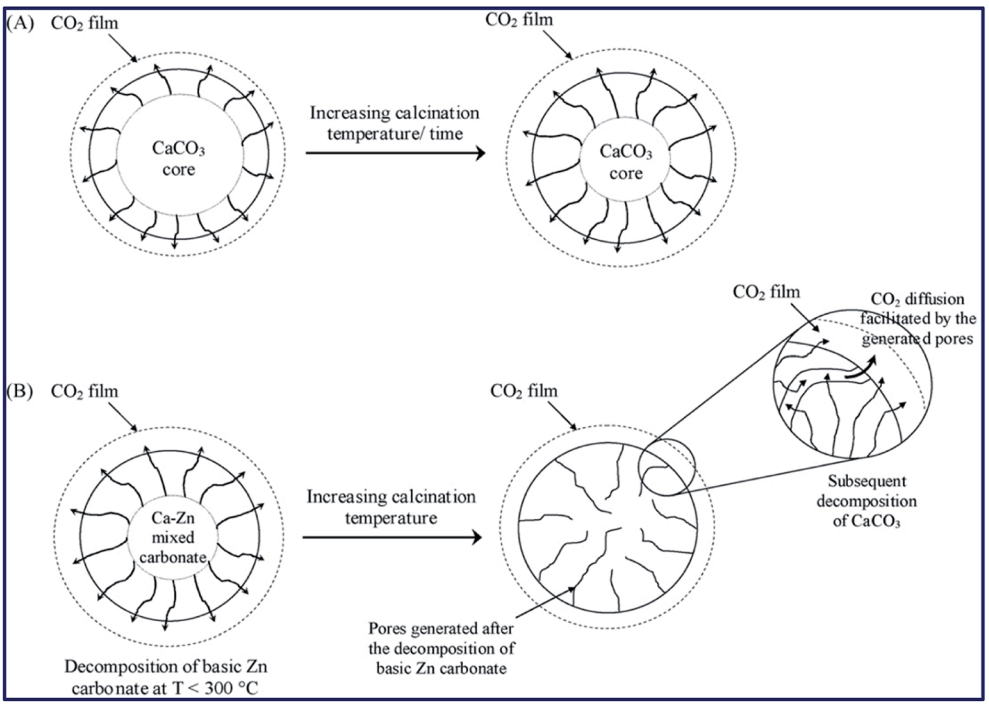

Scheme 3 Proposed models for $CaCO_3$ decomposition to CaO (A) and mixed precipitate of Ca–Zn (B). Reproduced from ref. 150.

Table 12 Various eggshells-derived solid base catalyst yields for FAME production[c]

No.	Catalyst source	Catalyst	Feedstock	Conditions[a]	Yield (%)	Ref.
1	Chicken eggshell	CaO	Soybean oil	9 : 1, 3, 65, 180	>95	161
2	Chicken eggshell	CaO	Soybean oil	10 : 1, 7, 57.5, 120	93	216
3	Chicken eggshell	CaO	Soybean oil	8 : 1, 10, 65, 180	90	163
4	Chicken eggshell	CaO	Soybean oil	14 : 1, 4, 60, 180	91	164
5	Ostrich eggshell	CaO	Karanja oil	8 : 1, 2.5, 65, 150	95	165
6	Chicken eggshell	CaO	WCO	22.5 : 1, 3.5, 65, 330	91	166
7	Chicken eggshell	CaO	WCO	12 : 1, 1.5, 65, 120	94	167
8	Chicken eggshell	CaO	WCO	4 : 1, 2, 65, 120	NR	168
9	Chicken eggshell	CaO	WFO	9 : 1, 3, 65, 180	95.05	169
10	Chicken eggshell	CaO	WCO	12 : 1, 1.5, 60, 60	96.23	191
11	Chicken eggshell	CaO	WCO	24 : 1, 4, 60, 240	100	217
12	Chicken eggshell	CaO	WCO	12 : 1, 5, 65, 60	94.52[b]	172
13	Chicken eggshell	CaO	WCO	10 : 1, 1.5, 60, 50	96.07	173
14	Chicken eggshell	CaO	WCO	6 : 1, 3, 60, 30	97.50	174
15	Chicken eggshell	CaO	WCO	9 : 1, 5, 65, 165	87.8	175
16	Chicken eggshell	CaO	WCO	15 : 1, 6, 65, 420	75.92	218
17	Chicken eggshell	CaO	Palm oil	18 : 1, 10, 60, 90	>90	176
18	Chicken eggshell	CaO	Palm oil	18 : 1, 15, 900 W, 4	96.7	177
19	Chicken eggshell	CaO	Palm oil	12 : 1, 10, 60, 120	94.1	178
20	Chicken eggshell	CaO	Palm oil	6 : 1, 5, NR, 30	95	179
21	Chicken eggshell	CaO	Rape seed oil	9 : 1, 3, 60, 180	96	180
22	Chicken eggshell	CaO	Rapeseed oil	9 : 1, 4, 60, 60	95.12	181
23	Chicken eggshell	CaO	Sunflower oil	9 : 1, 3, 60, 180	96	182
24	Chicken eggshell	CaO	Sunflower oil	11 : 1, 5, 60, 3	83.2	183
25	Chicken eggshell	CaO	Sunflower oil	9 : 1, 3, 60, 240	97.75	219
26	Chicken eggshell	CaO	Sunflower oil	12 : 1, 2, 60, 180	100	185
27	Chicken eggshell	CaO	JCO	81, 2, 65, 150	90	186
28	Chicken eggshell	CaO	Microalgae *Chlorella vulgaris*	10 : 1, 1.39, 70, 180	92.03	187
29	Chicken eggshell	CaO	Microalgae	10 : 1, 1.7, 70, 216	86.41	188
30	Chicken eggshell	CaO	Micro algae/*S. armatus*	10 : 1, 1.61, 75, 240	90.44	189
31	Chicken eggshell	CaO	Chicken fat	13 : 1, 8.5, 57.5, 300	90.41	190
32	Chicken eggshell	CaO	Catfish oil	12 : 1, 1.5, 60, 60	87.77	191
33	Chicken eggshell	CaO	*Helianthus annuus* L oil	8 : 1, 2.5, 65, 120	99.2	192
34	Chicken eggshell	CaO	Cotton oil	9 : 1, 3, 60, 180	98.08	193
35	Chicken eggshell	CaO	*C. sativa* oil	12 : 1, 1, 65, 120	97.2	194
36	Chicken eggshell	CaO	*C. inophyllum* L oil	9 : 1, 3.88, MW, 12.47	98.90	195
37	Chicken eggshell	CaO/W/Mo	WCO	15 : 1, 2, 70, 120	96.2	196
38	Chicken eggshell	CaO/anthill	WCO	6 : 1, 5, 60, 120	70	197
39	Chicken eggshell	CaO/Zn	WCO	20 : 1, 5, 65, 240	96.74	198
40	Chicken eggshell	CaO/KF/Fe_3O_4	WCO	15 : 1, 6, 65, 120	97	199
41	Chicken eggshell	CaO/SiO_2 based on PEFB	WCO	14 : 1, 8, 60, 90	96	200
42	Chicken eggshell	Mo–Zr/CaO	WCPO	15 : 1, 3, 80, 180	90.1	201
43	Chicken eggshell	ZnO/CaO	JCO	12 : 1, 5, 65, 60	98.2	164
44	Chicken eggshell	CaO NPs	JCO	6 : 1, 2, 90, 120	98	202
45	Chicken eggshell	$K_y(MgCa)_{2x}O_3$	Palm oil	16 : 1, 5.53, 65, 273	88	203
46	Chicken eggshell	CaO/SiO_2	Palm oil	15 : 1, 9, 65, 480	80.21	204
47	Chicken eggshell	CaO/SiO_2	Palm oil	15 : 1, 3, 60, 120	87.5	205
48	Chicken eggshell	CaO/Rice husk	Palm oil	9 : 1, 7, 65, 240	91.5	206
49	Chicken eggshell	CaO/Coconut waste	Palm oil	24 : 1, 5, 65, 180	81	207
50	Chicken eggshell	Li/CaO	Nahor oil	10 : 1, 5, 65, 240	94	208
51	Chicken eggshell	CaO/Zn	Eucalyptus oil	6 : 1, 5, 65, 150	93.2	209
52	Chicken eggshell	CaO/KF/Fe_3O_4	Neem oil	15 : 1, 6, 65, 120	97	199
53	Chicken eggshell	CaO/fly ash	Soybean oil	6.9 : 1, 1, 70, 300	96.97	210
54	Chicken eggshell	CaO/KF	Soybean oil	12 : 1, 2, 65, 120	99.1	211
55	Chicken eggshell	Na/CaO	*Madhuca indica* oil	9 : 1, 5, 60, 120	81.1	212
56	Ostrich eggshell	CaO	Palm oil	9 : 1, 8, 60, 60	92.7	213
57	Duck eggshell	CaO	SODD	10 : 1, 10, 60, 80	94.6	2
58	Quail eggshell	CaO	Palm oil	12 : 1, 1.5, 65, 120	98	214
59	Quail eggshell/crab shell	CaO	Jatropha oil	18 : 1, 4, MW, 5	94	215

[a] Methanol-to-oil molar ratio, catalyst loading (wt%), temperature (°C), reaction time (min). [b] Conversion. [c] NR = not reported, WCPO = waste cooking palm oil.

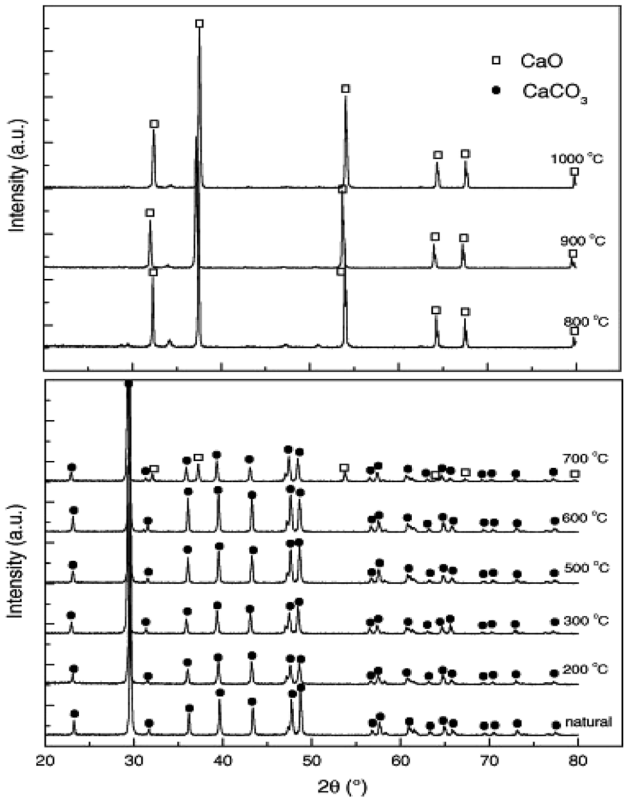

Fig. 12 XRD patterns of natural eggshell and the materials obtained by calcining natural eggshell in the range of 200–1000 °C. Reproduced from ref. 161.

Therefore, with the growing high demand for renewable energy, there is a need to search for an ideal heterogeneous catalyst that is easy to synthesize, non-toxic, low cost, widely available, biodegradable and eco-friendly in nature, yet exhibits high catalytic activity in biodiesel production. In light of this, the utilization of CaO (derived from the high-temperature calcination of waste shells containing $CaCO_3$) has been a front-runner in recent times. The use of waste shells as a source of CaO not only make the whole production of biodiesel sustainable, but also solved the problem associated with the waste disposal of huge quantities of waste shell generated due to human consumption.

7.1.7.1.1 Eggshell. Various eggshell-derived heterogeneous catalysts are available for the transformation of edible/non-edible oils to FAME, as listed in Table 12. For the first time, CaO originated from chicken eggshell calcined at 1000 °C was utilized for biodiesel synthesis by Wei *et al.*[161] Biodiesel yield greater than 95% was obtained. They calcined the eggshell at different temperatures from 200 °C to 1000 °C, and then tested their efficacy for the transformation of soybean oil to FAME. They observed that those calcined above 800 °C were the most active catalysts, where the XRD spectra display a crystalline CaO (Fig. 12). Samples calcined at 700 °C for 2 h contain $CaCO_3$ as the principal constituent and CaO as a minor one; hence, a medium yield (90%) was obtained. Calcinations below 600 °C did not result in the formation of CaO; hence, low catalytic activity was observed (<30% biodiesel yield). Hence, CaO in the catalyst is the principal basic constituent, which led to the high reactivity of the catalyst. From this experiment, it is suggested that waste shells have to be calcined at a temperature of at least 800 °C for 2 h to fully convert $CaCO_3$ to CaO, a highly basic catalyst.

In recent years, CaO derived from eggshell has been widely investigated in the transformation of various edible/non-edible oils, such as soybean oil,[162–164] karanja oil,[165] WCO,[166–175] palm oil,[176–179] rapeseed oil,[180,181] sunflower oil,[182–185] JCO,[186] micro-algae oil,[187–189] chicken fat,[190] catfish oil,[191] *Helianthus annuus* L oil,[192] cotton oil[193] and sativa oil[194] for FAME production. In 2014, Niju *et al.*[172] examined a highly active modified chicken eggshell derived CaO catalyst for the synthesis of FAME from WFO. The authors reported that highly reactive CaO can be obtained from eggshells *via* calcination–hydration–dehydration treatment. While the FAME conversion was only 67.57% for the commercial CaO catalyst, CaO obtained from the eggshell calcined at 900 °C followed by hydration and dehydration at 600 °C (eggshell-CaO-900-600) gave 94.52% conversion under the optimized reaction conditions. Calcination followed by hydration and dehydration greatly increased the surface area of the eggshell-derived CaO as compared to those obtained with the only calcination. The high activity of the modified CaO

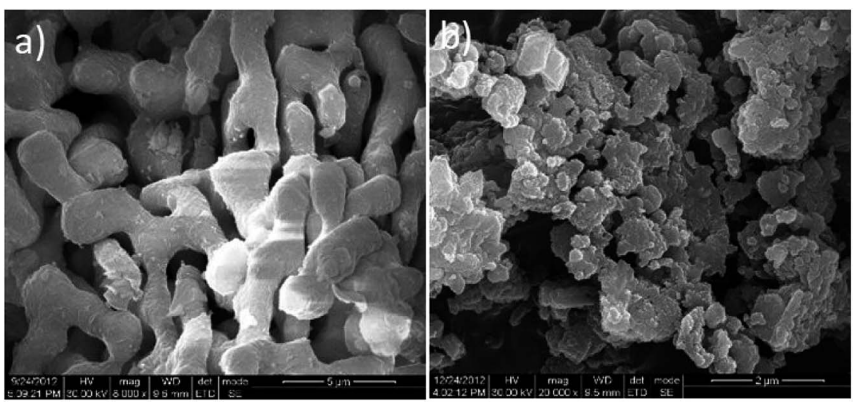

Fig. 13 SEM image of (a) eggshell-CaO-900 and (b) eggshell-CaO-900-600. Reproduced from ref. 172.

(eggshell-CaO-900-600) is attributed to the high surface area (8.6401 $m^2 g^{-1}$) compared to both commercial CaO (3.0022 $m^2 g^{-1}$) and eggshell derived-CaO calcined at 900 °C (eggshell-CaO-900) (3.7262 $m^2 g^{-1}$). The basicity of the modified catalyst lies in the region $12.2 < H_- < 15.0$. Fig. 13b depicts the SEM image of CaO generated from the calcination–hydration–dehydration treatment of eggshells (*i.e.*, egg shell-CaO-900-600), which shows a honeycomb-like porous surface. However, in the case of eggshell-CaO-900, a rod-like structure with microporous particles (size ranging from 1.29 to 2.0 μm) was observed (Fig. 13a).

In another work, waste chicken fat obtained from a slaughterhouse was converted to FAME using calcined chicken eggshell catalyst under microwave irradiation (Fig. 14).[190] Esterification was carried out to lessen the FFA content of the chicken oil below 1 mg KOH per g of oil, followed by transesterification to yield FAME. A flow diagram of the biodiesel production using chicken eggshell as a catalyst is presented in Fig. 15. Optimization of the transesterification process parameters by response surface methodology was performed.

Similarly, *Helianthus annuus* L oil was converted to FAME using eggshell-derived CaO.[192] The preparation route of CaO

Fig. 14 Microwave-assisted synthesis of FAME using an eggshell catalyst. Reproduced from ref. 190.

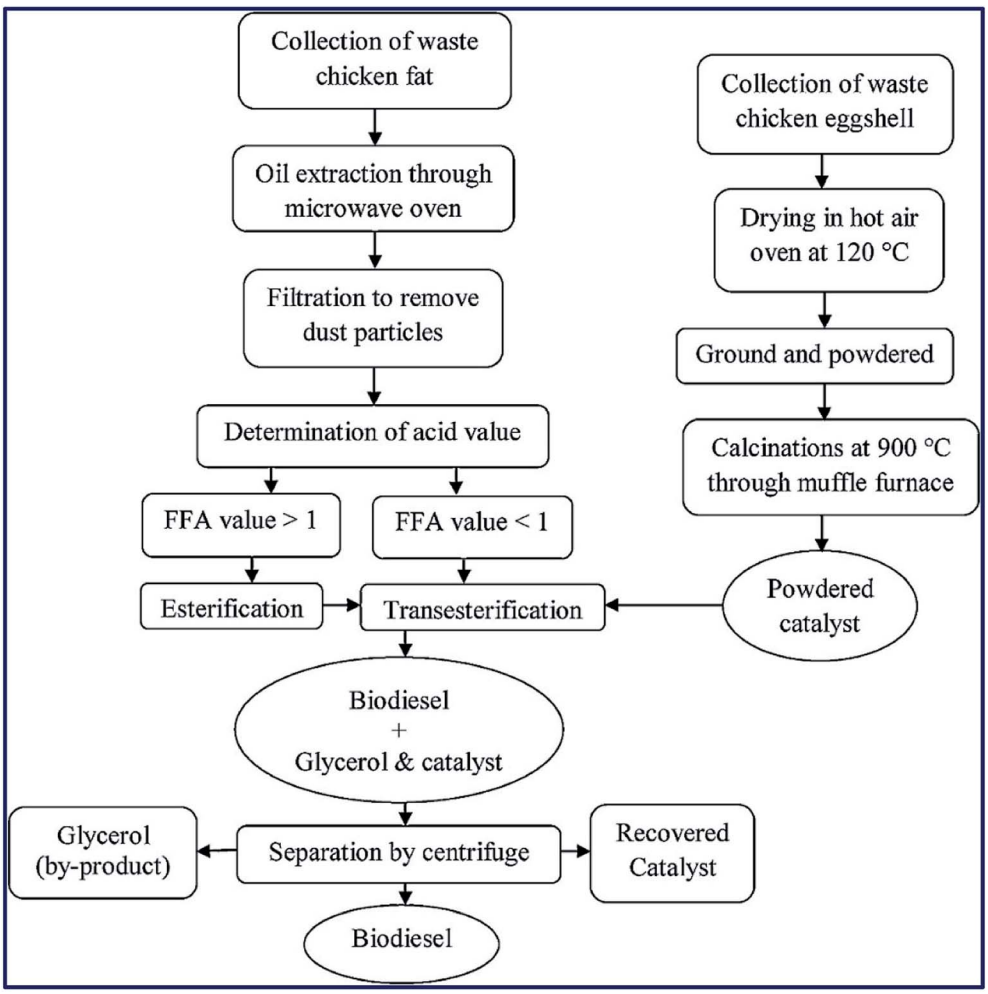

Fig. 15 Flow diagram of biodiesel production utilizing chicken eggshell catalyst. Reproduced from ref. 190.

starting from the shell is presented in Fig. 16. Under the optimized reaction conditions, 99.2% of the FAME yield was achieved. The catalyst is stable up to the fourth cycle, where 87.8% yield was observed.

Earlier, Ansori *et al.*[195] reported a chicken shell-derived CaO catalyzed synthesis of FAME from *C. inophyllum* L oil under a microwave (MW) irradiation. Initially, the oil FFA content was pre-esterified utilizing H_2SO_4, which was then transesterified by utilizing the CaO catalyst (originated from chicken shell), and they reported 98.90% FAME yield in 12.47 min. In another work, Mansir *et al.*[196] examined the application of the W/Mo/CaO catalyst, where tungsten and molybdenum were impregnated on CaO derived from waste eggshell, for the transformation of WCO *via* a concerted esterification/transesterification to produce FAME in a one-pot process. Moreover, the authors investigated the influence of W and Mo loading on CaO in its catalytic activity, and found that catalytic activity increased when the wt% of W was higher than the wt% of Mo over the range of 0.3–0.7%. A maximum yield of 96.2% was reported under the optimum reaction conditions using 0.6 W/0.4 Mo/CaO. In addition, several studies in the literature are available for the transesterification of WCO having FFA content in the range of 4–7.1% to produce the methyl ester using various eggshell-derived CaO catalysts impregnated with acidic and basic compounds. Examples of such catalysts are CaO/anthill,[197] CaO/Zn,[198] CaO/KF/Fe_3O_4,[199] CaO/SiO_2 based on palm empty fruit bunch (PEFB),[200] and Mo–Zr/CaO.[201]

In 2015, Joshi *et al.*[164] synthesized various metal oxides, for example, ZnO, MnO_2, Fe_2O_3 and Al_2O_3 impregnated on CaO derived from eggshell *via* calcination at 900 °C, and exploited these catalysts in the conversion of non-edible JCO to FAME. Among all of the mixed metal oxides, the surface area and pore volume of ZnO–CaO were highest and thus showed an excellent 95.2% JCO conversion. The authors also reported that the catalyst is very stable towards the transesterification of JCO, and can be reused for 4 cycles. Similarly, Teo *et al.*[202] synthesized CaO NPs derived from *Gallus domesticus* eggshell *via* precipitation method, and utilized it for the conversion of JCO to give FAME with 97% yield under the optimal reaction conditions.

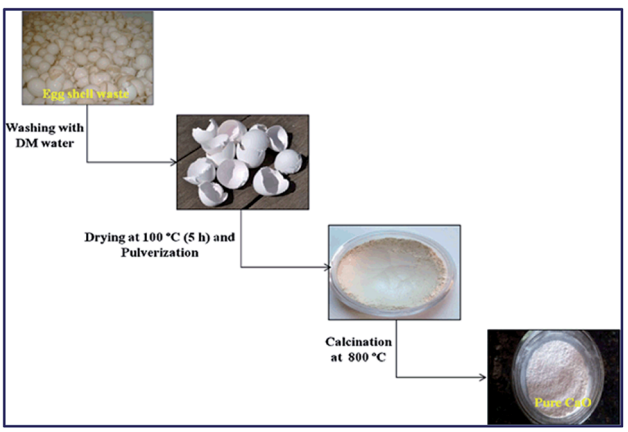

Fig. 16 Schematic layout for eggshell-originated CaO synthesis. Reproduced from ref. 192.

The TEM images and particle size distribution of the waste eggshell of *Gallus domesticus* derived nano-CaO catalyst is displayed in Fig. 17(a–c), which revealed that the particles were regular spheroidal shape and the average particle diameter is 16–27 nm. Fig. 17d displays the basicity measurement of the catalyst and commercial CaO using CO_2-TPD technique. All CaO catalysts showed a broad desorption peak owing to the existence of the strong basic strength. The desorption peaks of both catalysts observed over the temperature ranging from 550 to 700 °C are attributed to the super-basic characteristics of the nanoparticles.

In 2011, Olutoye *et al.*[203] reported a mixed metal solid catalyst, where $Mg(NO_3)_2$ and KNO_3 were impregnated on CaO originated from eggshell, and exploited it in the transformation of palm oil to FAME. The authors made three sets of a catalyst by changing the loading amount of $Mg(NO_3)_2$ and KNO_3 on CaO with wt% ratios of 6 : 1 : 1, 2 : 1 : 1 and 1 : 1.5 : 1.5, and investigated their influence on the transesterification reaction. They reported that the catalyst with wt% ratio of 6 : 1 : 1 showed the maximum yield of 85.8%. In addition, several works are reported in the literature regarding the transesterification of palm oil using chicken shell-derived CaO modified solid catalysts, such as CaO/SiO_2 (ref. 204 and 205) and CaO/rice husk.[206] Recently, Sulaiman *et al.*[207] successfully synthesized a mixture of calcined coconut waste and egg waste for the transformation of palm oil to biodiesel. The authors employed RSM based on CCD to study the ideal reaction conditions: coconut waste/eggshell waste ratio, M/O molar ratio, catalyst amount, reaction temperature and reaction time. After a successful investigation, they reported that 5 : 1 wt% ratio of coconut waste/eggshell waste showed the maximum yield of 81% under the optimal reaction conditions.

In another work, A Li-doped CaO catalyst derived from eggshell was examined for the transformation of nahor oil to produce FAME by Boro *et al.*[208] They measured the FFA content in the nahor oil and found 15 mg KOH per g. Due to this high FFA contents, a two-step process was investigated. First, an esterification was performed using sulfuric acid to bring down the FFA amount to <1, followed by transesterification reaction using the Li/CaO catalyst. They also examined the impact of Li doping on the conversion of oil to FAME, and reported a maximum 94% conversion when the Li doping was 2 wt%. Recently, Rahman *et al.*[209] modified CaO derived from chicken eggshell with transition metals, such as Zn and Cu, and applied the catalyst in the transformation of eucalyptus oil to FAME. The authors reported that the surface area and basicity of Zn/CaO are higher than the Cu/CaO, therefore Zn/CaO showed better results with 93.2% FAME yield. Moreover, the impregnation of Zn on CaO improved the stability of the catalyst and can be used for 7 consecutive cycles. In another report, a magnetically recoverable KF-modified CaO derived from eggshell was prepared and employed in the transformation of neem oil to FAME.[199] The author reported that the primary advantage of the catalyst is that the catalyst circumvented the saponification reaction. Therefore, the transesterification of neem oil (FFA content 4.2%) can proceed through the one-step process, and 94.5% FAME can be achieved.

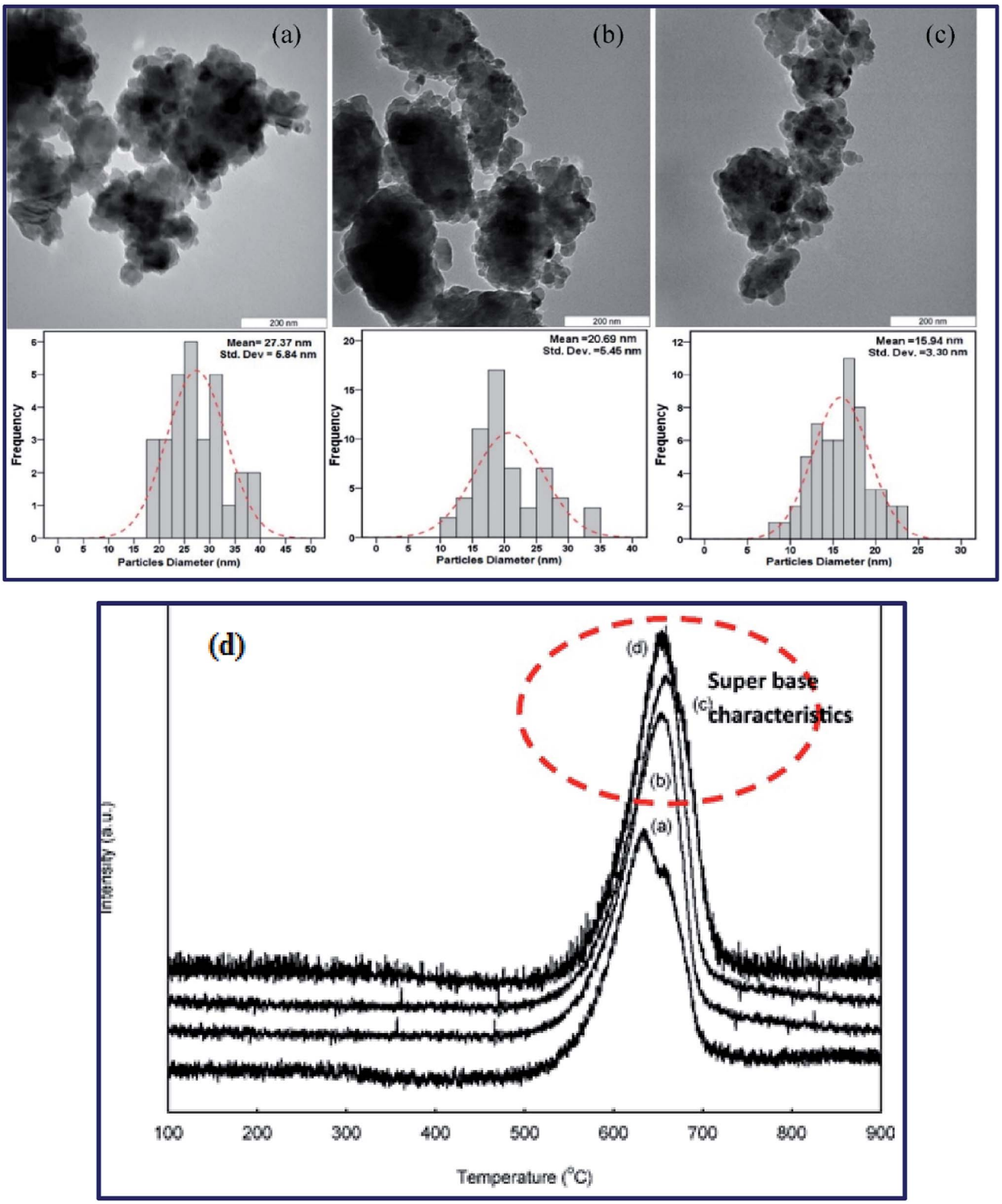

Fig. 17 TEM images and particle size distributions of the surfactant assistant CaO nanocatalysts: after 40 min (a), after 80 min (b), and after 120 min (c). CO_2 desorption performance commercial of CaO (a), and nano CaO catalysts: after 40 min (b), after 80 min (c), and after 120 min (d). Reproduced from ref. 202.

In 2010, a novel eggshell originated CaO impregnated with fly ash was reported for the transesterification of soybean oil to form FAME. The influence of CaO loading was studied by the authors, and it was found that 30 wt% CaO loading showed a maximum yield of 96.97%. Moreover, CaO supported on fly ash enhanced the catalyst reusability and reactivity compared to

the neat eggshell originated CaO.[210] In addition, a KF modified CaO originated from eggshell was examined for the transformation of soybean oil to FAME. The modified catalyst has higher basicity than the neat CaO due to the addition of KOH in the process.[211] Recently, Chowdhury *et al.*[212] synthesized a Na-doped CaO derived from chicken eggshell, and exploited it in the transesterification of *Madhuca indica* oil. A two-step process was employed as the oil has 45% of FFA content. They first esterified the oil using 5 wt% sulfuric acid to lessen the FFA content of the oil, followed by transesterification using Na-doped CaO catalyst. To study the influence of the reaction parameters on the transformation of oil to biodiesel, the Taguchi approach was used, where they observed that the M/O molar ratio and the reaction temperature have the highest impact, and the reaction time has minimal impact on the transformation of oil to FAME. In 2014, Chen *et al.*[213] demonstrated the synthesis of FAME from palm oil using CaO catalyst derived from ostrich egg-shell *via* ultrasonication. They compared the production of biodiesel using both mechanical stirring and ultrasonication process, and reported that the latter case showed higher yield (92.7%). Moreover, the catalyst can be used for 8 consecutive cycles. A transesterification process for soybean oil deodorizer distillate (SODD) to produce FAME was reported using CaO derived from the duck eggshell. They measured the FFA content of SODD and found 53.2%. Therefore, to overcome the saponification problem, the oil was pre-

Table 13 Various mollusk and seashell-derived solid catalyst yields for biodiesel production[d]

No.	Catalyst source	Catalyst	Feedstock	Conditions[a]	Yield (%)	Ref.
1	Oyster shell	CaO/KI	Soybean	10 : 1, 1 mmol g^{-1}, 50, 240	79.5	220
2	Oyster shell	CaO	Soybean oil	6 : 1, 25, 65, 300	73.8	221
3	Oyster and *Pyramidella* shells	CaO	Jatropha oil	15 : 1, 4, MW, 6	93	222
4	River snail shell	CaO	WCO	9 : 1, 3, 65, 60	92.5[b]	223
5	River snail shell	CaO	Palm oil	12 : 1, 5, 65, 90	98.5	224
6	River snail shell	CaO	Soybean oil	9 : 1, 3[c], 65, 180	98	225
7	River snail shell	CaO	WFO	6.03 : 1, 2, 60, 420	87.28	226
8	Snail shell	CaO/KBr/kaolin	Soybean oil	6 : 1, 2, 65, 120	98.5	227
9	Snail shell	CaO	Soybean oil	6 : 1, 3, RT, 420	98	228
10	Snail shell	CaO	WFO	6 : 1, 3, 60, 60	96	229
11	Snail shell	CaO	WCO	9 : 1, 9, 60, 180	84.14	230
12	Snail shell (*S. canarium*)	CaO	WCO	12 : 1, 3, 65, 240	83.5	231
13	Snail shell	Nano-CaO	*H. wightiana* oil	12.4 : 1, 0.892, 61.6, 145.154	98.93	232
14	Snail shell	CaO	*A. africana* seed oil	6 : 1, 1.5, 55, 65	85	233
15	Mussel/cockle/scallop shell	CaO	Palm oil	9 : 1, 10, 65, 180	95	234
16	Mussel shell (*Perna varidis*)	C/CaO/NaOH	Palm oil	0.5 : 1, 7.5, 65, 180	95.12	235
17	Mussel shell	CaO/KOH	Castor oil	6 : 1, 2, 60, 180	91.17	236
18	Mussel shell	CaO	Soybean oil	24 : 1, 12, 60, 480	94.1	237
19	Mussel shell	CaO	Soybean oil	9 : 1, 4, 65, 180	>98[b]	238
20	Fresh water mussel shell	CaO	Chinese tallow oil	12 : 1, 5, 70, 90	97.5	239
21	Mussel/clamp/oyster	CaO	*Camelina sativa* oil	12 : 1, 1, 65, 120	95/93/91	240
22	Angel wing shell	CaO	*N. oculata* (microalgae) oil	150 : 1, 9, 65, 60	84.11	241
23	Angel wing shell	CaO–SO_4	PFAD	15 : 1, 5, 80, 180	98[b]	242
24	Clamshell	CaO	Palm oil	9 : 1, 1, 65, 120	98	243
25	Short necked clam (*O. orbiculata*) shell	CaO	JCO	20 : 1, 4, 65, 360	93	244
26	Clamshell (*M. mereterix*)	CaO	WFO	6.03 : 1, 3, 60, 180	> 89	245
27	White bivalve clamshell	CaO	WFO	18 : 1, 8, 65, 180	95.84	246
28	Venus clam (*Tapes belcheri* S.)	CaO	Palm oil	15 : 1, 5, 65, 360	97	247
29	Abalon shell	CaO	Palm oil	9 : 1, 7, 65, 150	96.2	248
30	*T. jourdani* shell	CaO	Palm oil	3 : 1, 10, 80, 420	99.33[b]	249
31	*A. cristatum* shell	CaO	Palm oil	8 : 1, 3, 60, 360	93	250
32	Cockleshell	CaO	Palm oil	0.54 : 1, 4.9, reflux, 180	99.4	251
33	Obtuse horn shell	CaO	Palm oil	12 : 1, 5, reflux, 360	86.75	252
34	Biont (turtle) shell	CaO/KF	Rape seed oil	9 : 1, 3, 70, 180	97.5	253
35	*Turbonilla striatula* shell	CaO	Mustard oil	9 : 1, 3, 65 ± 5, 360	93.3	254
36	*Turbonilla striatula* shell	CaO/Ba	WCO	6 : 1, 1, 65, 120	> 98[b]	255
37	*Chicoreus brunneus* shell	CaO	Rice bran oil	30 : 1, 0.4, 65, 120	93	256
38	Shrimp shell	CaO/KF	Rape seed oil	9 : 1, 2.5, 65, 180	89.1[b]	257
39	*P. erosa* seashells	Nano-CaO	Jatropha oil	5.15 : 1, 0.02, RT, 133.1	95.8	258
40	Crab shell (*S. tranquebarica*)	CaO	Sunflower oil	12 : 1, 8, 95, 75	94.2	259
41	Crab shell	CaO/Na-ZSM-5	Neem oil	12 : 1, 15, 75, 360	95	260
42	Crab shell (*S. serrata*)	CaO	Palm oil	0.5 : 1, 5, 65, 150	98.8	261
43	Crab shell	CaO	Karanja oil	8 : 1, 2.5, 65, 120	94	262

[a] Methanol-to-oil molar ratio, catalyst loading (wt%), temperature (°C), reaction time (min). [b] Conversion. [c] w/w. [d] PFAD = palm fatty acid distillate.

esterified with sulfuric acid and then the transesterification was performed for the pre-esterified SODD oil using the CaO catalyst to produce FAME with an overall yield of 94.6%.[2] In addition, CaO derived from quail eggshell was utilized for the transformation of palm oil[214] and JCO[215] to biodiesel in high yield.

7.1.7.1.2. Mollusk shell and other seashells. Mollusk shell and other seashell-derived solid catalysts have been widely investigated in the transformation of edible/non-edible oils to produce biodiesel, and are listed in Table 13. Examples include a basic solid catalyst developed by the impregnation of KI on the calcined oyster shell, which was utilized in the transformation of soybean oil to FAME.[116–119] The authors reported that the impregnation and calcination increased the surface area to an extent of 32-fold, and therefore increased the catalytic activity. The main disadvantages of the catalyst are the reusability factor and higher loading of KI.[220] In addition, there are various studies in the literature, where neat CaO derived from oyster shell was utilized for the transformation of soybean oil to FAME[221] and microwave-assisted (800 W) biodiesel synthesis from jatropha oil.[222] Recently, a basic heterogeneous catalyst was developed from the river snail shell by calcination at 800 °C for 4 h. The catalyst was employed for the transesterification of WCO for biodiesel production. They performed KOH titration and found that the FFA content in the WCO is 0.3%. Therefore, direct transesterification was carried out and 98.19% yield was achieved under the optimal reaction conditions.[223] Elsewhere, other reports are also available where CaO derived from calcined river snails were used for the transesterification of various edible/non-edible oils, for example, palm oil,[224] soybean oil[225] and WFO.[226]

In 2016, Liu *et al.*[227] developed a solid catalyst, where KBr was loaded on calcined snail shell and kaoline mixture, followed by activation of the catalyst *via* calcination at 500 °C for 4 h, and applied the catalyst in the transformation of soybean oil to FAME. They also investigated the effect of the loading of KBr and the wt% ratio of the snail shell/kaoline mixture on biodiesel yield. It was found that the catalyst showed a maximum yield of 98.5% when the KBr loading and wt% ratio of the snail shell/kaoline were 40 wt% and 4 : 1, respectively. The mixing of the snail shell and kaoline together provides the catalyst with extra stability compared to their pure form.[227] In addition, Laskar *et al.*[228] developed a solid basic catalyst CaO derived from a calcined snail shell for the conversion of soybean oil to biodiesel. Under the ideal reaction states, 98% biodiesel yield was achieved. It is reported that at 400–600 °C calcination temperature, $CaCO_3$ of the snail shell was transformed to calcite. When the calcination temperature was further increased to 700 and 800 °C, a minor and major component of CaO was achieved, which was later completely transformed into CaO at 900 °C calcination temperature. Fig. 18 reveals that 100% transformation of $CaCO_3$ into CaO can be achieved above 800 °C calcination temperature.

In another work, El-Gendy *et al.*[229] reported on a CaO catalyst originated from snail shell calcined at 800 °C, and utilized it in the transesterification reaction. RSM was utilized to investigate the influence of the reaction parameters on biodiesel production, and it was reported that 96.76% yield was observed under the optimized reaction conditions. Similarly, there are various studies in the literature available for the transesterification of WCO to FAME using CaO derived from snail shell collected from different sources.[230,231] Very recently, Krishnamurthy *et al.*[232] developed a solid catalyst, CaO nanoparticles derived from snail shell *via* the hydrothermal method, and investigated its application in the transesterification of *H. wightiana* oil to produce FAME. However, a high FFA content (7.57%) in the oil led the authors to follow a two-step process: (1) pre-esterification and (2) transesterification for the production of FAME. RSM was utilized to examine the impact of reaction parameters on FAME synthesis, which resulted in 96.92% yield under the optimal reaction conditions. In a similar vein, CaO derived from snail shell was also investigated for the transformation of *A. africana* seed oil[233] and showed 85% FAME yield.

A calcined mussel/cockle/scallop shell-derived CaO was developed for the transformation of palm oil for FAME production. The authors reported on the high catalyst reactivity catalytic activity with great stability towards the transesterification of palm oil with 95% conversion.[234] In the meantime, Hadiyanto *et al.*[235] developed a solid catalyst, modified CaO (derived from green mussel shell) with activated carbon (C), followed by impregnation of NaOH, and utilized the catalyst in the transformation of palm oil. The wt% C/CaO ratio of 2 : 3 showed the maximum yield of 95.12% under the optimal reaction conditions. Similarly, KOH impregnated mussel shell derived CaO was examined for castor oil transformation to biodiesel. The authors made a comparison between the non-impregnated and KOH impregnated catalysts, and revealed

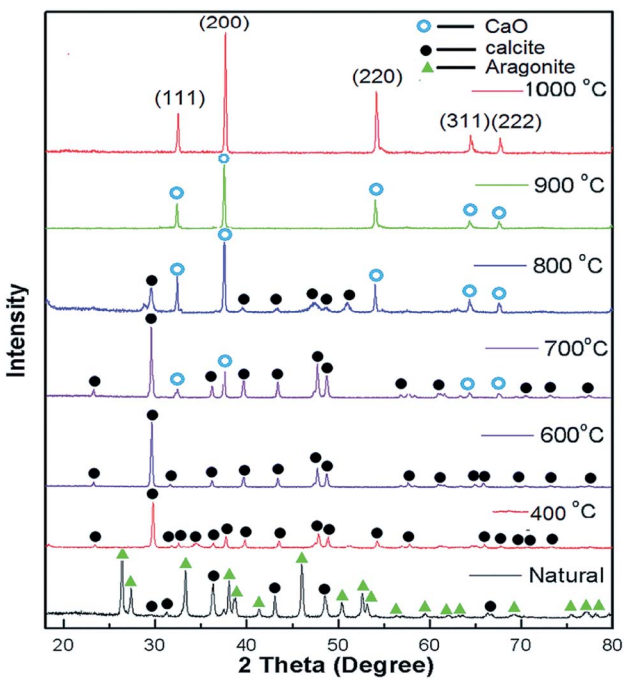

Fig. 18 XRD spectra of normal and calcined (400–1000 °C) snail shells. Reproduced from ref. 228.

that the KOH impregnated catalyst displayed higher reactivity, as well as basicity, and they reported 91.7% FAME yield using the KOH impregnated catalyst.[236] Moreover, the calcined mussel shell-derived catalysts were widely examined for the transformation of vegetable oils, for example, soybean oil,[237,238] chinese tallow oil,[239] and *Camelina sativa* oil[240] for biodiesel production.

Syazwani *et al.*[241] examined CaO, which originated from angel wing shell (AWS) and was calcined at 900 °C for 2 h, for the conversion of *N. oculata* micro-algae oil to FAME. The catalyst possessed high reactivity with great stability, and could be reused for 3 consecutive cycles. Furthermore, a bifunctional catalyst was developed for the conversion of palm fatty acid distillate (PFAD) to FAME. The angel wing shell was calcined to form CaO, followed by sulfonation to afford the catalyst. The authors reported that the catalyst surface area increased by two-fold after the modification. As a result, the catalyst showed excellent activity towards the esterification of PFAD. Unfortunately, the catalyst was reusable only for two cycles as blocking of active sites occurred in each reaction cycles. Therefore to enhance the reusability of the catalyst, pretreatment of the catalyst such as washing and re-calcination are necessary before each reaction cycles.[242] In 2015, Asikin-Mijan *et al.*[243] developed a waste clam shell-derived CaO using hydration–dehydration treatment, and investigated its catalytic application in the conversion of palm oil to FAME. They also examined the effect of the hydration–dehydration time on biodiesel conversion. The authors found that the catalytic activity increased with increasing hydration time. This was because the extended hydration enhanced the formation of $Ca(OH)_2$, increased the basicity, reduced the crystallinity, and enhanced the surface area. They reported that the rehydration for 12 h showed the maximum 98% FAME yield under optimized reaction conditions. Similarly, an investigation of the naked CaO catalyst, derived from a calcined short-necked clamshell, recorded 93% biodiesel yield under the optimal reaction conditions.[244] In addition, CaO derived from various calcined clamshell was utilized for the transformation of diverse edible/non-edible oils, for example, palm oil[245,246] and WFO,[247] to produce biodiesel.

A solid ethanol-treated catalyst CaO, derived from calcined abalone shell, was examined for the production of FAME from palm oil. The authors investigated the impact of ethanol treatment at different temperatures (RT, 100 °C and 160 °C). They found that the catalyst treated with ethanol at 100 °C showed the maximum yield of 96.2%, as the ethanol treatment provides high basicity, high surface area and lowered the catalyst crystallinity. Moreover, a comparison of the modified CaO with naked CaO showed that the modified CaO has higher reusability and provided higher biodiesel yield.[248] In addition, there are several reports available in the literature regarding the transesterification of palm oil to FAME utilizing the CaO-based solid catalyst originating from various waste shells, such as *T. jourdani* shell,[249] *A. cristatum* shell,[250] cockle shell[251] and obtuse horn shell.[252]

In 2009, Xie *et al.*[253] synthesized a solid catalyst *via* three-step process: (i) incomplete carbonization of a biont shell at 500 °C, (ii) KF impregnation and (iii) catalyst activation at 300 °C. The developed catalyst was utilized for the conversion of rapeseed oil to FAME. They reported that the catalyst displayed excellent reactivity due to the formation of a higher amount of active sites during the reaction between the incomplete carbonized shell and KF. The effect of KF loading was also examined, and it was found that 25% KF loading is optimal and showed 97% FAME yield under the optimized reaction conditions. Correspondingly, Boro *et al.*[254] demonstrated the synthesis of the CaO catalyst by calcination of *Turbonilla striatula* shell, and utilized it for the transformation of mustard oil to FAME. The effect of the calcination temperature was examined, and it was observed that the catalyst calcined at 900 °C displayed the maximum 93.3% FAME yield. In addition, CaO derived from calcined *Turbonilla striatula* was modified with Ba in the range of 0.5–1.5 wt%. It was utilized for the transformation of WCO to biodiesel. Due to the high acid value of 22 mg KOH per g, the oil was pretreated with sulfuric acid to reduce the acid value to <1. Then, the pretreated oil was transesterified with Ba/CaO catalyst. The authors also examined the effect of Ba loading and found that 1% of Ba doping showed >98% biodiesel yield.[255] In addition, *Chicoreus brunneus* shell was calcined above 800 °C to convert $CaCO_3$ to CaO, followed by hydration/dehydration to form a solid base catalyst. It was then examined for the transformation of rice bran oil. Calcination and hydration provided the catalyst with high porosity, enhancing the basicity, catalytic activity and reusability.[256] In addition, shrimp shell originated catalysts have been utilized for the transformation of various edible/non-edible oils to FAME. Yang *et al.*[257] synthesized a catalyst *via* a three-step process; (i) inadequate carbonization of shrimp shell, (ii) reaction with KF, and (iii) activation of the catalyst under the heating condition for the rapeseed oil transformation. The authors examined the impact of the carbonization temperature, KF amount and activation temperature. They found that 89.1% biodiesel was achieved under the reaction states: carbonization temperature of 450 °C, KF amount of 25 wt%, and an activation temperature of 250 °C. The excellent catalyst reactivity is attributable to the formation of active sites during the reaction between the incomplete carbonized shrimp shell and KF. Moreover, a solid catalyst, CaO nanoparticles with a diameter of 66 nm derived from *Polymedosa erosa* shell *via* calcination–hydration–dehydration process was developed for the transformation of JCO to FAME in a two-step procedure: (1) pre-esterification and (2) transesterification. The influence of the reaction parameters on the oil conversion was examined by RSM technique, and displayed 98.54% FAME yield.[258]

In the recent past, Sivakumar *et al.*[259] developed a solid catalyst derived from *Scylla tranquebarica* crab shell calcined at 750 °C for sunflower oil transformation to FAME. The developed catalyst displayed similar reactivity to that of commercial CaO, and reported a very high conversion of 94.2% under the optimal reaction conditions. Similarly, Shankar *et al.*[260] prepared a solid catalyst, where CaO (derived from crab shell calcined at 900 °C) was impregnated on Na-ZSM-5 followed by activation at 550 °C for 10 h. It was utilized for the production of FAME from neem oil. The impact of CaO loading was examined, and it was found that 15 wt% CaO impregnation showed a maximum 95% biodiesel

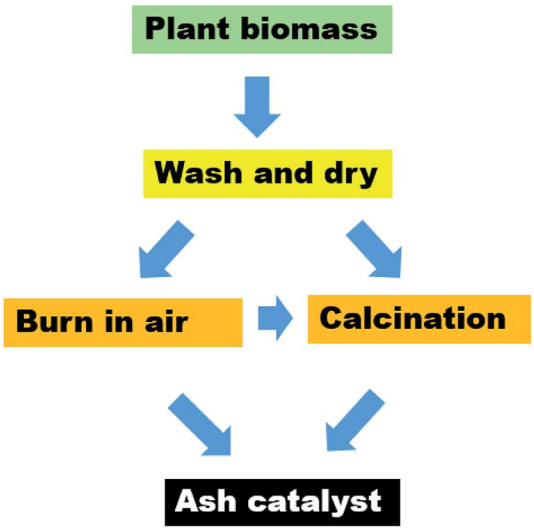

Fig. 19 Flowchart for the synthesis of ash catalyst derived from plant biomass.

formation. Moreover, various reports are available for the transesterification of edible/non-edible oils, such as palm oil[261] and karanja oil,[262] utilizing CaO originated from calcined crab shells.

7.1.7.2 Ashes of biomass. In recent years, the application of waste plant ashes as a highly active heterogeneous catalyst has drawn increasing attention in the realm of biodiesel production. A huge amount of alkali or alkaline earth elements, mostly K, Ca and Mg present in the ashes of waste plant biomass, acted as a highly basic catalyst in the transesterification reaction to produce biodiesel from vegetable oil with low FFA. In the case of vegetable oil with high FFA, a reduction of FFA to <1% (by acid-catalyzed esterification) before the transesterification reaction is mandatory to elude catalyst consumption in soap formation, which otherwise leads to low biodiesel yield. Usually, the biomass is collected, washed and dried either in oven or sunlight, burnt in the open air or burnt in the air. This is followed by calcination to produce a highly basic ash catalyst, as shown in Fig. 19. Different basic ash catalysts were utilized, and their efficacy in the synthesis of biodiesel is presented in Table 14. In a pioneering work, Chouhan *et al.*[263] reported the use of amphibian plant *L. perpusilla* Torrey ash as a solid catalyst in biodiesel synthesis from JCO. The plant biomass was subjected to calcination at 550 ± 5 °C for 2 h to obtain the ash catalyst. The crystallinity of the catalyst was affirmed by XRD patterns. The impact of catalyst loading revealed that 5 wt% (w.r.t. oil) is enough to obtain a high 89.43% biodiesel yield under the optimal reaction conditions. Nevertheless, the reusability study

Table 14 Different plant ash catalyst yields in biodiesel production

No.	Catalyst source	Feedstock	Conditions[a]	Yield (%)	Ref.
1	*L. perpusilla* Torrey	JCO	9 : 1, 5, 65 ± 5, 300	89.43	263
2	Oil palm ash	WCO	18 : 0, 5.35, 60, 30	71.74	264
3	Oil palm ash/boiler ash (BA)	Palm olein	15 : 1, 3, 60, 30	90	265
4	*Musa paradisiaca* L. (plantain) peels	*Thevetia peruviana* oil	3.3 : 1, 3, 60, 60	95.2	266
5	Ripe plantain fruit peel	*Azadirachta indica* oil	1 : 0.73, 0.65, 65, 57	99.2	267
6	Coconut husk	JCO	12 : 1, 7, 45, 30 min	99.86	268
7	Cocoa pod husks	Soybean oil	6 : 1, 1, 60, 60/120	98.7/91.4	269
8	*Musa balbisiana* Colla peel	*Thevetia peruviana* seed oil	20 : 1[c], 20, RT, 180	96[b]	270
9	*Musa balbisiana* Colla underground stem	JCO	9 : 1, 5, 275, 60	98	271
10	Musa 'Gross Michel' peel	Napoleon's plume seed oil	7.6 : 1, 2.75, 65, 69.02	98.5	272
11	Rubber seed shell	Rubber seed oil	0.20 : 1[d], 2.2, 60, 60	83.06	273
12	*Musa balbisiana* Colla peel	WCO	6 : 1, 2, 60, 180	100[b]	274
13	*M. acuminata* peel	Soybean	6 : 1, 7, RT, 240	98.95	275
14	Wood (*Acacia nilotica*) stem	JCO	12 : 1, 5, 65, 180	98.7[b]	276
15	Birch bark/fly ash	Palm oil	12 : 1, 3, 60, 180	88.06 ± 0.72/99.92 ± 0.01	277
16	Musa spp "Pisang Awak" peduncle	*Ceiba pentandra* oil	9.20 : 1, 1.978, 65, 60	98.69 ± 0.18	278
17	*Musa acuminata* peduncle	*Ceiba pentandra* oil	11.46 : 1, 2.68, 65, 106	98.73 ± 0.50[b]	279
18	*Theobroma grandiflorum* seeds	Soybean oil	10 : 1, 10, 80, 480	98.36[b]	280
19	*Brassica nigra* plant	Soybean oil	12 : 1, 7, 65, 25	98.79	281
20	Kola nut pod husk	Kariya seed oil (KSO)	6 : 1, 3, 65, 75	98.67 ± 0.01	156
21	Orange peel	Soybean oil	6 : 1, 7, RT, 420	98[b]	282
22	*Sesamum indicum* plant	Sunflower oil	12 : 1, 7, 65, 40	98.9	283
23	Tucumã peels	Soybean oil	15 : 1, 1, 80, 240	97.3[b]	284
24	*Tectona grandis* leaves	WCO	6 : 1, 2.5, RT, 180	100[b]	285
25	Cocoa pod husk	*Azadirachta indica* oil	0.73 : 1[d], 0.65, 65, 57	99.3	286
26	Walnut shell	Soybean oil	12 : 1, 5, 60, 10	98	287
27	Sugar beet waste	Sunflower oil	4.5 : 1, 1, 75, 60	93[b]	288
28	*M. acuminata* trunk	Soybean oil	6 : 1, 14, RT, 360	98.39[b]	289
29	Banana peel/cocoa pod husk	Palm kernel oil	0.80 : 1[d], 4, 65, 65	99.5/99.3	290
30	*Carica papaya* stem	*Scenedesmus obliquus*	9 : 1, 2, 60, 180	93.33[b]	291
31	*Musa balbisiana* underground stem	*Mesua ferrea* oil	9 : 1, 5, 60, 275	95[b]	292

[a] Methanol-to-oil molar ratio, catalyst loading (wt%), temperature (°C), reaction time (min). [b] Conversion. [c] mL g^{-1}. [d] v/v.

demonstrated that the catalyst lost its reactivity in each progressive reaction cycle, owing to leaching of the reactive elements in the catalyst. Thereby, the catalyst was recycled up to 3 cycles only.

In another work, oil palm ash was seen as an active catalyst for biodiesel synthesis from WCO by Chin *et al.*[264] Fig. 20 depicts the SEM micrograph of the palm ash, which displayed the porous nature of the ash catalyst, while Table 15 lists the elements existing in the palm ash determined from the EDX analysis. It was observed that the palm ash consisted of a large amount of potassium, while a relatively low quantity of aluminum, zinc, and magnesium was also found. Besides, it was seen that K_2O was the primary driver for the high basicity and catalytic activity of the catalyst towards biodiesel synthesis. CCD was utilized to investigate the impact of the optimized reaction conditions in biodiesel synthesis, such as M/O ratio, reaction time, temperature and catalyst loading. Accordingly, the predicted and experimental biodiesel yields were found to be 60.07% and 71.74%, respectively.

In the meantime, Boey *et al.*[265] reported on a solid base, derived from boiler ash (BA) *via* calcination, that catalyzed biodiesel synthesis from palm oil. BA effectively transformed palm oil to FAME at moderate reaction conditions and delivered 90% FAME yield. Ironically, the ash is intolerant of the presence of moisture and FFA at 1 wt% in the feedstock. Betiku *et al.*[266] reported a process for biodiesel synthesis from *Thevetia peruviana* oil by utilizing calcined *Musa paradisiaca* L. (plantain) peel ash catalyst. The dried powdered plantain peels were calcined at 500 °C for 3.5 h to produce plantain peels ash. A biodiesel yield of 95.2% was acquired using the optimized reaction conditions. In addition, Etim *et al.*[267] utilized ripe plantain fruit peel as a solid catalyst in biodiesel synthesis from *Azadirachta indica* oil. At the onset, pre-esterification of the oil was performed to diminish the FFA contents from 5.81 wt% to 0.90 wt%, utilizing a M/O molar ratio of 2.19 v/v and 6 wt% of $Fe_2(SO_4)_3$. Finally, the pre-esterified oil was transformed to FAME *via* transesterification reaction catalyzed by plantain fruit peel ash. Coconut husk ash catalyst was also reported for biodiesel synthesis from JCO.[268] The husks were subjected to calcination at various temperatures ranging from 250–500 °C. It was identified that the catalyst produced at 350 °C calcination temperature was found to be the most reactive one for biodiesel synthesis, giving 99.86% yield within 30 min at the moderate reaction temperature. XRD patterns of the catalysts are presented in Fig. 21, which revealed the presence of several components of ash, such as KCl, $K_2Si_2O_5$, K_2SO_4, K_2S_3, $KAlO_2$, $K_4CaSi_3O_9$, and $FeCa_2Al_2BSi_4O_{15}OH$.

Table 15 EDX data for compositions of palm ash by Ref. 264

Elements	Atomic wt%
Potassium (K)	40.59
Magnesium (Mg)	0.76
Silicone (Si)	2.63
Aluminum (Al)	0.50
Zinc (Zn)	0.33
Oxygen (O)	29.36
Carbon (C)	14.56
Chlorine (Cl)	7.07

Cocoa pod husks (CPHs) were used as a solid catalyst for biodiesel synthesis from soybean oil by Ofori-Boateng *et al.*[269] The authors examined the reactivity of MgO impregnated CPH (MgO@CPH) and bare CPH in biodiesel synthesis under the optimal reaction states, and achieved 98.7% and 91.4% biodiesel yields, respectively. Moreover, the synthesized fuel satisfies the European biodiesel quality norm (EN 14112). In another study, the production of biodiesel from yellow oleander (*Thevetia peruviana*) seed oil using banana (*Musa balbisiana* Colla) peel ash was reported.[270] The K, Na, CO_3, and Cl present in the ash are responsible for the high basicity, and thus the reactivity of the catalyst. Oil transformation of 96% was demonstrated in just 3 h time under room temperature. The produced biodiesel conforms to standards set for ASTM D6751, EN 14214 and others. The BET surface area measurement of the catalyst revealed that the surface area is 1.487 $m^2\ g^{-1}$. The biodiesel was free from sulfur, and has displayed a high cetane number. Meanwhile, *Musa balbisiana* Colla underground stem (MBCUS) ash was examined as a solid base catalyst for biodiesel synthesis from high FFA containing JCO by Sarma *et al.*[271] Characterization of the ash catalyst revealed that it is composed of oxides and carbonates of various alkali and alkaline earth metals, which leads to the high basicity of the catalyst, and the surface area is 39 $m^2\ g^{-1}$. It was reported that the catalyst is very effective during the biodiesel synthesis process at 275 °C and internal pressure (4.2 MPa), and resulted in 98.0% biodiesel yield.

Betiku *et al.*[272] led an investigation on the application of banana (*Musa* 'Gross Michel') peel waste as a catalyst for biodiesel synthesis from *Bauhinia monandra* (Napoleon's plume) seed oil (BMSO), with a motive to develop a low-cost fuel. The burnt ash of the banana peel was further calcined at 700 °C for 4 h to produce a highly active catalyst. They utilized the RSM model to determine the optimal reaction conditions for biodiesel synthesis using the ash catalyst. The RSM plot of the M/O molar ratio and catalyst loading on *Bauhinia monandra* (Napoleon's plume) methyl ester (BMME) yield is shown in Fig. 22a. It

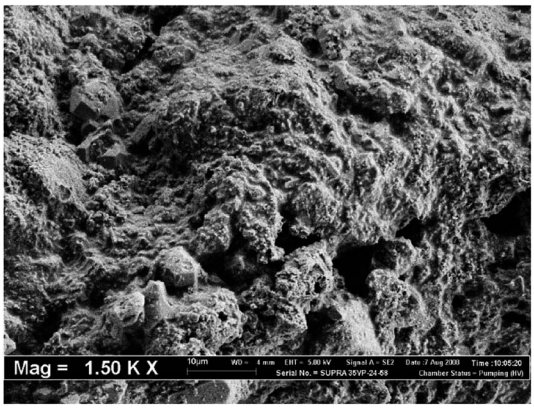

Fig. 20 SEM micrograph of palm ash. Reproduced from ref. 264.

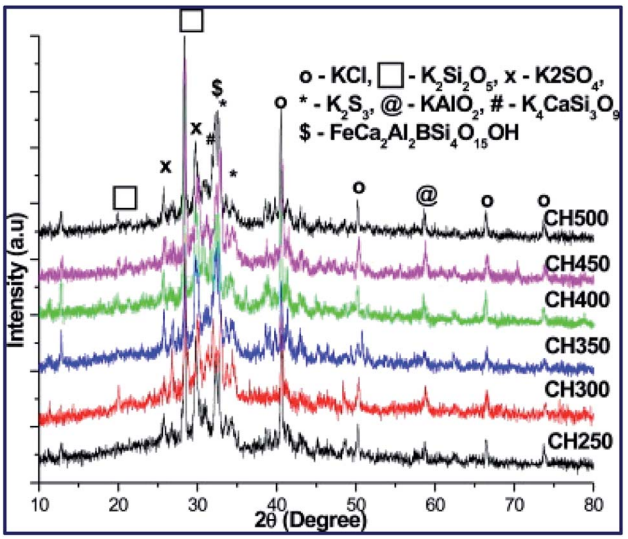

Fig. 21 XRD patterns of calcined coconut husk calcined at different temperatures. Reproduced from ref. 268.

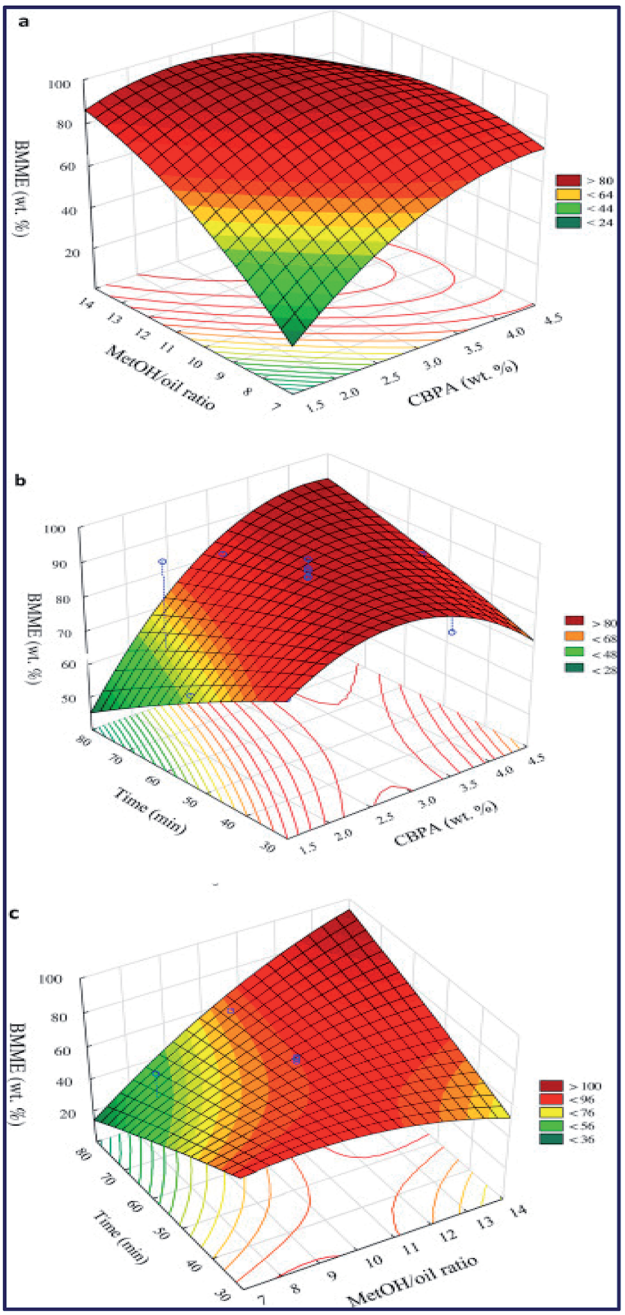

Fig. 22 3-D plots of biodiesel yield. (a) Impact of M/O molar ratio and catalyst loading, (b) reaction time and catalyst loading, and (c) M/O molar ratio and reaction time on the biodiesel yield. Reproduced from ref. 272.

was observed that the BMME yield improved from 0 to >90 wt% as the M/O molar ratio expanded from 7 : 1 to 14 : 1, and the catalyst loading increased from 1.5 to 3.5 wt%. This might be ascribed to the increase in the active site number as a result of the increased catalyst loading. Besides, the BMME yield diminished marginally when the catalyst loading was above 3.5 wt% (Fig. 22a). In addition, the plot revealed a direct connection between the M/O molar ratio and catalyst loading on the biodiesel yield. As the two parameters increased, the biodiesel yield also increased (Fig. 22a). The transformation of the pre-esterified oil to biodiesel was done inside the time span of 33.79–76.21 min. The extended reaction time, somewhere in the range of 33.79 and 55 min, favoured biodiesel yield. After 55 min, the yield diminished. Fig. 22b displays the impact of the reaction time and catalyst loading on the biodiesel yield. It was observed from the surface plot that the rise in catalyst loading and reaction time led to an increase in the biodiesel yield. Moreover, the plot displayed that 90 wt% biodiesel yield was reached using 4.5 wt% catalyst loading within 80 min reaction time. In addition, Fig. 22c illustrates the surface plot to examine the impact of the M/O molar ratio and reaction time on the biodiesel yield. It was observed from the plot that the increases in two parameters, such as the M/O molar ratio and reaction time, led to a rise in the biodiesel yield. It can be seen from the figure that the increases in M/O molar ratio from 7 : 1 to 14 : 1 improved the biodiesel yield from 33% to 100%. Therefore, the highest biodiesel yield was recorded at 14 : 1 M/O molar ratio and 80 min reaction time.

Meanwhile, Onoji *et al.*[273] built up a novel technique to utilize rubber seed shell (RSS) ash calcined at 800 °C as a solid base catalyst for the transformation of rubber seed oil to biodiesel. The high FFA content of the RSS (9.01 ± 0.07%) was pre-esterified using H_2SO_4 to >1% FFA. The reusability study of the catalyst revealed that >80% biodiesel yield was noticed after 4 successive reaction cycles. The surface area and pore size of the calcined RSS was found to be 2.29 nm and 352.51 $m^2\ g^{-1}$, respectively. Similarly, Gohain *et al.*[274] studied the application of the *Musa balbisiana* Colla peel ash catalyst to produce biodiesel from WCO. It was observed that the calcination procedure improved the mesoporous and microporous morphology of the catalyst, and upgraded its surface area, bringing about the higher catalytic activity. The external morphology of the catalyst examined by SEM analysis revealed aggregation of the particles, and porosity in the range of micro and meso. Moreover, 100%

conversion of WCO to biodiesel was confirmed by ^{1}H NMR spectra (Fig. 23b), utilizing the Knothe and Kenar eqn (1). The ^{1}H NMR spectrum of WCO (Fig. 23a) displays two peaks at 4.1 and 5.3 ppm because of the glyceridic protons (Fig. 23a). The presence of a peak of the methoxy protons at ~3.6 ppm and the vanishing of the signs of the glyceridic peak close to 4–4.2 ppm (Fig. 23b) confirmed the formation of biodiesel.

In recent year, Pathak *et al.*[275] utilized the *Musa acuminata* peel ash (MAPA) catalyst for biodiesel synthesis from soybean oil at room temperature. The catalyst characterization reported the existence of various alkali and alkaline earth metals that enhance the catalyst basicity and reactivity of the ash catalyst. K (14.27%), C (47.51%) and O (30.27%) are the primary/main elements that exist in MAPA, as revealed by the XPS data (Fig. 24). The authors reported 98.95% biodiesel yield under the optimized reaction conditions.

Sharma *et al.*[276] investigated the reactivity of wood ash catalyst calcined at different temperatures for biodiesel synthesis from JCO. Ester conversion in the range of 97–99% could be achieved with wood ash catalysts. Wood ash calcined at 800 °C afforded 98.7% oil conversion under the ideal reaction conditions. Uprety *et al.*[277] studied the application of wood ash derived from birch bark and fly ash blazed at 800 °C for 4 h synthesis of biodiesel from palm oil. Birch bark ash gave a FAME yield of 88.06 ± 0.72, whereas fly ash from wood pellet afforded 99.92 ± 0.01% yield. Recently, the application of banana peduncle ash as an efficient solid base catalyst for the synthesis of biodiesel from *Ceiba pentandra* oil (CPO) was investigated.[278] Based on the response surface methodology (RSM) study, the ideal reaction conditions for the transformation of CPO into FAME was found to be 1.978 wt% catalyst loading, 60 min response time, 9.20 : 1 M/O molar ratio with a maximum predicted FAME yield of 99.36%, which was assessed experimentally as 98.69 ± 0.18%. The same research team also investigated the utilization of *Musa acuminata* peduncle for biodiesel preparation from CPO.[279] The authors calculated the surface area and pore diameter of the calcined ash catalyst from BET analysis data, and reported 45.99 m^2 g^{-1}

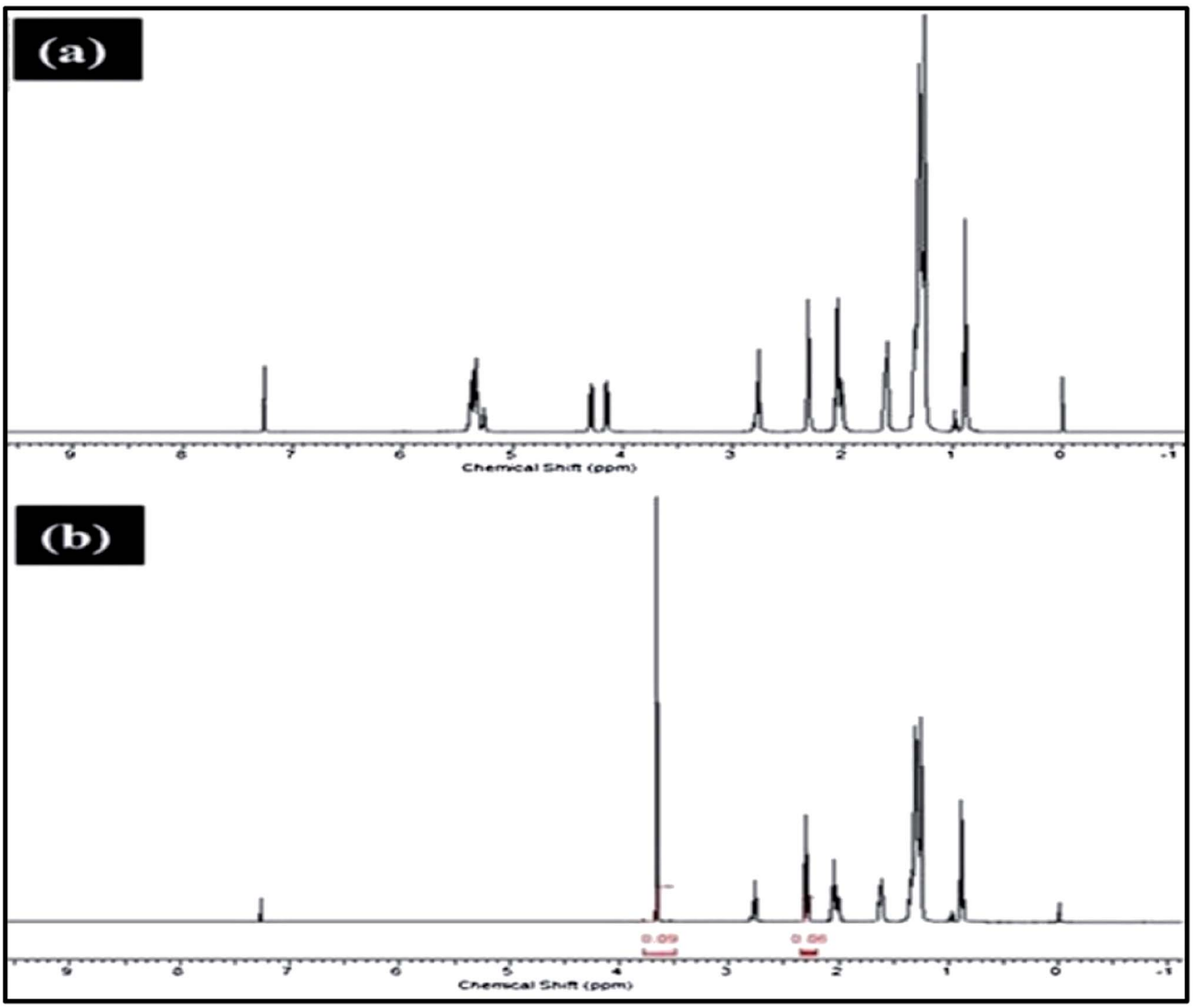

Fig. 23 ^{1}H NMR spectrum of (a) WCO and (b) Biodiesel. Reproduced from ref. 274.

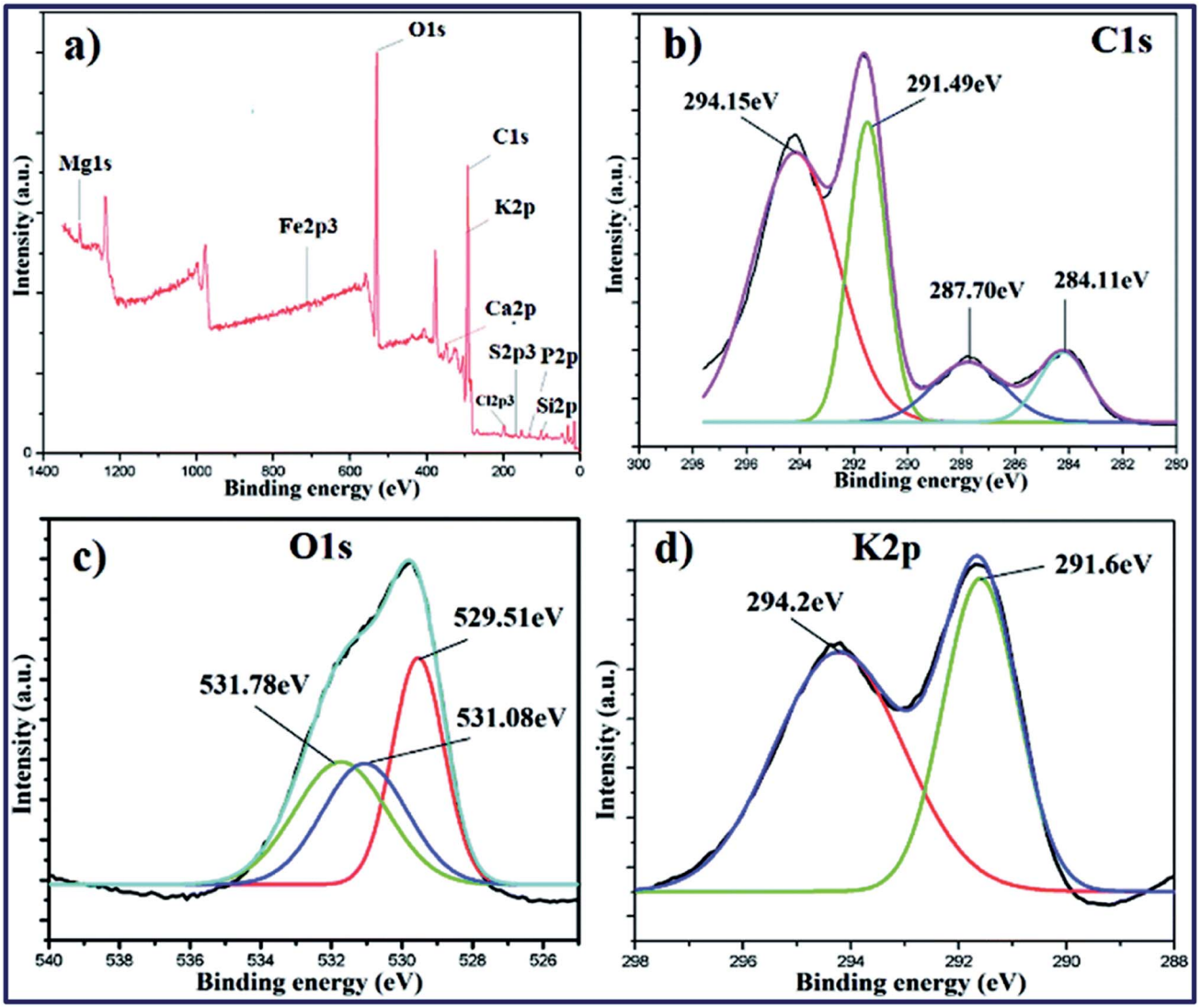

Fig. 24 XPS survey (a), C 1s (b), O 1s (c), and K 2p (d) spectra of MAPA. Reproduced from ref. 275.

and 9.77 nm, respectively. Moreover, the catalyst consists of diverse minerals (along with potassium) as primary components, which leads to the higher reactivity of the catalyst (Fig. 25). A high conversion of 98.73 ± 0.50% FAME was observed under the optimum reaction conditions.

In 2019, Mendonça *et al.*[280] reported the utilization of calcined (800 °C for 4 h) waste cupuaçu seeds as a solid base catalyst in the synthesis of biodiesel from soybean oil and ethanol. Similarly, Nath *et al.*[281] utilized a solid base catalyst derived from waste *Brassica nigra* plant for the efficient preparation of biodiesel. The SEM-EDX analysis of the catalyst revealed the existence of potassium (56.13%) and calcium (26.04%) in a huge amount, which may be considered as key ingredients for the high basicity of the catalyst. The authors also measured the surface area pore volume of the catalyst *via* BET analysis, and came about 7.308 $m^2\ g^{-1}$ and 0.011 $cm^3\ g^{-1}$, respectively. The catalyst possessed excellent reactivity in transforming the soybean oil to FAME and displayed 98.79% FAME yield in a short time frame of 25 min under the optimum states. Betiku *et al.*[156] prepared an ash catalyst from kola nut pod husk and used it to convert Kariya seed oil (KSO) to biodiesel, namely Kariya oil methyl esters (KOME), *via* transesterification process. A maximum of 98.67 ± 0.01 wt% of FAME yield was observed. Moreover, the reusability examination of the catalyst suggests that it can be reused for 4 progressive cycles. Recently, Changmai *et al.*[282] converted soybean oil to biodiesel using orange peel ash in 98% yield. XRF analysis showed the presence of potassium oxide (51.64%) and calcium. The Hammet indicator strategy was employed to examine the catalyst basicity, and it was seen as $9.8 < H_- < 12.2$. The authors measured the catalyst pore volume and surface area from BET analysis, and found 0.428 $cm^3\ g^{-1}$ and 605.60 $m^2\ g^{-1}$, respectively. Moreover, GC-MS analysis (Fig. 26) revealed the existence of six components in the synthesized FAME; methyl palmitate (11.63%), methyl oleate (25.32%) and methyl linoleate (54.34%) were found to be the major components.

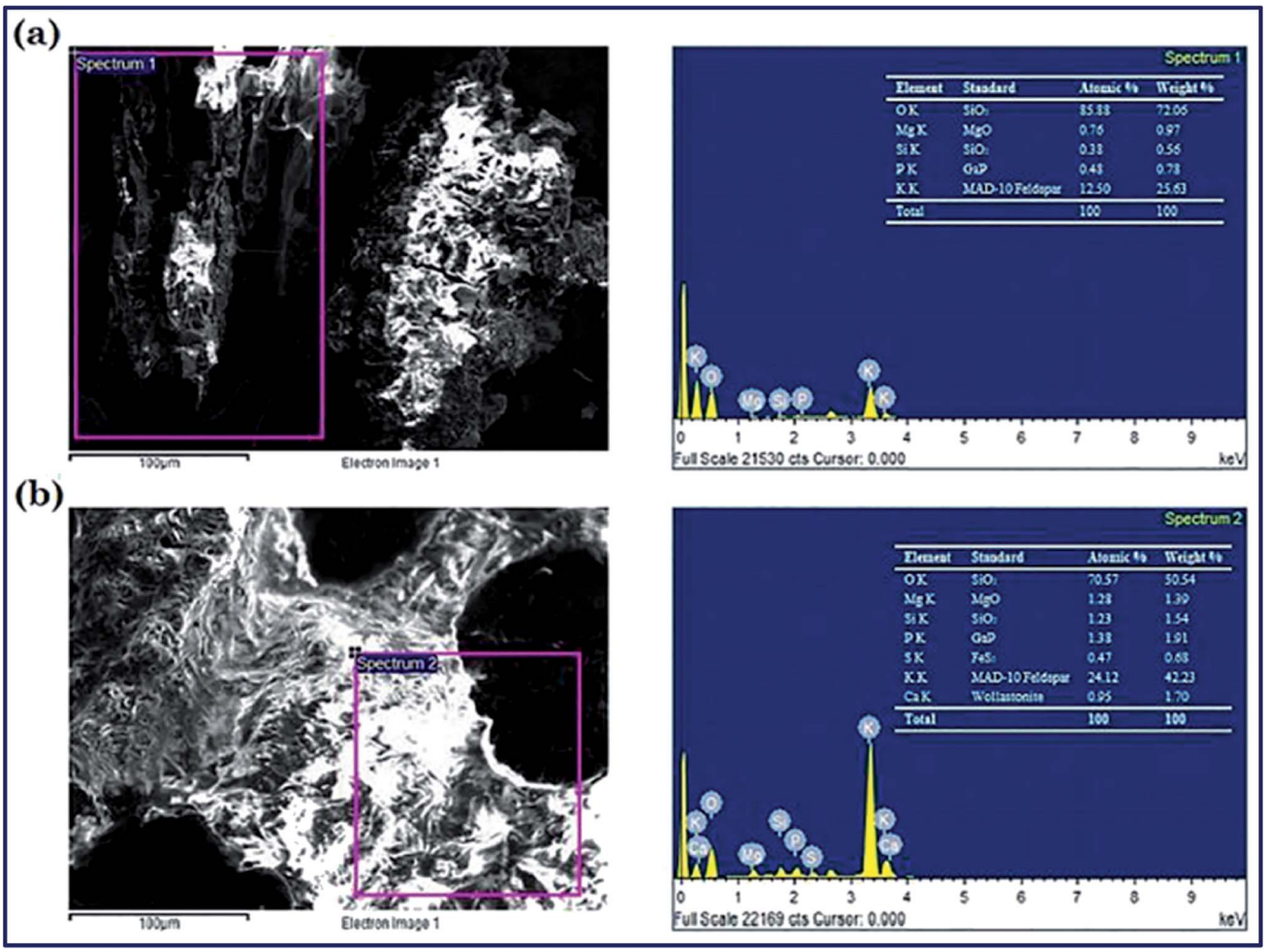

Fig. 25 EDS images of (a) uncalcined and (b) calcined banana peduncle. Reproduced from ref. 279.

The waste *Sesamum indicum* plant ash catalyst was also successfully utilized for the transformation of sunflower oil to biodiesel.[283] The measured surface area of the catalyst was 3.66 $m^2\ g^{-1}$, as obtained from the BET analysis data. A high 98.9% biodiesel yield was accomplished. They reused the catalyst up to the 3rd cycle, which yielded 94.2% biodiesel. In addition, Mendonça *et al.*[284] utilized waste tucumã peels ash catalysts for biodiesel synthesis from soybean oil. The catalyst characterization by XRF showed that it was mostly composed of potassium oxides, calcium and magnesium. Because of its heterogeneous and non-leachable nature, the catalyst derived from *tucumã* peels could be reused at least 5 times. In another study, an ash catalyst from *Tectona grandis* leaves was developed and utilized for the transformation of WCO to FAME by Gohain *et al.*[285] The measured surface area and pore size of the catalyst were 116.833 $m^2\ g^{-1}$ and 112.210 Å, respectively, as calculated from BET data. 100% oil transformation to FAME was accomplished at room temperature using the optimized reaction conditions. Furthermore, cocoa pod husk-derived solid base catalyst was employed in the transformation of neem seed oil to FAME.[286] A two-step process was employed for the conversion of neem seed oil to FAME: (i) pretreatment of the oil was performed using the $Fe_2(SO_4)_3$ catalyst to reduce the FFA content from 28.76% to 0.39%, and (ii) the transesterification of the pretreated oil using the calcined bio waste-derived catalyst. The authors also studied the effect of the reaction parameters using the Box–Behnken design (BBD), and the CCD of RSM was utilized to determine the optimized reaction conditions. Similarly, a walnut shell derived catalyst was developed for the transformation of sunflower oil to biodiesel.[287] The catalyst was

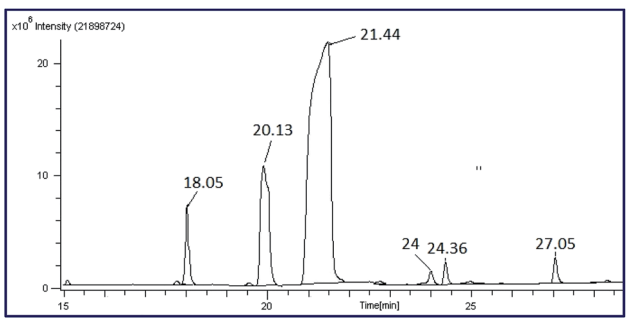

Fig. 26 GC-MS spectrum of biodiesel from soybean oil. Reproduced from ref. 282.

prepared from walnut shells *via* air combustion, thereby bringing down the cost involved in the calcination process to afford ash. The authors reported a 98% FAME yield within a brief time frame of 10 min. Recently, the transformation of sunflower oil to synthesize FAME using calcined sugar beet generated from agro-industry waste was reported.[288] The catalyst has a high amount of highly basic CaO, and showed very high reactivity towards the transesterification process to afford

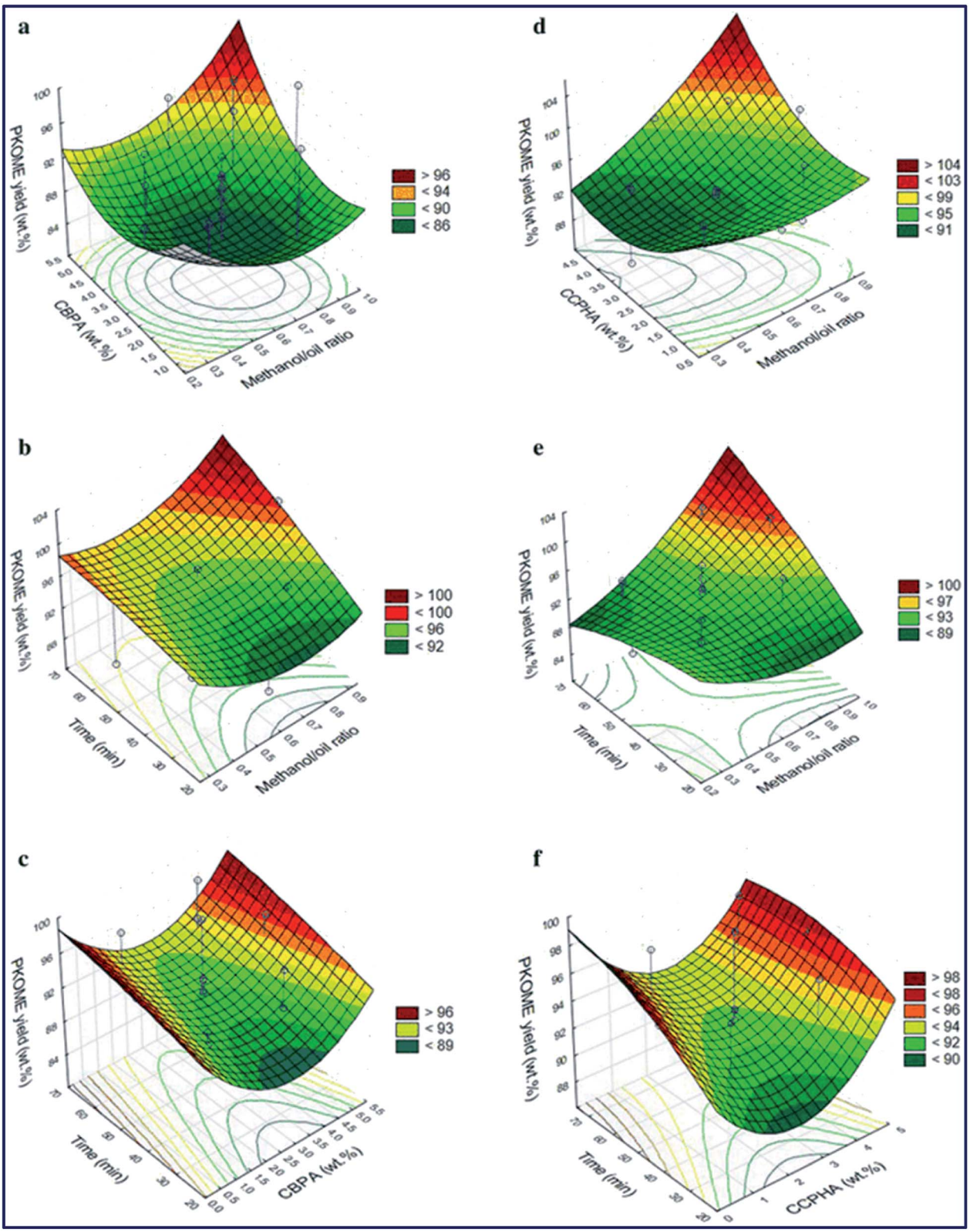

Fig. 27 Contour and surface plots for PKOME synthesis. Reproduced from ref. 290.

about 93% FAME yield. 98.39% soybean oil transformation to FAME under room temperature was recently reported using *M. acuminata* trunk ash catalyst.[289]

Most biomass ash catalysts are usually applied for the transesterification reactions of different biodiesel feedstocks and different reaction conditions. These make a comparison of the effectiveness of such catalysts under the same reaction condition impossible. Hence, to have a better insight into the activities of the catalysts under the same reaction conditions and feedstock, Odude *et al.*[290] examined the transformation of the pre-esterified palm kernel oil (PKO) to FAME utilizing two diverse catalysts, *viz.*, calcined banana peel ash (CBPA) and calcined cocoa pod husk ash (CCPHA) under the same reaction conditions. The RSM technique was utilized for the optimization of both CBPA and CCPHA catalyzed transformation processes of PKO to FAME. CCD was utilized to acquire the best possible combination of the M/O ratio, catalyst loading and reaction time for the highest conversion of oil to FAME, as portrayed in Fig. 27. The observed FAME yields under the optimized conditions utilizing the catalysts CBPA and CCPHA were 99.5 and 99.3 wt%, respectively. The created models, when exposed to statistical assessment, demonstrated that the CBPA-catalyzed transformation model was better than the CCPHA-catalyzed transformation model. In the meantime, the *Carica papaya* stem[291] and *Musa balbisiana* underground stem[292] were also reported as a solid catalyst to convert *Scenedesmus obliquus* and *Mesua ferrea* oil, respectively, to FAME.

7.2 Acid catalysts

Acids can catalyze both transesterification and esterification reactions without soap formation.[293] Hence, unlike base catalysts, an acid catalyst has the potential to afford biodiesel from poor quality oil with high FFA and high water content. In the transesterification reaction, alkaline catalysts are superior in promoting methoxide anion formation from methanol. In contrast, acidic catalysts are less active in methoxide anion formation, but could activate the carbonyl bonds *via* H^+ addition (Brønsted acidic sites) or *via* coordination of the carbonyl oxygen with the coordinatively unsaturated metal ion sites (Lewis acidic sites), and thereby promote transesterification. Hence, an increase in the number of either Brønsted or Lewis acidic sites promotes faster FAME formation *via* transesterification. Delightfully, heterogeneous acid catalysts are endorsed as a potential alternative to homogeneous acid catalysts as they possess certain advantages. These include their ease of separation and reuse, lower corrosiveness and lower toxicity.[294] In recent years, several research groups have studied the feasibility of solid acid catalysts for esterification/transesterification processes, and proposed economical and environment-friendly approaches for biodiesel production.[295–297]

7.2.1 Ion exchange resin. It is a well-known fact that several catalysts have been employed for FAME production from various feedstocks. However, due to the certain disadvantages of conventional catalysts, researchers are always in search of an ideal catalyst that should overcome all associated limitations. These specifications include the ability of the catalyst to be active at lower temperatures, exhibit high catalytic efficacy in terms of conversion of FAME, and have easy availability, low cost, easy downstream processing and reusability. Such an ideal catalyst can be considered as potential and economically viable candidates for biodiesel production.[298] In this context, one of them is ion exchange resin, which meets most of the specifications of an ideal catalyst. Thus, many research groups have studied the role of ion exchange resins as solid catalysts in FAME production.[299,300] Resin is the insoluble solid material that can retain and discharge ions simultaneously.[301] Resins are broadly categorized into cationic and anionic resin based on their functional groups and degree of cross-linkages. It possesses specific functional groups responsible for the permutation of ions.[301] Having one of the important properties, the resin-based catalyst undergoes easy recovery from liquid mixtures by simple methods and are active at low temperature.

Since the last few years, the cationic resins have gained considerable attention due to their advantages, such as functioning at soft reaction conditions, non-corrosive nature, more numbers of active sites and lower residual water production.[302,303] The cationic resin catalysts possess numerous active acid sites that play a crucial role in FAME production *via* esterification/transesterification reactions.[304,305] Various ion exchange resin catalysts utilized for FAME production, together with ideal reaction conditions, are listed in Table 16. In 2007, Shibasaki-Kitakawa *et al.*[302] reported in a comparative study that cation exchange resins showed less efficacy than anion exchange resins towards the conversion of triacylglycerols to biodiesel. Moreover, while evaluating the conversion rates of various commercial resins, such as Diaion PA308, PA306, PA306S and Diaion HPA25, it was observed that highly porous resin-like Diaion HPA25 showed a low conversion rate. It is believed that this might be due to resistance of the resin towards water. According to Ren *et al.*,[303] transformation of soybean oil to FAME was reduced from 95.2% to 87.7% in the presence of D261 anion-exchange resin when the water content was enhanced from 0.0% to 1.0% by the mass of oil. Similarly, in another study, Deboni *et al.*[304] also reported a lowering of the reaction rate due to the presence of water inside the resins.

Generally, ion exchange resins are utilized for the purification and softening of water at room temperature. Recently, Kansedo *et al.*[305] compared the catalytic efficiencies of different ion exchange resins like Amberlyst 15, Dowex DR-2030 and DR-G8 for the transformation of FFA into FAME *via* esterification of the sea mango oil (hydrolyzed) at RT. The results revealed that Amberlyst 15 showed maximum efficacy with the highest FAME production compared to Dowex DR-2030 and Dowex DR-G8. However, Jaya *et al.*[306] utilized ion exchange resin catalysts at a moderately lower temperature (50 °C to 80 °C) for biodiesel production, which is analogous to those of the homogeneous catalytic process. Furthermore, Umer and co-worker investigated the transformation of *Lagenaria vulgaris* seed oil to biodiesel, exploiting the Amberlyst 15 resin and calcium oxide (egg cell) catalyst. The authors reported 93.2% yield of biodiesel when the Amberlyst 15 ion exchange resin was used as a catalyst with the loading of 5% w/w and M/O ratio of 40% w/w for 40 min

Table 16 Different ion exchange resin catalysts used for the production of biodiesel[c]

No.	Catalyst	Feedstocks	Conditions[a]	Yield (%)	Ref.
1	D261 anion-exchange resin	Soybean oil	9 : 1, 50.15, 56	95.2[b]	303
2	Amberlyst A26 OH anion exchange resin	Acid soybean oil	9 : 1, 2, 50, NR	78	304
3	Amberlyst-15	Hydrolyzed sea mango oil	6 : 1, 30, 30, NR	>90	305
4	Basic anion exchange resin.	Pongamia oil	9 : 1, 75, 60	85	306
5	Amberlyst 15 ion exchange resin	*Lagenaria vulgaris* seed oil	40 : 1, 5, 60, 40	93.2	307
6	Amberlyst	Hydrolyzed sea mango oil	3 : 12, 100, 60	>80	308
7	Amberlyst-26	Canola oil	6 : 1, 3, 45, 90	67	309
8	Amberlyst-A26 OH	Tallow fat	6 : 1, 2 mol L^{-1}, 65, 360	95	310
9	Amberlite gel resin	WCO	7 : 1, 60, 120	85.94	311
10	Cation-exchange resin	Rice bran oil	6 : 1, 20, 63.83, 120	79.7	313
11	Purolite-PD206	Corn oil	18 : 1, 65, 2880	79.45	315

[a] Methanol-to-oil molar ratio, catalyst loading (wt%), temperature (°C), reaction time (min). [b] Conversion. [c] NR: not reported, PFAD: palm fatty acid distillate.

reaction time at 60 °C.[307] Similarly, Kansedo and Lee[308] investigated the esterification of hydrolyzed sea mango oil utilizing different cationic ion exchange resins, and over 80% yield of FAME was recorded using the Amberlyst 15 catalyst at a comparatively lower temperature within 1 h of reaction time and with catalyst loading of less than 5% w/w.

Recently, Deboni *et al.*[304] reported 99% yield of methyl and ethyl esters from soybean oil with methanol and ethanol, respectively, using optimal reaction conditions. Conversely, Ilgen *et al.*[309] recorded 63% yield of FAME from canola oil using Amberlyst-26 under the optimized reaction conditions. Moreover, in another study, a yield of about 67% was observed for canola oil and methanol with almost similar reaction conditions.[301,309] The conversion of tallow fat with methanol showed the yield of methyl and ethyl esters around 95% using Amberlyst-A26 OH with reaction conditions, like a tallow fat-to-methanol molar ratio of 6 : 1, and a resin loading of 2 mol L^{-1} at 65 °C temperature for about 8.5 hours.[310]

Hartono *et al.*[311] investigated the catalytic efficacy of a heterogeneous catalyst obtained from a different source, like Lewatit macroporous resin, Amberlite gel resin and natural zeolite from Bayah, to transform WCO to biodiesel. Authors reported the 85.94% yield of biodiesel production by Lewatit macroporous anion exchanger with 6 M NaOH. Whereas, Amberlite gel with 6 M HCl displayed 65.22% biodiesel generation. Previously, Shibasaki-Kitakawa *et al.*[312] reported the usefulness of the anion-exchange resin from their catalytic and adsorption abilities for the transformation of WCO to FAME. In their other study, Shibasaki-Kitakawa *et al.*[313] also developed an ion-exchange resin catalyst-based continuous process for the production of biodiesel. The FFA conversion rate was estimated for different catalysts with reactions conditions, like the mole ratio of M/O (6 : 1), temperature (63.83 °C), reaction time (2 h) and catalyst load (20 wt%). The maximum FFA conversions of 79.7% were recorded for NKC-9. For 001 × 7 and D61 catalysts, it was found to be only 32.2% and 10.3%, respectively.[314] Jalilnejad-Falizi *et al.*[315] achieved the highest FFA conversions by ion exchange resins (PD206-Na^+ and PD206-H^+) under the optimal reaction conditions. All of the above-mentioned reports are enough to summarize that ion exchange resins can be employed as one the potential heterogeneous catalysts in biodiesel production.

7.2.2 Sulfated catalyst. Among the solid acid catalysts, the sulfated catalysts have attracted considerable attention for transesterification due to their super-acid property. Sulfated inorganic metal oxides are reported to be chemically stable, and have super acidity comparable to 100% sulfuric acid, remarkable acid–base and redox properties.[316] Different kinds of sulfated catalysts, such as sulfated zirconia, tin oxide, and zirconia-alumina, have been successfully exploited in the production of biodiesel. However, among these, sulfated zirconia is the most widely studied catalyst (Table 17). Various reports are available on the transformation of oil to FAME utilizing the sulfated zirconia catalyst, but there are some studies that presented certain drawbacks of these catalysts, which include low catalytic activities, drastic reaction conditions, and reusability issues. Moreover, the lack of uniform pore size and low surface area are the other factors that restrict their wide uses in catalyzing bulky oil molecules of biodiesel feedstocks. In this context, several attempts have been made to modify the sulfated zirconia catalysts with an intention to increase their catalytic efficacy.

Xia *et al.*[317] demonstrated the synthesis of mesoporous materials, which has the potential to improve the activity of the sulfated zirconia catalyst owing to their promising and outstanding properties, like high surface area, uniform and controllable pore size. According to Alexander *et al.*,[318] the modification of the sulfated zirconia catalyst enhanced the total acidity, which basically increased the catalyst active sites. In another study, Guoliang *et al.*[319] proposed that a change in the phase structure of sulfated zirconia can also increase its catalytic activity. Therefore, they developed tetragonal sulfated zirconia, which showed enhanced catalytic activity in the FAME synthesis procedure. Moreover, some of the studies proposed the modification of sulfated zirconia on a MCM-41 (Mobil Composition of Matter No. 41) support for the generation of methyl *tert*-butyl ether to improve its catalytic performance. The results obtained revealed that the catalytic performance of the

Table 17 Different types of sulfated catalyst yields reported for biodiesel production[b]

No.	Catalyst	Feedstocks	Conditions[a]	Yield (%)	Ref.
1	SO_4^{2-}/ZrO_2	Neem oil	9 : 1, 1, 65, 120	95	321
2	SO_4^{2-}/SnO_2–SiO_2	WCO	15 : 1, 3, 150, 180	92.3	322
3	$SnSO_4$	Soybean oil	3.5 : 1, 5, 100 180	92	323
4	SO_4^{2-}/SnO_2–SiO_2	Jatropha oil	15 : 1, 3, 180, 120	97	324
5	SO_4^{2-}/TiO_2	Rapeseed oil	12 : 1, NR. 80, 720	51	325
6	$Ti(SO_4)O$	WCO	9 : 1, 1.5, 75, 180	97.1	328
7	$TiO_2/PrSO_3H$	WCO	15 : 1, 4.5, 60, 540	98.3	329

[a] Methanol-to-oil molar ratio, catalyst loading (wt%), temperature (°C), reaction time (min). [b] NR: not reported.

prepared supported sulfated zirconia catalyst was 2.5–3.0 times greater than neat sulfated zirconia.[317,320] Similarly, Muthu *et al.*[321] reported the preparation of FAME from neem (*Azadirochta indica*) oil using sulfated zirconia catalyst. It was revealed that the catalyst is highly stable to oils with high FFA concentration. The strong acid sites of this catalyst showed a considerable impact on its reactivity in the transformation of neem oil.

Recently, Lam *et al.*[322] developed a SO_4^{2-}/SnO_2 catalyst by impregnation method, and exploited it for the conversion of WCO to biodiesel. Furthermore, the authors studied the bimetallic impact of the catalyst, in which SnO_2 was blended in with SiO_2 and Al_2O_3, at various weight ratios to increase the activity of SnO_2. The finding confirmed that the SO_4^{2-}/SnO_2–SiO_2 weight ratio of 3 showed exceptionally high reactivity with 92.3% biodiesel yield using optimal reaction conditions. Similarly, Pereira *et al.*[323] demonstrated the application of the $SnSO_4$ catalyst for the esterification of oleic acid (as model feedstock) and acid soybean oil having high contents of FFA. It was found that the model feedstock containing 70 wt% of FFA showed 92% FAME yield using excess ethanol, 5 wt% $SnSO_4$ at 100 °C for 3 h. Moreover, it was also reported that the catalyst is stable up to ten cycles without any significant decrease in the biodiesel yield. Moreover, one of the studies involved the application of sulfated tin oxide modified with the SiO_2 (SO_4^{2-}/SnO_2–SiO_2) catalyst to produce FAME from JCO.[324] The sulfated titania-based solid superacid catalysts are another kind of sulfated catalysts. Li *et al.*[325] prepared three different titania-based solid superacid catalysts, and these were exploited for the transformation of rapeseed oil to FAME at 353 K with a 12 : 1 molar ratio of M/O under atmospheric pressure. It was found that all three prepared catalysts showed a significant yield of biodiesel due to their stronger surface acidities. Moreover, Alaba *et al.*[316] reviewed that apart from these, there are various other sulfated metal oxides, such as titania and silica, and a combination of both also showed remarkable performance. It was also proved thorough the investigation led by several researchers, who applied sulfated silica as catalysts for esterification and transesterification.[326,327] In this context, Gardy and co-workers demonstrated a facile preparation of the sulfated doped TiO_2 catalyst that was utilized efficiently in the petroleum refinery. The authors reported that the synthesized catalyst has better reactivity than other sulfated metal oxides, primarily because of the acidic properties of the TiO_2 particles, which was subjected to sulfonation to enhance its acidity. The catalyst displayed great efficiency in the synthesis of FAME from WCO.[328,329]

7.2.3 Mixed metal oxides. A wide range of acidic mixed metal oxide catalysts has been utilized to overcome the problem associated with high FFA content in low-cost biodiesel feedstock employed in FAME production (Table 18). Suzuta *et al.*[330] reported the utilization of the Fe_2O_3–SiO_2 catalyst in the conversion of JCO to FAME. The catalyzed reaction displayed 95.6% FAME yield under the optimized reaction conditions. When the Fe loading was raised from 0.07 to 2.1 wt%, the acidity of the catalyst drastically increased. The Fe-oxide species scattered over the SiO_2 surface were recognized as the active sites. In the meantime, the $ZnAl_2O_4/ZnFe_2O_4$ catalyst was also examined for the transformation of oil, such as sunflower oil, WCO and JCO.[331] During the reaction, the Zn 3d electrons of the $ZnAl_2O_4$ and $ZnFe_2O_4$ spinels were likely to take part in the electronic excitation; thereby, the Zn 3d electrons are probably going to undertake a vital job to enhance the catalyst reactivity. In 2012, Xie *et al.*[332] synthesized the SnO_2–SiO_2 catalyst by loading 8 wt% Sn onto SiO_2, followed by calcination (550 °C) and exploited it in the transformation of soybean to FAME, yielding 81.7% under the optimal reaction conditions.

Impregnation followed by calcination (600 °C) was used to synthesize the Fe–Mn–MoO_3/ZrO_2 catalyst, which could provide a high 95.6 ± 0.15% yield of FAME.[333] It is interesting to observe that ZrO_2 and MoO_3/ZrO_2 gave a lower FAME yield of 48.6 ± 1.14 and 73.0 ± 0.25%, respectively. The high activity of the Fe–Mn–MoO_3/ZrO_2 catalyst is attributed to the high surface area (49.5 $m^2\ g^{-1}$) and availability of huge active sites (2411 μmol g^{-1}) in the catalyst. Moreover, the catalyst reusability examination revealed that it is stable up to 6 progressive reaction cycles of transesterification of WCO without a loss in its efficiency. On the other hand, the enhanced catalytic activity was observed in a mixed metal oxide of WO_3/SnO_2 in the soybean oil transformation in comparison with the individual WO_3 and SnO_2 species.[334] The bonding of WO_3 with SnO_2 was believed to upgrade the WO_3/SnO_2 acidity. The catalyst is highly stable and was reused up to 4 times without much depreciation in the biodiesel yield.

Further, Xie *et al.*[335] studied 30 wt% WO_3 loading on the $AlPO_4$ catalyst and recorded a good 72.5% conversion to biodiesel under the optimized reaction condition. The high catalyst reactivity was attributed to the existence of WO_3 that enhanced the surface acid sites. Similarly, Amani *et al.*[336] reported a series of $Mn_{3.5x}Zr_{0.5y}Al_xO_3$ catalysts for the transformation of WCO to FAME. The $Mn_{1.4}Zr_{0.35}Al_{0.6}O_3$ catalyst demonstrates better catalyst reactivity, as far as the FAME yield (>93%), than the $Mn_{1.4}Zr_{0.35}O_3$ catalyst (52.8%). The bonding between metals in the crystal structure efficiently influenced the catalyst reactivity. It was observed that the amphoteric component of the Al developed the surface region of the catalyst and framed a complex structure with other metal oxides, although Mn alternated the morphology and catalyst basic site density. In the meantime, Zhang *et al.*[337] reported the Zr–Mo mixed metal oxide functionalized with various carboxylic acids, for example, lauric

Table 18 Different types of solid acid catalysts for the FAME production

No.	Catalyst	Feedstocks	Conditions[a]	Yield (%)	Ref.
1	Fe_2O_3–SiO_2	Jatropha oil	218 : 1, 15, 220, 180	95.6	330
2	$ZnAl_2O_4$/$ZnFe_2O_4$	Sunflower oil, WCO, Jatropha oil	9 : 1, 5, 180, 600	>90	331
3	SnO_2–SiO_2	Soybean oil	24 : 1, 5, 180, 300	81.7	332
4	Fe–Mn–MoO_3/ZrO_2	WCO	25 : 1, 4, 200, 300	95.6 ± 0.15	333
5	WO_3–SnO_2	Soybean oil	30 : 1, 5, 110, 300	79.2	334
6	WO_3 (30 wt%)/$AlPO_4$	Soybean oil	30 : 1, 5, 180, 300	72.5	335
7	$Mn_{1.4}Zr_{0.35}Al_{0.6}O_3$	WCPO	14 : 1, 2.5, 150, 300	>93	336
8	Zr–Mo	Oleic acid	10 : 1, 4, 180, 120	94.2[b]	337
9	FMWMo	WCO	25 : 1, 6, 200, 480	92.3 ± 1.12	338

[a] Methanol-to-oil molar ratio, catalyst loading (wt%), temperature (°C), reaction time (min). [b] Conversion.

acid, stearic acid, palmitic acid and myristic acid for the biodiesel production from oleic acid. The modification of the Zr–Mo metal oxide using such monofunctional carboxylic acids enhances the catalyst acidity and surface area, and thus upgraded the rate of the reaction. They also reported that among all catalysts, the stearic acid-functionalized Zr–Mo metal oxide showed the best result with the maximum oleic acid conversion of 94.2%. The catalyst reusability test revealed that the catalyst is stable for up to 6 progressive cycles. Similarly, WCO was utilized for the FAME production using ferric-manganese doped tungstate molybdena nanoparticles (FMWMo).[338] The Fe–Mn dopants enhance the surface area, density of acidic sites, and the stability towards the esterification of WCO. A maximum yield of 92.3 ± 1.12% methyl ester was achieved under the optimized reaction conditions.

7.2.4 Sulfonated carbon-based catalyst. In the last few decades, various carbon materials with different shapes, sizes, and structures have been developed by several research groups and utilized as low-cost catalysts for diverse industrial processes, including transesterification.[339] Currently, sulfonated carbons, *i.e.*, SO_3H-functionalized acidic carbon materials, are considered as a new group of the metal-free solid acid catalyst described by their original carbon structure and Brønsted acidity equivalent to concentrated H_2SO_4. Sulfonated carbon acid catalysts can be easily prepared by processes, like the incomplete carbonization of aromatic compounds in concentrated H_2SO_4 (ref. 340) or sulfonation of incompletely carbonized natural organic matter, such as sugar[341–343] and cellulosic materials.[344,345] Sulfonation can also be achieved by treating the carbon material with a sulfonating reagent, such as gaseous SO_3, $ClSO_3H$, *p*-toluenesulfonic acid, 4-benzenediazonium sulfonate or SO_3H-containing aryl diazoniums.[346–349] These materials possess promising features, such as biogenic, environment-friendly, lower production costs, distinctive surface chemistry, high chemical and thermal stability.

The acid-catalyzed chemical reactions, such as saccharification, esterification, transesterification and acetylation, are vital operations commonly used for the valorization of biomass or their components to useful products in various food, fuel and chemical industries.[350] The functionalized acidic carbons from inexpensive sources, including natural organic carbon matter (such as sugars, carbohydrates, cellulosic materials, and lignin), have been achieved by several researchers.[341,351–353] Besides this, agro waste such as husk, straw, seed cover, cow manure, corn cob,[342,343,354,355] carbonaceous waste from industries (char, oil pitch, coke, glycerol)[346,348,356,357] and polymer resins[349,358,359] were also used. Various carbon supports (*e.g.*, zeolite-templated carbons, mesoporous carbons, active carbon)[352,353,360,361] and more recently nanostructured carbons (such as graphene, graphene oxide, carbon nanotubes, and carbon dots)[362–367] have been exploited for the same purpose.

Over the last few years, there is growing interest from researchers towards the application of sulfonated carbon-based catalysts due to their noteworthy efficacies mentioned earlier. Many reports are available, which demonstrated the efficient nature of the sulphonic acid-functionalized catalyst in biodiesel production using various feedstocks.[356,362,367] One of the reports presented the synthesis of organosulfonic acid (*i.e.*, propylsulfonic and arenesulfonic groups) functionalized mesoporous silicas through a simple one-step process. The synthesized novel catalysts that possessed propylsulfonic groups and arenesulfonic groups were further evaluated for their catalytic efficacy in the esterification of fatty acids with methanol to produce methyl esters, and the authors also compared the efficacy of these heterogeneous catalysts with a variety of commercially available catalysts (such as sulfuric acid, *p*-toluene sulfonic acid, Nafion NR50, and Amberlyst-15). The obtained results indicated that the organosulfonic acid-functionalized mesoporous silica catalysts showed the highest reactivity compared to all of the above-mentioned commercial solid acid catalysts in the fatty acid esterification process. Moreover, it was also recorded that the efficiency of these catalysts largely depended on important factors, such as the median pore diameter of the catalyst and the acidic strength of the organosulfonic acid group present over this catalyst. Considering these findings, it can be proposed that there is a huge potential to develop catalysts using organic–inorganic mesoporous materials.[363] In general, the activity of the carbon-based catalysts upon fatty acid (C16–C18) esterification to produce biodiesel primarily depends on three primary factors: (i) $-SO_3H$ group density, (ii) total acid density, and (iii) porosity. Different sulfonated carbon-based acid catalysts utilized for

FAME production are listed in Table 19. Numerous reported catalysts demonstrated promising outcomes in the (trans) esterification of biodiesel feedstocks with high FFA and afforded >85% FAME yield. In the meantime, several investigations had been conducted using model acids (*e.g.*, palmitic acid, oleic acid, which are the major components of vegetable oil as a reactant) that mainly focused on the esterification reaction.

In a pioneering work towards the preparation of the biomass-based sulfonated carbon catalyst, Toda *et al.*[364] synthesized the sulfonated carbon catalyst by partial carbonization of sugar, followed by sulfonation in fuming H_2SO_4. The prepared catalyst consists of sheets of indistinctive carbon having a high amount of sulfonic groups, along with hydroxyl and carboxyl as a minor group (Fig. 28). The highly active bio-based carbon catalyst was utilized for the transformation of oleic and stearic acid to FAME *via* esterification. Apart from the $-SO_3H$ group, the presence of the –OH and –COOH groups in the catalyst greatly enhance the catalytic activity and make it highly water tolerant. The successful incorporation of the $-SO_3H$ group and the formation of carbonized materials can be easily confirmed by using FT-IR and ^{13}C MAS NMR analysis, respectively, as depicted in Fig. 33.[368] The FT-IR spectra (Fig. 29a) displayed two bands at 1040 and 1377 cm^{-1} (in SO_3H), ascribed to the SO_3 and O=S=O stretching vibrations, respectively, suggesting the existence of the $-SO_3H$ groups. ^{13}C MAS NMR (Fig. 29b) depicted three major peaks at 130, 155, and 180 ppm, ascribed to the polycyclic aromatic carbon atoms, phenolic OH, and COOH groups, respectively.

In another work, Hara *et al.*[356] examined the sulfonated carbon catalyst in biodiesel synthesis. The findings showed that the amorphous carbon material-containing sulfonic acid groups enhances the catalytic performance, and thus displayed

Table 19 Different sulfonated carbon-based acid catalyst yields used for biodiesel production[d]

No.	Catalyst	Feedstock	Conditions[a]	Yield (%)	Ref.
1	Sulfonated sugar	Oleic acid	10 : 1[c], 7.4, 80, 240	NR	364
2	Sulfonated carbon	Oleic acid	2.92 : 1[c], 17.2, 95, 240	99.9	365
3	$ACPhSO_3H$	Rapeseed oil	20 : 1, 10, 65, 420	95	366
4	Sulfonated AC	Soybean oil	6 : 1, 20, 75, 20	88.7	355
5	H_2SO_4/C	Castor oil	12 : 1, 5, 65, 60	94	369
6	SAM	Vegetable oil	10 : 1, 6, 180, 120	95	370
7	SO_3H/SBA-15	Soybean oil	6 : 1, 5, 190, 30	90	371
8	$SiO_2–Pr–SO_3H$	Acid oil	15 : 1, 4, 100, 480	96.78[b]	372
9	$OPPSO_3H$	Soybean oil	50 : 1[c], 10, 70, 600	93[b]	373
10	Coal based solid acid	Oleic acid	10 : 1, 8, 240, 67	97.6[b]	375
11	Sulfonated carbon-based solid acid	Oleic acid	10 : 1, 10, 65, 120	97.3	376
12	Sulfonated activated carbon	Oleic acid	7 : 1[c], 12, 180, 85	96[b]	377
13	$C–SO_3H$	Waste cooking oil	20 : 1, 10, 60, 180	93.6	378
14	Sulfonated multiwalled carbon nanotube	Triglycerides	10 : 1[c], 3.7, 60, 150	97.8[b]	379
15	$ICS-SO_3H$	Palm fatty acid distillate	10 : 1, 2, 180, 75	90.4	380
16	$CMR-DS-SO_3H$	Waste palm oil	12 : 1, 5, 65, 72	92.7	381
17	$HS/C–SO_3H$	Oleic acid	5 : 1, 3.5, 80, 300	96.9[b]	382
18	SOMC	Oleic acid	10 : 1, 3.5, 80, 600	73.59[b]	383
19	SO_4^{2-}/corncob	Oleic acid	15 : 1, 5, 60, 480	>80	384
20	$C–SO_3H$	Oleic acid	10 : 1, 1.5, 67, 120	93.04	385
21	$C–SO_3H$	Oleic acid	16 : 1, 17, 95, 240	99.9	386
22	$C–SO_3H$	WCO	10 : 1, 10, 110, 240	89.6	387
23	$C–SO_3H$	PFAD	15 : 1, 2.5, 80, 240	95.3[b]	388
24	$C–SO_3H$	*Mesua ferrea* Linn oil	40 : 1, 5, 120, 1440	97.79	389
25	Coconut shell-SO_3H	Palm oil	30 : 1, 6, 60, 360	88.03	390
26	Oil palm trunk/sugarcane bagasse-SO_3H	Waste oil	1.17 mL min^{-1}, 12, 130, 240	80.6/83.2	391
27	Corn straw-SO_3H	Oleic acid	3 : 1, 3, 60, 240	92	392
28	Bamboo-SO_3H	Oleic acid	7 : 1[c], 2, 90, 360	98.4	393
29	*Jatropha curcas* Seed-SO_3H	JCO	12 : 1, 7.5, 60, 60 99.13	99.13[b]	394
30	Bio-glycerol	Karanja oil	45 : 1, 20, 160, 240	99.5	395
31	Glycerol	Palmitic acid	9.7 : 1[c], 10, 65, 240	99[b]	396
32	Microalgae residue	Oleic acid	NR, 5, 80, 720	98[b]	397
33	Oil cake waste-SO_3H	JCO/*M. ferrea* L. oil	43 : 1, 5, 80, 480	99	398
34	Oil cake waste-SO_3H	Oleic acid	12 : 1, 20, 60, 120	94[b]	399
35	De-oiled waste cake	Oleic acid	20 : 1, 3, 64, 600	97[b]	400
36	De-oiled canola meal-SO_3H	Oleic acid	60 : 1, 7.5, 65, 1440	93.8[b]	401
37	Pine chip char	Palmitic acid	6 : 1, 5, 55–60, 300	97	402
38	Biochar	Canola oil	15 : 1[c], 5, 65, 1440	92	403
39	Biochar	Canola oil, oleic acid	30 : 1, 5, 315, 180	48	404

[a] Methanol-to-oil molar ratio, catalyst loading (wt%), temperature (°C), reaction time (min). [b] Conversion. [c] Ethanol to oil molar ratio. [d] NR: not reported.

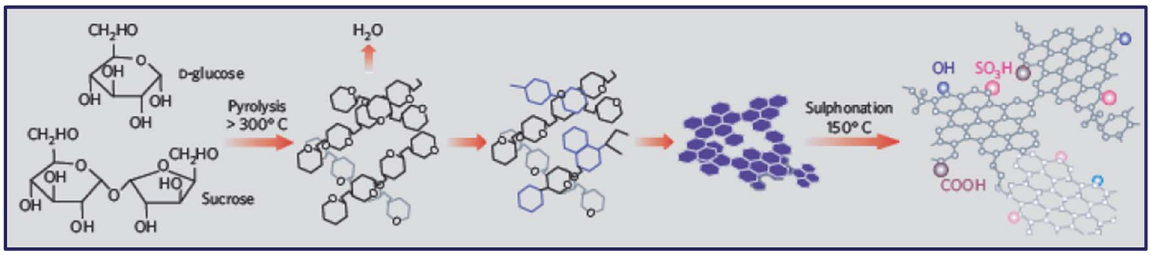

Fig. 28 Synthesis of sulfonated carbon catalyst from sucrose and D-glucose. Reproduced from ref. 364.

extraordinary reactivity in the esterification/transesterification reactions in comparison with the ordinary solid acid catalyst.

Likewise, Nakajima *et al.*[365] synthesized an amorphous cellulose-originated carbon solid acid (CCSA) catalyst and exploited it in the transformation of oleic acid to FAME, and observed a 99.9% yield under the optimized conditions. The carbon material displayed much higher catalytic activity in the esterification reaction in comparison with the ordinary solid acid catalysts examined, such as niobic acid, Amberlyst-15 and Nafion NR50. Interestingly, those CCSA catalysts prepared at a lower carbonization temperature before being subjected to sulfonation gave a much better biodiesel yield, as compared to those prepared at higher carbonization temperature. This is attributed to the huge amount of –OH and –COOH groups in the former, which enhanced its acidic nature, and thereby its catalytic activities (Fig. 30). The catalyst reactivity remains intact after 10 progressive cycles.

The simultaneous carbonization and sulfonation in a one-pot synthesis of solid acid catalyst directly from biomass have also been explored by various experts, as it is a straightforward, cost and time-efficient approach. Malins *et al.*[366] synthesized C–SO_3H *via* the simultaneous carbonization-sulfonation approach, and utilized it for FAME production. The C–SO_3H catalysts with the highest density of SO_3H groups (0.81 mmol Hβ per g) were prepared using optimal reaction conditions. It was noted that under these optimized reaction conditions, 96.5% of FAME was recorded. Interestingly, the catalyst has great stability, and can be easily recovered and reused for subsequent reaction cycles. Moreover, in the comparative study of the esterification reactions of rapeseed oil fatty acids, the prepared catalyst exhibited similar reactivity to Amberlyst-15.

Another recent report proposed a synthesis of the heterogeneous sulfonated catalyst using activated carbon to overcome several problems, like drastic reaction conditions (such as very high temperature, pressure, longer reaction time and expensive overall process cost). The above-mentioned activated carbon catalyst was prepared from corncobs as a precursor, and utilized in the microwave-assisted conversion of soybean oil with ethanol to FAME. In this study, about 88.7% yield of pure biodiesel was reported at 0–600 W of microwave power. Moreover, the catalyst was reused for up to 5 cycles.[355] Fig. 31 represents the schematic illustration of the application of the activated carbon-based catalyst in the transesterification of various oils using methanol.

In 2009, Yuan *et al.*[369] examined the application of a solid acid catalyst originated from sulfonated activated carbon (H_2SO_4/C) for catalyzing the transesterification of castor oil and methanol as feedstock. Melero *et al.*[370] synthesized the sulfonic acid-modified mesostructured (SAM) catalysts and studied their efficacy in the transformation of crude vegetable oils to FAME. The results obtained noted that this catalyst has the ability to yield 95 wt% pure FAME and oil transformation close to 100%. Despite the presence of FFAs, this catalyst displayed significantly high activity toward the simultaneous esterification and transesterification reactions. Similarly, Zuo *et al.*[371] developed various sulfonic acid-functionalized mesoporous SBA-15

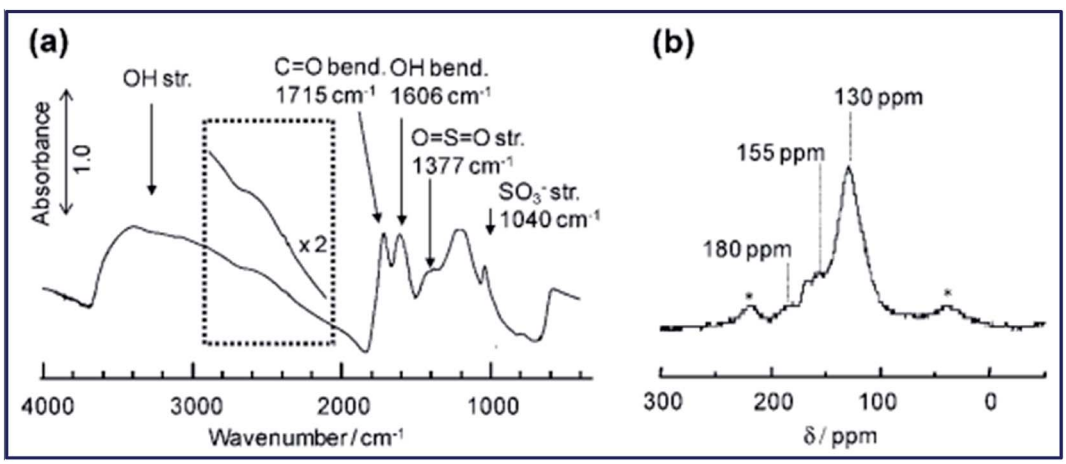

Fig. 29 FT-IR (a) and ^{13}C MAS NMR (b) spectra for the sulfonated carbon catalyst originated from cellulose. Reproduced from ref. 368.

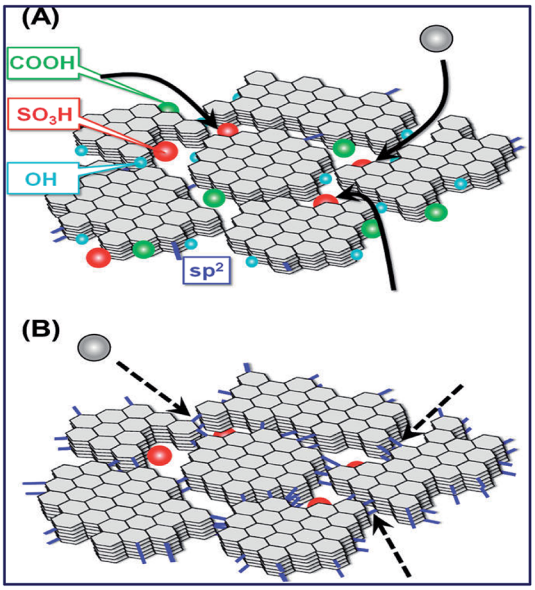

Fig. 30 Schematic structures of the SO_3H-bearing CCSA materials carbonized at below 723 K (A) and above 823 K (B). Reproduced from ref. 365.

catalysts, and tested their catalytic activity in the microwave-assisted conversion of soybean oil and 1-butanol to biodiesel. The authors observed that the catalytic efficacy of these catalysts mainly depends on the acid strength and not on the number of acid sites. Furthermore, propyl-SO_3H and arene-SO_3H functionalized SBA-15 catalysts were found to have comparatively better reactivity in the transesterification process. However, the perfluoro-SO_3H functionalized SBA-15 catalyst displayed leaching of the active sites in each progressive cycle, and thus, the reactivity decreased. Shah *et al.*[372] demonstrated esterification of FFAs in acid oil (which is a byproduct of oil refining) using a sulfonic acid-functionalized silica (SiO_2–Pr–SO_3H) catalyst to prepare the biodiesel. Furthermore, the authors optimized various reaction conditions, such as temperature, reaction time, catalyst concentration, and M/O molar ratio, which usually affect the conversion to FAME. A high conversion (*i.e.*, 96.78% conversion after 8 h was reported at optimized conditions) can be achieved using these solid acid catalysts.

Moreover, in the recent past, Varyambath *et al.*[373] developed different sulfonic acid-functionalized organic knitted porous polyaromatic microspheres (OPPSO$_3$H) utilizing pyrene, anthracene, and naphthalene as monomers *via* Friedel–Crafts alkylation, followed by crosslinking reactions. Furthermore, these heterogeneous catalysts were utilized for the transformation of long-chain fatty acids and triglycerides to biodiesel. These solid acid catalysts were found to be very promising for biodiesel synthesis, as they showed excellent surface acidity. In addition, several other sulphonic acid-functionalized catalysts were successfully developed and exploited in the production of biodiesel. In this context, Shagufta *et al.*[374] reviewed all such sulphonic acid-functionalized catalysts in esterification and transesterification reactions. This review can be consulted for more detailed information.

Yu *et al.*[375] studied biodiesel production by exploiting coal-based acid catalysts, and reported an oleic acid conversion of 97.6% under the optimal reaction conditions. Similarly, Tang and Niu[376] investigated the synthesis of carbon-based solid acid catalysts from bamboo through the partial carbonization and sulfonation approach. The microstructure of the catalyst was activated by phosphoric acid impregnation. The catalyst

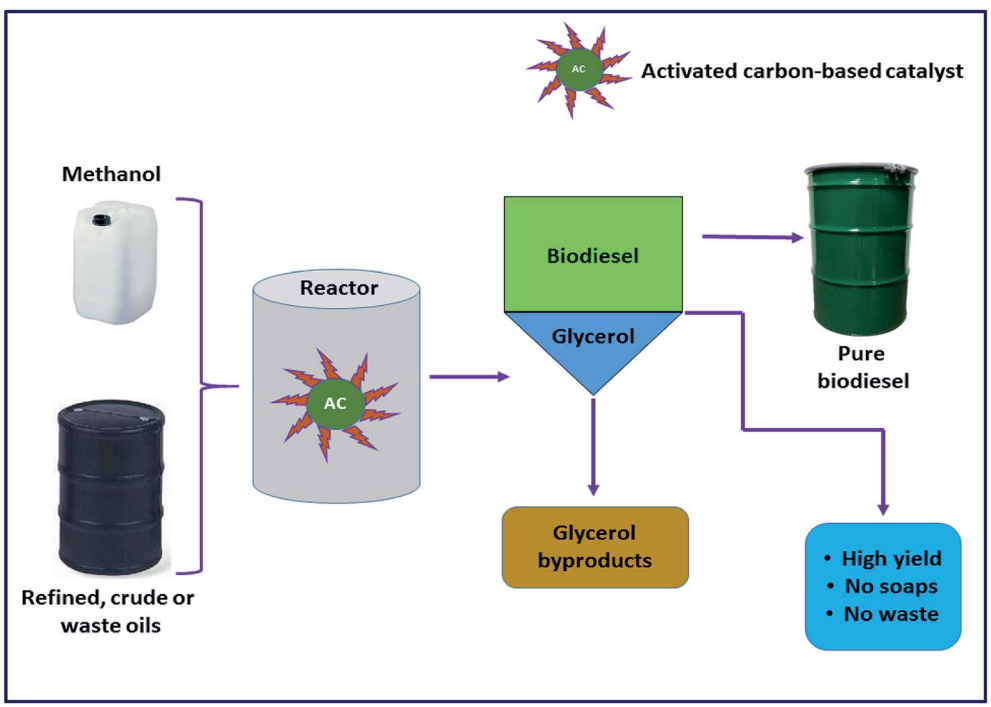

Fig. 31 Schematic representation of transesterification of various oils using activated carbon-based catalysts.

afforded a biodiesel yield of 97.3% at optimum conditions, which decreased to 83.7% in the fourth reaction cycles. In addition, biodiesel production from oleic acid was reported using sulfonated activated carbon from bamboo.[377] A sulfonated carbonaceous material synthesized *via* the single-step hydrothermal sulfonation of glucose has also been used as a catalyst for the esterification of waste cooking oil to produce biodiesel.[378] FESEM images of the carbonaceous material (C) (Fig. 32a) and the sulfonated carbonaceous material (C–SO_3H) (Fig. 32b) showed the carbonaceous microsphere and the sulfonated carbonaceous microsphere with an attached sulfonic group on the surface, respectively. The catalyst showed great stability with 93.4% FAME yield under the optimized reaction conditions.

Guan *et al.*[379] synthesized the sulfonated multi-walled carbon nanotube (S-MWCNT) for the conversion of triglyceride to FAME in 97.8%. The high catalytic reactivity is because of the high surface area (198.9 $m^2\ g^{-1}$), high porosity (10–15 nm) and high acid sites. Similarly, the sulfonated carbonaceous material from starch was utilized as a solid catalyst for the esterification of PFAD.[380] A novel, efficient, inexpensive and environment-friendly acid catalyst was synthesized from coconut meal residue (CMR). The CMR-DS-SO_3H catalyst was prepared by a one-step direct *in situ* carbonization in concentrated H_2SO_4, and reported for the transformation of the waste palm oil (WPO) to biodiesel. The prepared sulfonated catalyst has an acid density of 3.8 mmol g^{-1}, surface area of 1.33 $m^2\ g^{-1}$ and means pore volume of 0.31 $cm^3\ g^{-1}$. The results obtained recorded a high yield of 92.7% biodiesel from WPO.[381] Moreover, Wang *et al.*[382] investigated the application of the monodispersed hollow carbon/silica solid acid catalyst HS/C–SO_3H, which was prepared by chemical activation approach, in the esterification of oleic acid with methanol to produce the biodiesel.

Besides this, another kind of sulfonated functionalized carbon material, *i.e.*, sulfonated ordered mesoporous carbon (SOMC) catalyst, showed promising biodiesel production (73.59% yield).[383] Recently, the sulfonated acid catalyst obtained from corncob (SO_4^{2-}/corncob) has been reported as an excellent catalyst for the conversion of oleic acid to obtain methyl oleate in good yield (>80% after 8 h at 60 °C).[384] Mahdavi and Darab[385] prepared a sulfonated carbon catalyst by treatment of sucrose and concentrated H_2SO_4 at high temperature (sulfonation and carbonization approach). The synthesized C–SO_3H catalyst was further utilized for the conversion of oleic acid to FAME in 93.04% yield. Moreover, a solid acid catalyst generated from the sulfonation of microcrystalline cellulose powder was successfully applied for oleic acid esterification, showed 99.9% biodiesel yield under the optimized reaction conditions.[386] In another investigation, waste cooking oil was transformed to produce biodiesel, utilizing an environmentally benign sulfonated carbon microsphere catalyst.[387] The catalyst with surface area 86 $m^2\ g^{-1}$ and acidity 1.38 mmol g^{-1} was developed by consecutive hydrothermal carbonization and sulfonation of xylose. Using this catalyst, a biodiesel yield of 89.6% was recorded at optimal reaction conditions. The catalyst reusability report revealed that in each cycle, the biodiesel yield was reduced by 9%. Furthermore, the sulfonated carbon-based solid acid catalyst was also utilized for the transformation of PFAD[388] and *Mesua ferrea* Linn oil[389] to biodiesel.

To bring down the cost of biodiesel production, several sulfonated raw biomasses have been prepared and investigated for their catalytic activities. In this line, a sulfonated solid-acid catalyst obtained from coconut shells (SO_4^{2-}/coconut shell) reported 88.03% biodiesel yield.[390] In the same vein, oil palm trunk/sugarcane bagasse,[391] corn straw,[392] bamboo,[393] *Jatropha curcas* seed,[394] bio-glycerol,[395] glycerol,[396] microalgae residue,[397] oil cake waste,[398,399] de-oiled waste cake,[400] de-oiled canola meal-SO_3H,[401] pine chip char[402] and biochar[403,404] are reported as a catalysts for FAME production.

7.3 Enzyme catalyst

In recent years, enzyme catalysts have been widely examined for the production of biodiesel, as they produce high-quality biodiesel, improve the product separation process, mild reaction conditions and most importantly, their ecological benignness (Table 20).[405,406] Besides, they do not form soap with FFA, contrary to the alkaline catalyst. Hence, they can be utilized in biodiesel production on the industrial scale.

In biocatalyst-mediated reactions, enzymes can usually be used in the free form or they can be immobilized on a matrix, *i.e.*, immobilized lipase.[407] The free enzymes are more sensitive

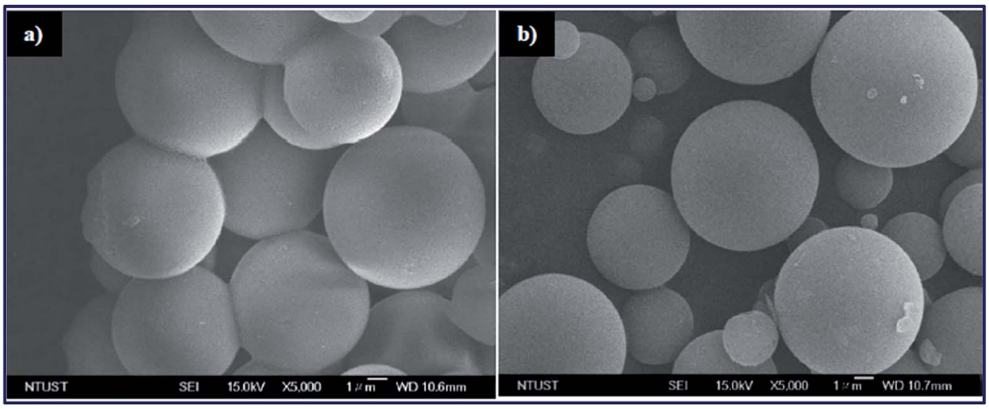

Fig. 32 FESEM images of (a) C and (b) C–SO_3H. Reproduced from ref. 378.

towards the pH, temperature and impurities of the reactants, which may create an obstacle in the bioprocesses. However, these problems can be overcome by immobilizing the enzyme onto different types of support materials.[408] The commonly adopted immobilization methods for biological processes include entrapment, adsorption and covalent bonding. Among these techniques, the entrapment method was found to be effective, offering greater advantages, such as ease of process scale-up, higher stability of the enzyme, and longer enzymatic activity retention.[409,410] Mostly, the lipase enzymes obtained from microbial sources that have been used for biodiesel production[411] proposed the entrapment method for the large scale production of bacterial or fungal lipases due to their extracellular nature. Moreover, lipases obtained from diverse plant sources are also considered as the potential substitute for catalysing the transesterification process.[412] The advantages associated with the lipase catalyst over the other catalysts used in biodiesel production are its superior quality and higher yield of biodiesel, freedom from soap formation, lower reaction temperature and ability to work on a variety of feedstock.[413]

Compared to homogeneous and heterogeneous catalysts, enzymatic catalysts are less studied; hence, there is scant literature that is available when compared with reports on the above-mentioned two catalysts. However, the high cost of the free lipase catalyst along with the limited long-term use has led to the exploitation of the immobilized lipase catalyst to reduce the cost of the catalyst and its reusability. Apart from that, the immobilized lipase catalyst showed greater tolerance to pH variation, high thermal stability and high substrate selectivity.[414,415] To date, a large number of studies in the literature are available in the field of biodiesel production using both free[416–418] and immobilized[419–422] enzyme catalysts.

Recently, Jayaraman *et al.*[423] demonstrated the lipase enzyme-mediated transesterification of waste cooking oil (WCO), and reported 88% of biodiesel yield. Marín-Suárez *et al.*[424] demonstrated the lipase-catalyzed transesterification of low quality fish oil through the process optimization. Moreover, the reusability of the enzyme was also studied. Authors evaluated the efficacy of the commercially available immobilized enzymes, such as Liposome RM IM, Lipozyme TL IM and Novozym 435 (ref. 425) for biodiesel production from waste fish oil. The results obtained revealed that Novozym 435 showed the maximum catalytic activity, resulting in the highest yield of FAME, *i.e.*, 82.91 wt% and the enzyme can be reused for about ten successive cycles. In another study, it was reported that the immobilized lipase (Epobond *P. cepacia*) employed in the transesterification of waste vegetable oil was reported to achieve an ester yield of 46.32%.[426] Similarly, the *Candida cylindracea* lipase immobilised on the functionalised activated carbon was tested as a catalyst in the transesterification of *Jatropha curcas* oil. It was found that a free fatty acid yield of 78% was achieved at the optimized reaction conditions. Furthermore, the biocatalyst was found to be stable for up to four consecutive cycles of transesterification.[427] Besides, the lipase obtained from the plant source (like the rice bran lipase) produced 83.4 wt% FAME yield from rice bran oil under optimized conditions.[428]

Moreover, Muanruksa and Kaewkannetra[429] examined the biodiesel production from sludge palm oil (SPO) *via* two steps of extraction and enzymatic esterification. The immobilised *Rhizopus oryzae* lipases on alginate-polyvinyl alcohol (PVA) beads were used for the conversion of FFAs from SPO to fatty acid methyl esters (biodiesel). It was found that at the optimum condition, the maximum biodiesel yield of 91.30% was achieved and the biocatalyst showed higher stability and catalytic efficiency for up to 15 cycles. It is reported that the enzymatic transesterification reaction for producing biodiesel is the slowest pathway among all of the known transformations. Taking this into account, the application of ultrasonication in the enzyme-catalyzed transesterification improves the reaction rate and hence, reduces the reaction time.[414,422] Thus, it can be a promising technique for the industrial-scale production of biodiesel in a very short time.

Table 20 Different enzyme catalyst yields reported for the production of biodiesel

S. no.	Catalyst	Feedstock	Conditions[a]	Yield	Ref.
1	Lipase immobilized on biosupport beads	Hybrid non edible oils	6 : 1[c], 10, 50, 1440	~78	407
2	Lipase	WCO	3 : 1, 1.5, 65, 240	88	423
3	Thermolysis lanugonosus lipase	Rubber seed oil	4 : 1, 5, NR, 65	92.83	416
4	CalleraTM Trans L lipase	Soybean oil	4.51 : 1, 1.45, 35, 1440	96.9	417
5	Lipase@AC	Sardine oil	9 : 1, 10, 30, 600	94.5	418
6	Lipase@APTES-Fe_3O_4	*Aspergillus* lipid	4 : 1, 300[b], 45, 240	84	419
7	Lipase@ZIF-67	Soybean oil	6 : 1, 10, 45, 3600	78	420
8	Lipase@[bmim][PF_6]	Food compost	6 : 1, 40, 50, 840	72	421
9	Lipase@[bmim][NTf_2]	Food compost	6 : 1, 40, 50, 840	48	421
10	Lipase@Immobead	Blended non-edible oils	7.64 : 1, 3.55, 36, 120	94	422
11	Novozym 435 lipase	Waste fish oil	35.45 : 1[d], 50, 35, 480	82.91 wt%	424
12	Novozym 435 lipase	BSFL fat	14.64 : 1[e], 17.58, 39.5, 720	96.97	425
13	Immobilized lipase (Epobond-*Pseudomonas cepacia)*	Waste vegetable oil	3 : 1[d], 3, 37, 90	46.32	426
14	Immobilized *Candida cylindracea* lipase	*Jatropha curcas* oil	HR, 8, 40, 1440	78	427
15	Immobilised *Rhizopus oryzae* lipase	Sludge palm oil (SPO)	3 : 1, 5, 40, 240	91.30	428
16	Lipase (from rice bran)	Rice bran oil	6 : 1, NR, 40, 17 280	83.4 wt%	429

[a] Methanol-to-oil molar ratio, catalyst loading (wt%), temperature (°C), reaction time (min). NR: not reported. [b] Miligram. [c] 2-Propanol/oil molar ratio. [d] Ethanol/oil molar ratio. [e] Methyl acetate/fat molar ratio.

7.4 Bifunctional solid catalysts

Despite the high reactivity of the basic solid catalyst towards biodiesel production, they are not an effective catalyst for the transesterification of oils having a high amount of FFA, as such catalysts are highly sensitive to the FFA, which leads to soap generation and thus interferes in the separation process of glycerol from biodiesel. On the other hand, solid acid catalysts are insensitive to the FFA content and esterify waste oils or low-cost oils without any requirement of pretreatment. However, water formed during the course of the reaction may lead to the decomposition of triglycerides to diglycerides, resulting in the formation of more FFA and catalyst leaching.[430] Taking these difficulties into account, developing a new type of solid catalyst that possesses dual characteristics, such as solid acidic character, to tackle the FFA and solid basic character for easy transesterification of triglycerides to FAME has been a recent interest in the realm of biodiesel research. To date, numerous bifunctional catalysts are reported for the FAME production (Table 21), which will be discussed in this section. Farooq *et al.*[78] developed a bifunctional Mo–Mn/γ-Al_2O_3–MgO catalyst and utilized it for the simultaneous esterification/transesterification of WCO, having FFA content of 3.27 mg KOH per g. The authors investigated the effect of MgO loading (5–20 wt%) on its catalytic activity, and found that 15 wt% MgO loading showed the highest catalytic activity with 91.4% biodiesel yield under the ideal reaction conditions. Moreover, the catalyst showed excellent stability towards the biodiesel production from WCO, as it is stable for up to 8 progressive reaction cycles without any major loss of its activity. In another study, the Cu/Zn/γ-Al_2O_3 catalyst was utilized for the simultaneous esterification/transesterification of WCO for the production of FAME *via* RSM.[431] The effect of the Cu/Zn wt% ratio and calcination temperature on the catalytic reactivity was also examined, and it was found that the 10 : 90 Cu/Zn wt% ratio and 800 °C calcination temperature showed 88.82% FAME yield. The authors also studied the structure and particle size of the synthesized catalyst *via* TEM micrographs (Fig. 33). Fig. 33a showed that the average diameter of the particles lies in between 4–6 nm. The lattice fringes measured from Fig. 33b, c and d are 0.201, 0.282 and 0.242 nm, and matched with the *hkl* planes (400), (220) and (311) of alumina, respectively. The lattice fringe in Fig. 33e is 0.240 nm fitted with the *hkl* plane (200) of CuO, and the lattice fringe 0.281 nm (Fig. 33f) fitted with the ZnO plane (100). Similarly, the biodiesel production from WCO was reported using diverse bifunctional solid catalysts, such as Mg/MCM-41,[432] γ-Al_2O_3–CeO_2,[433] KAcZX[434] and Sr/ZrO_2.[435]

Nizah *et al.*[436] synthesized a bifunctional catalyst Bi_2O_3–La_2O_3 *via* wet impregnation procedure, and employed it for the one-pot esterification/transesterification of JCO, having a FFA content of 6.1 mg KOH per g. The authors investigated the influence of Bi_2O_3 impregnation on La_2O_3 support by varying the wt% of Bi_2O_3 in the range of 1–7 wt%, and found that 5 wt% Bi_2O_3 impregnated on La_2O_3 showed the maximum biodiesel yield of 94%. The high catalyst reactivity is attributed to the good dispersion of Bi_2O_3 on the La_2O_3 support, which directly enhanced the surface area, and thus increases the selectivity and rate of the reaction. Similarly, the biodiesel production from JCO having a high amount of FFA was reported by using a bifunctional solid catalyst CaO–La_2O_3.[437] The esterification/transesterification was performed in a high-temperature reactor (Fig. 34). The effect of the Ca/La atomic ratio on the catalytic activity was examined, and it was observed that a Ca/La atomic ratio of 0.8 showed the maximum biodiesel yield of 98.76% under the optimized reaction conditions. The high catalytic reactivity is because of the good dispersion of CaO on the surface of La_2O_3, which led to an increase in the catalyst surface area. Moreover, the synthesized catalyst is chemically stable and can be used for 4 consecutive cycles.

Another study revealed the synthesis of the mixed metal oxide Mn@MgO–ZrO_2 *via* co-precipitation and impregnation method, and the utilization of the catalyst in the FAME production from kernel oil.[438] The efficiency of the catalyst in the FAME production was tested by changing the Mg/Zr ratio from 0.2 to 0.5, and it was found that 0.4 Mg/Zr has the optimal active sites, followed by impregnation of 4 wt% Mn to the MgO–ZrO_2 composite to enhance its reactivity and displayed 96.4% biodiesel yield. The high catalyst reactivity is due to a large number of active sites and

Table 21 Different bifunctional solid catalyst yields reported for biodiesel production

No	Catalyst	Feedstocks	Conditions[a]	Yield (%)	Ref.
1	Mo–Mn/γ-Al_2O_3-15% MgO	WCO	27 : 1, 3, 100, 240	91.4	78
2	Cu/Zn(10 : 90)/γ-Al_2O_3-800 °C	WCO	18 : 1, 6, 65 ± 5, 180	88.82	431
3	Mg/MCM-41	WCO	8 : 1, 10, 80, 180	94	432
4	γ-Al_2O_3–CeO_2	WCO	30 : 1, 7, 110, 270	81.1	433
5	KAcZX	WCO	48 : 1, 6, 120, 180	80.8	434
6	Sr/ZrO_2	WCO	29 : 1, 2.7, 115.5, 169	79.7	435
7	Bi_2O_3–La_2O_3	JCO	15 : 1, 2, 150, 240	94	436
8	CaO–La_2O_3	JCO	25 : 1, 3, 160, 180	98.76	437
9	Mn@MgO–ZrO_2	Kernel oil	15 : 1, 3, 90, 240	96.4	438
10	HPA@ZIF-8	Rapeseed oil	10 : 1, 4, 240, 300	98.02[b]	439
11	AWS/SO_4^{2-}	PFAD	15 : 1, 5, 80, 180	98	441
12	$[Zn(4,4'\text{-bipy})(OAc)_2]_n$	Soybean oil	3.2/5 (v/v), 2, 180, 120	98	442
13	K/TiO_2	Canola oil	36 : 1, 6, 70, 180	100[b]	443

[a] Methanol-to-oil molar ratio, catalyst loading (wt%), temperature (°C), reaction time (min). [b] Conversion.

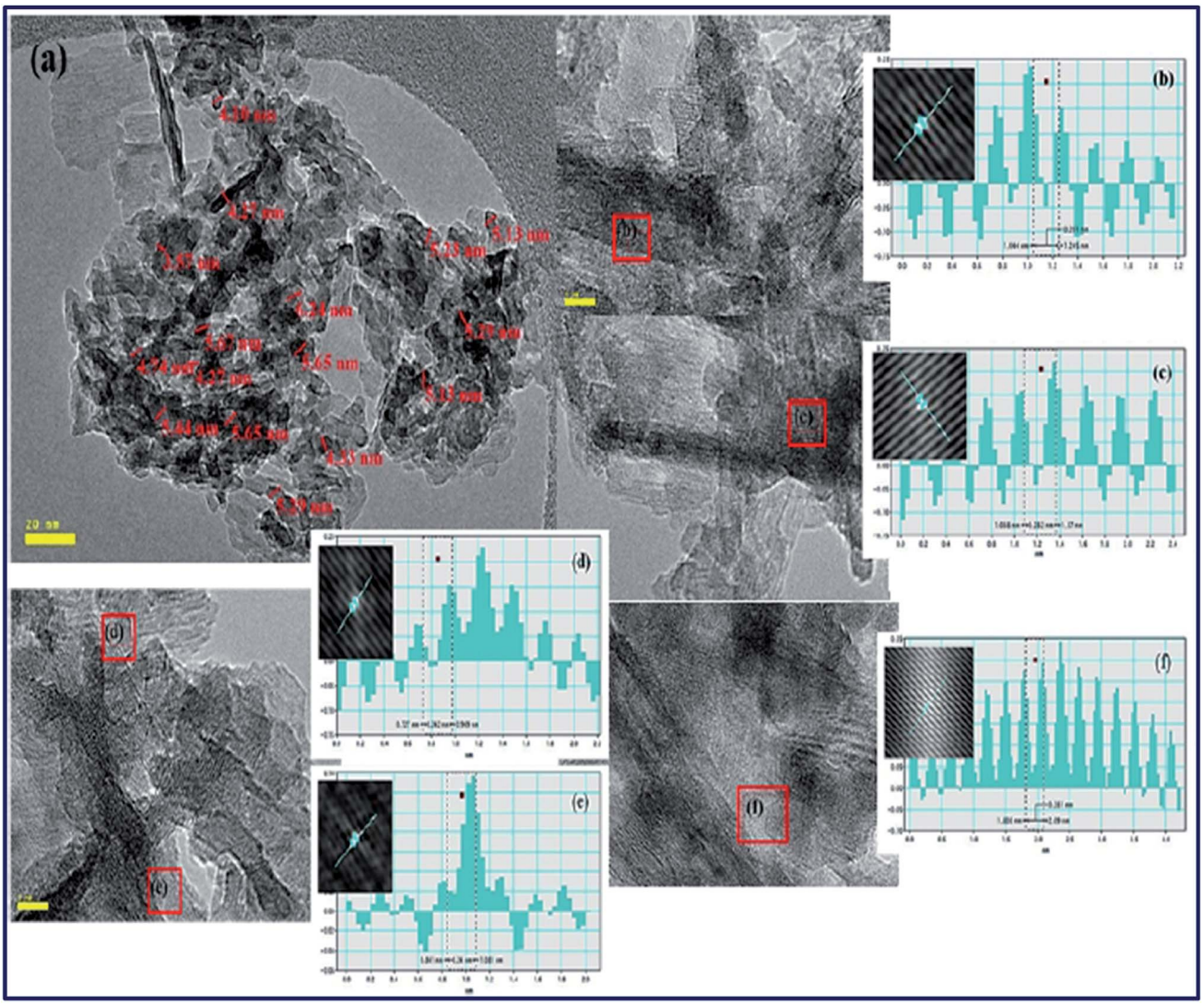

Fig. 33 TEM micrograph for Cu/Zn(10 : 90)/γ-Al_2O_3-800 °C (a). The HRTEM images displayed the lattice fringes of (b) Al_2O_3 (400), (c) Al_2O_3 (220), (d) Al_2O_3 (311), (e) CuO (200) and (f) ZnO (100). Reproduced from ref. 431.

the mesoporous nature of the catalyst. Jeon *et al.*[439] synthesized heteropolyacid (HPA) functionalized ZIF-8 (zeolite imidazole framework-8) to form a bifunctional catalyst for the production of biodiesel from rapeseed oil in a batch reactor. The catalyst possesses a core–shell nanostructure as displayed by the TEM micrograph (Fig. 35), where the rhombic dodecahedral ZIF-8 core was surrounded by thin-wrinkled HPA shell, and thus enhances the surface area and catalyst reactivity. Moreover, the effect of the concentration of HPA for the functionalization was also tested by varying the amount of HPA, such as 0.05, 0.1, 0.3 and 0.5. It was found that 0.1 g HPA functionalized ZIF-8 showed a maximum FAME conversion of 98.02% under the optimized reaction conditions. Similarly, another bifunctional catalyst organo-triphosphonic acid-functionalized ferric alginate (ATMP-FA) was developed for the oleic acid esterification to produce biodiesel.[440] The reaction conditions were optimized by using the Box–Behnken model of RSM. Moreover, the catalyst is very stable towards the esterification reaction, and can be reused for 5 consecutive cycles.

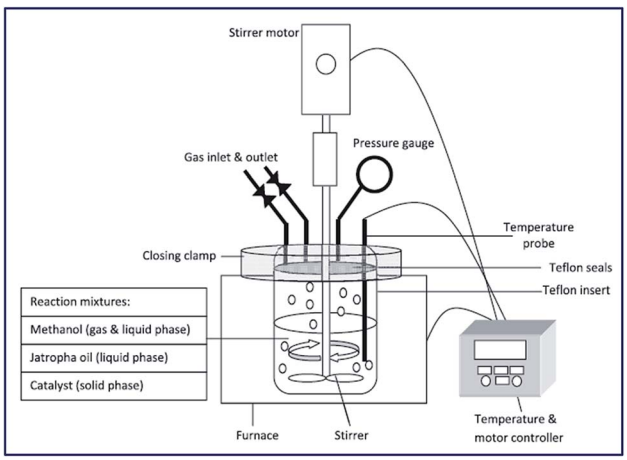

Fig. 34 Schematic diagram of a high-temperature reactor. Reproduced from ref. 437.

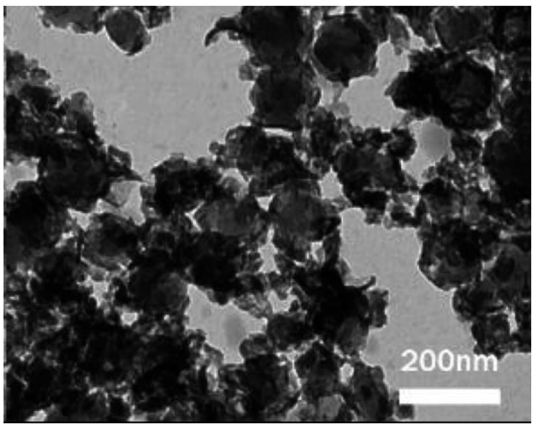

Fig. 35 TEM image of HPA-ZIF-8. Reproduced from ref. 439.

Recently, a solid bifunctional catalyst originating from the bio-waste angel wing shell (AWS) *via* two-step processes: (i) calcination of angel wing shell, and (ii) sulfonation of the calcined angel wing shell to produce sulfonated angel wing shell (AWS/SO_4^{2-}), was reported for the esterification of PFAD to produce biodiesel.[441] The sulfonation procedure increases the surface area of bare AWS from 3.88 to 6.53 $m^2\ g^{-1}$, and thus enhanced the catalytic reactivity. The authors tested the influence of the sulfuric acid concentration by varying the sulfuric acid amount from 3 to 11 M, and found that the sulfonation with 7 M sulfuric acid showed 98% FAME yield. The authors also checked the reusability of the catalyst, and observed a blockage of the active sites of the catalyst after the 2nd consecutive cycles, which necessitated pretreatment of the spent catalyst to increase its reusability. In addition, a coordinated polymer of Zn, $[Zn(4,4'\text{-bipy})(OAc)_2]_n$, was tested for the soybean oil transformation to FAME.[442] The catalyst showed excellent reactivity and showed 98% FAME yield under the optimized reaction conditions. The authors reported that the high reactivity of the catalyst is attributed to the bipyridine present in the catalyst. In another study, the conversion of canola oil to FAME was reported using potassium-impregnated titania (K/TiO_2).[443] The addition of K on the surface of titania increases the surface energy from 86 to 102 $m^2\ g^{-1}$, and thus enhanced the catalytic activity. The authors investigated the effect of K loading on the catalytic activity, and found that 20 wt% K-loaded titania was optimal and showed 100% conversion of canola oil to biodiesel.

8. Biodiesel production process

Biodiesel can be produced by (trans)esterification, thermal cracking and pyrolysis.[444–447] Among all these methods, transesterification is generally utilized for the synthesis of biodiesel.[447] The generalized diagram for the biodiesel production process is presented in Fig. 36, which consists of the synthesis and purification steps.[447] Alkali, acid and enzyme are routinely exploited as a catalyst for the transesterification reactions. These catalysts had their own merits and demerits, as compiled in Table 22.[448] Until now, the homogeneous base catalysts (such as NaOH, KOH) are normally utilized for biodiesel synthesis in the industrial scale. In the meantime, owing to their capacity to catalyze both esterification/transesterification reactions, a homogeneous acid catalyst (such as H_2SO_4) and HCl are generally picked for feedstock having high FFA, such as non-edible vegetable oil, WCO and animal fats. Recently, the heterogeneous catalyst has attracted interest to a great extent

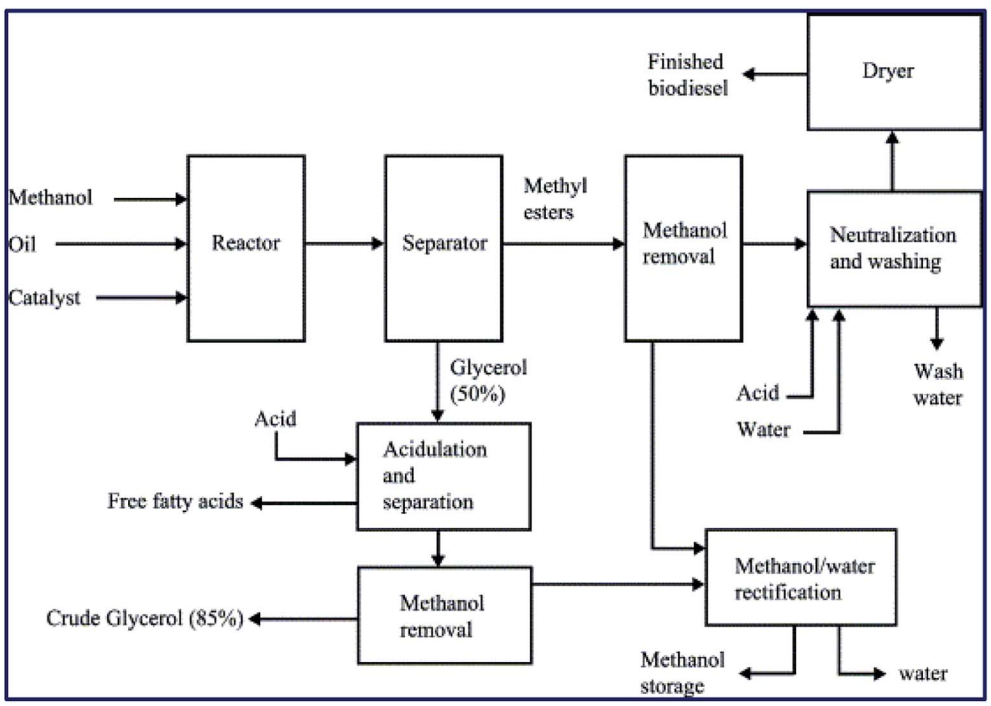

Fig. 36 Representative diagram for biodiesel production. Reproduced from ref. 447.

Table 22 Points of interest and detriments of different catalysts utilized for the transesterification/esterification reaction (reproduced from ref. 448)

Catalyst types	Examples	Advantages	Disadvantages
Homogeneous			
Alkali	NaOH, KOH	• High reactivity	• Inappropriate for high FFA in feedstocks
		• Faster reaction rate	• Deactivates in the presence of moisture and FFA.
		• Minimum cost	• Requirement of high amount of waste water
		• Encouraging kinetics	• Saponification occurs as a side reaction.
		• Moderate working conditions	• Non-recyclable
			• Corrosive in nature
Acid	H_2SO_4, HCl, HF.	– Non-reactive to moisture and FFA content in oil.	– Slow reaction rate
		– Catalyzed simultaneous esterification/ transesterification reactions.	– Long reaction time
		– Avoids formation of soap.	– Equipment corrosion
			– Higher reaction temperature and pressure
			– High alcohol/oil requirement
			– Weak catalytic activity
			– Catalyst is difficult to recycle
Heterogeneous			
Alkali	CaO, SrO, MgO, mixed oxide and hydrotalcite	• Non-corrosive	• Slow reaction rate compared to homogeneous one
		• Environmentally benign	• Low FFA requirement in the feedstock (<1 wt%)
		• Recyclable	• Highly sensitive to water and FFA
		• Fewer disposal problems	• Saponification as a side reaction
		• Easy separation	• Soap formation
		• Higher selectivity	• High volume of wastewater
		• Longer catalyst life	• Leaching of active catalyst sites
			• Diffusion limitations
			• Complex and expensive synthesis route
			• High cost of catalyst synthesis
Acid	ZrO, TiO, ZnO, ion-exchange resin, sulfonic modified	– Insensitive to FFA and water content in the oil	– Moderate reaction rate
	Mesostructured silica	– Catalyzed simultaneous esterification and transesterification reactions	– Long reaction time
		– Recyclable, eco-friendly	– Higher reaction temperature and pressure
		– Non-corrosive to reactor and reactor parts	– High alcohol/oil requirement
			– Weak catalytic activity
			– Low acidic site
			– Low micro porosity
			– Leaching of active catalyst sites
			– Diffusion limitations
			– Complex and expensive synthesis route
			– High cost of catalyst synthesis

for biodiesel synthesis because of their easy recyclability and reusability for successive reaction cycles.

9. Catalyst comparison

It can be seen from the literature that the reactivity of both homogeneous base and acid catalysts are very high compared to heterogeneous catalysts.[61,70] Despite the high reactivity, homogeneous catalysts have some serious shortfalls. These include the low quality of glycerol produced, the inability to regenerate the catalyst, and the lengthy process involved in the purification of biodiesel. Thus, the whole process becomes labour-intensive and uneconomical.[76] To overcome these shortfalls, solid catalysts have been widely investigated. Alkaline earth, basic metal oxides and supported solid base catalysts show excellent activity towards biodiesel production. However,

their low stability and high sensitivity against the FFA limit its industrial application.[143] In contrast, their acid counterparts are not efficient towards the transesterification reactions. Recently, mixed metal oxides are gaining immense attention in the field of biodiesel production due to their generally high surface area, excellent thermal and chemical stability, and tailored acid–base properties. Hence, they can be predominantly used for the (trans)esterification of vegetable oil having high FFA.[145]

Prior studies from literature revealed that the enzyme-based catalysts have various advantages over other catalysts, such as being environmentally benign, operating at mild reaction conditions and displaying high specificity.[432] Unfortunately, due to their sensitivity towards heat, poor operational stability and narrow pH range, the use of such catalysts for the industrial scale production of biodiesel is not a wise choice.[433] However, the immobilized lipase has various advantages compared to free lipase, such as cost-effectiveness, high thermal stability and greater tolerance to pH changes.[435] Thus, it has a scope for utilization in biodiesel production on the industrial scale. Besides, the present study suggests that the bio-waste derived catalyst can potentially be used in the industrial scale production of biodiesel as they are easily available, cost-effective and most importantly, environmentally benign.[161] The main limitation is their reusability due to the leaching of the active sites.[165] Apart from that, the metal-free carbon based solid acid catalyst is also a promising candidate for the industrial scale production of biodiesel as these materials possess promising features, such as being biogenic and environment-friendly, and having lower production costs, distinctive surface chemistry, high chemical and thermal stability.[383] The bifunctional catalyst has been of recent interest in the realm of biodiesel research, as it possesses dual characteristics such as solid acidic character to tackle the FFA and solid basic character for the easy transesterification of triglycerides to FAME. Hence, it can be utilized for the (trans)esterification of diverse oil systems. Apart from that, the bifunctional catalysts are highly reusable, thermostable and insensitive to the moisture.[438] Thus, the bifunctional solid catalyst can be utilized in the successful production of industrial scale biodiesel.

10. Conclusion and outlook

The exponential growth in the human population around the globe and industrial globalization tremendously increases the demand for petroleum fuels like diesel for various purposes. However, considering the limited resources of fossil fuels, searching for a novel, renewable and sustainable alternative fuel was required. In this context, researchers focused on the FAME production from different renewable sources as an effective way. A variety of methods have been proposed for biodiesel production. However, among all the existing methods, transesterification is considered as the foremost choice.

The transesterification reaction involves the use of a basic catalyst, such as homogeneous and heterogeneous catalysts. The use of homogeneous catalysts is found to be promising as far as the rate of biodiesel production is concerned. However, it is associated with certain limitations. The homogeneous catalyst-based transesterification reaction involves the consumption of high energy. Moreover, the treatment of wastewater generated is essential due to the presence of unreacted chemicals. These limitations created the need for the development of efficient catalysts, which was completed in terms of the heterogeneous catalysts. These catalysts attracted a great deal of attention from the scientific community all over the world because of its several advantages over homogeneous catalysts, such as the simple realization of continuous reactors, production of cleaner glycerol, and the absence of both the alkaline catalyst neutralization step and the necessity to replace the consumed catalyst. Due to these advantages, heterogeneous catalysts have opened up the chance for another powerful pathway for FAME production. However, the reactivity of the solid catalyst is dependent on several variables, which mainly involve the oil type, alcohol to oil molar ratio, temperature, and type of reactor. Therefore, the selection of these variables at an optimum level is a crucial step. The heterogeneous catalysts are considered comparatively promising because only the external-surface active species of the porous solid support is involved in the reaction, and these catalysts can be recovered in some cases. However, in the case of certain catalysts like CaO, leaching was reported, which adversely influences the reaction. Hence, researchers are looking at nanotechnology as a new hope.

Nanotechnology is the most emerging branch of science, having promising applications in catalysis. Moreover, it is reported to have the ability to fabricate the catalyst surface in order to meet the prerequisites of explicit applications, and beat the different issues related to both homogeneous and heterogeneous catalysts. Nanocatalysts can act as an interface between the homogeneous and heterogeneous catalysts having the possibility to develop promising solid-acid or solid-base catalysts, which can be easily recovered using conventional filtration and centrifugation techniques. The development and use of magnetic nanoparticle-supported catalysts is a path-breaking research because such catalysts can be easily recovered by using a simple magnetic field and reused for progressive reaction cycles, which helps to reduce the overall process cost involved in biodiesel production, which is the ultimate aim.

It is well proven that the application of a biological catalyst (enzyme) is more effective over all kinds of chemical catalysts, but the involvement of an expensive enzyme increases the overall cost of the FAME production process. In this context, immobilization of such enzymes on the surface of various magnetic nanoparticles was found to be a novel concept because of the easy recovery of the immobilized enzyme, along with magnetic nanoparticles and its reusability. Moreover, it also solves the problem of leaching the enzymes during the reaction due to immobilization. Although nanocatalysts were reported to have promising applications, the toxicological concerns associated with nanoparticles are a topic of debate because there are mixed opinions from the scientific community.

The present study revealed that the properties of the catalyst (such as basicity and acidity) play a pivotal role in the biodiesel production. Several literature studies suggest that the basicity of the catalyst is directly proportional to the transesterification

activity.[171,195] Similarly, the acidity of the catalyst decides the esterification activity of the catalyst.[383,390] The esterification activity increases with increasing acidity of the catalyst. Apart from the basicity and acidity, the catalytic activity of the solid catalyst depends on its surface area and porosity. Literature studies revealed that the high surface area of the catalyst enhances the rate of biodiesel production.[184,225]

It is believed that several newly introduced catalysts will take a central position in the near future, and help produce biodiesel through eco-friendly and economically viable processes. The development of a novel heterogeneous catalyst having both acid and basic sites on its surface will have a promising future in biodiesel production technologies because it will have the ability to overcome the issues usually caused because of the utilization of homogeneous catalysts. The application of bifunctional solids can be a novel way in heterogeneous catalyst-mediated biodiesel production because they showed the capability to accomplish the simultaneous esterification and transesterification reactions in a one-pot process. In addition, the development and application of the nanocatalysts will be a milestone in biodiesel production. These nanocatalysts will be the next-generation catalysts, which will help to develop the most effective, sensitive, sustainable and economically viable technology for the FAME production in the near future. Although recent advances in the developments of various homogeneous, heterogeneous and nanocatalysts showed a promising future for biodiesel industries or biorefineries, more efforts are required to develop even more effective and cheap catalysts, which will help overcome the present issues with all of the above-mentioned catalysts and increase the efficiency of sustainable biodiesel production.

Conflicts of interest

There are no conflicts to declare.

Acknowledgements

The Science and Engineering Research Board (SERB), India is thankfully acknowledged for the research fund (Grant No. SB/FT/CS-103/2013 and SB/EMEQ-076/2014).

References

1 G. Ciarrocchi, A. Montecucco, G. Pedrali-Noy and S. Spadari, *Biochem. Pharmacol.*, 1988, **37**, 1803–1804.
2 X. Yin, X. Duan, Q. You, C. Dai, Z. Tan and X. Zhu, *Energy Convers. Manage.*, 2016, **112**, 199–207.
3 International Renewable Energy Agency (IRENA), *Global Energy Transformation: A Roadmap to 2050*, 2018.
4 IEA, *Int. Energy Agency, Peris*, 2016, pp. 1–77.
5 M. G. Kulkarni and A. K. Dalai, *Ind. Eng. Chem. Res.*, 2006, **45**, 2901–2913.
6 S. Chatterjee, Dhanurdhar and L. Rokhum, *Renewable Sustainable Energy Rev.*, 2017, **72**, 560–564.
7 A. da Silva César, M. A. Conejero, E. C. Barros Ribeiro and M. O. Batalha, *Renewable Energy*, 2019, **133**, 1147–1157.
8 M. T. Lund, T. K. Berntsen and J. S. Fuglestvedt, *Environ. Sci. Technol.*, 2014, **48**, 14445–14454.
9 F. C. De Oliveira and S. T. Coelho, *Renewable Sustainable Energy Rev.*, 2017, **75**, 168–179.
10 J. Ling, S. Nip, W. L. Cheok, R. A. de Toledo and H. Shim, *Bioresour. Technol.*, 2014, **173**, 132–139.
11 L. E. Singer and D. Peterson, *International energy outlook*, 2010, p. 0484.
12 D. Y. C. Leung, X. Wu and M. K. H. Leung, *Appl. Energy*, 2010, **87**, 1083–1095.
13 G. Pathak, D. Das and L. Rokhum, *RSC Adv.*, 2016, **6**, 93729–93740.
14 G. Pathak and L. Rokhum, *ACS Comb. Sci.*, 2015, **17**, 483–487.
15 B. Mallesham, P. Sudarsanam and B. M. Reddy, *Ind. Eng. Chem. Res.*, 2014, **53**, 18775–18785.
16 B. H. Hameed, L. F. Lai and L. H. Chin, *Fuel Process. Technol.*, 2009, **90**, 606–610.
17 D. R. Lathiya, D. V. Bhatt and K. C. Maheria, *Bioresour. Technol. Rep.*, 2018, **2**, 69–76.
18 J. M. Encinar, N. Sánchez, G. Martínez and L. García, *Bioresour. Technol.*, 2011, **102**, 10907–10914.
19 L. Li, W. Du, D. Liu, L. Wang and Z. Li, *J. Mol. Catal. B: Enzym.*, 2006, **43**, 58–62.
20 J. Kansedo, K. T. Lee and S. Bhatia, *Biomass Bioenergy*, 2009, **33**, 271–276.
21 M. N. Nabi, M. M. Rahman and M. S. Akhter, *Appl. Therm. Eng.*, 2009, **29**, 2265–2270.
22 S. V. Ghadge and H. Raheman, *Biomass Bioenergy*, 2005, **28**, 601–605.
23 X. Meng, G. Chen and Y. Wang, *Fuel Process. Technol.*, 2008, **89**, 851–857.
24 S. A. Shaban, *Egypt. J. Chem.*, 2012, **55**, 437–452.
25 H. N. Bhatti, M. A. Hanif, M. Qasim and A.-u. Rehman, *Fuel*, 2008, **87**, 2961–2966.
26 P. Cao, M. A. Dubé and A. Y. Tremblay, *Biomass Bioenergy*, 2008, **32**, 1028–1036.
27 H. Y. Shin, S. H. Lee, J. H. Ryu and S. Y. Bae, *J. Supercrit. Fluids*, 2012, **61**, 134–138.
28 M. Gürü, A. Koca, Ö. Can, C. Çinar and F. Şahin, *Renewable Energy*, 2010, **35**, 637–643.
29 E. Alptekin and M. Canakci, *Fuel*, 2010, **89**, 4035–4039.
30 C. Y. Lin and R. J. Li, *Fuel Process. Technol.*, 2009, **90**, 130–136.
31 J. F. Costa, M. F. Almeida, M. C. M. Alvim-Ferraz and J. M. Dias, *Energy Convers. Manage.*, 2013, **74**, 17–23.
32 B. M. S. Hossain and S. Aishah, *Am. J. Biochem. Biotechnol.*, 2008, **4**, 250–254.
33 G. Najafi, B. Ghobadian and T. F. Yusaf, *Renewable Sustainable Energy Rev.*, 2011, **15**, 3870–3876.
34 L. Chen, T. Liu, W. Zhang, X. Chen and J. Wang, *Bioresour. Technol.*, 2012, **111**, 208–214.
35 U. Zur and R. V. O. N. Oel-proteinpflanzen, *Union Zur Förderung Von Oel- Und Proteinpflanzen E.V.*, 2017, p. 51.
36 I. M. Atadashi, M. K. Aroua, A. R. Abdul Aziz and N. M. N. Sulaiman, *J. Ind. Eng. Chem.*, 2013, **19**, 14–26.

37 S. P. Singh and D. Singh, *Renewable Sustainable Energy Rev.*, 2010, **14**, 200–216.
38 S. D. A. P. Apptanaidu, A. M. Ali and M. H. Alias, *J. Ekon. Malaysia*, 2014, **48**, 29–40.
39 B. Flach, S. Lieberz, M. Rondon, B. Williams and C. Teiken, *GAIN Report: EU-28 Biofuels Annual,* 2015, pp. 14–21.
40 R. Delzeit, T. Heimann, F. Schuenemann and M. Soeder. *GTAP*, 2019.
41 U. Zur and R. V. O. N. Oel-proteinpflanzen, *Union Zur Förderung Von Oel- Und Proteinpflanzen E.V*. 2015.
42 J. L. Shumaker, C. Crofcheck, S. A. Tackett, E. Santillan-Jimenez and M. Crocker, *Catal. Lett.*, 2007, **115**, 56–61.
43 K. Bélafi-Bakó, F. Kovács, L. Gubicza and J. Hancsók, *Biocatal. Biotransform.*, 2002, **20**, 437–439.
44 S. Yan, H. Lu and B. Liang, *Energy Fuels*, 2008, **22**, 646–651.
45 D. A. G. Aranda, R. T. P. Santos, N. C. O. Tapanes, A. L. D. Ramos and O. A. C. Antunes, *Catal. Lett.*, 2008, **122**, 20–25.
46 M. R. Avhad and J. M. Marchetti, *Renewable Sustainable Energy Rev.*, 2015, **50**, 696–718.
47 A. Karmakar, S. Karmakar and S. Mukherjee, *Bioresour. Technol.*, 2010, **101**, 7201–7210.
48 M. M. Gui, K. T. Lee and S. Bhatia, *Energy*, 2008, **33**, 1646–1653.
49 K. Shikha and C. Y. Rita, *J. Chem. Pharm. Res.*, 2012, **4**, 4219–4230.
50 A. L. Ahmad, N. H. M. Yasin, C. J. C. Derek and J. K. Lim, *Renewable Sustainable Energy Rev.*, 2011, **15**, 584–593.
51 S. L. Dmytryshyn, A. K. Dalai, S. T. Chaudhari, H. K. Mishra and M. J. Reaney, *Bioresour. Technol.*, 2004, **92**, 55–64.
52 S. Yusup and M. A. Khan, *Biomass Bioenergy*, 2010, **34**, 1500–1504.
53 J. M. Dias, M. C. M. Alvim-Ferraz and M. F. Almeida, *Fuel*, 2008, **87**, 3572–3578.
54 U. Rashid and F. Anwar, *Fuel*, 2008, **87**, 265–273.
55 J. M. Encinar, J. F. González and A. Rodríguez-Reinares, *Fuel Process. Technol.*, 2007, **88**, 513–522.
56 A. A. Refaat, N. K. Attia, H. A. Sibak, S. T. El Sheltawy and G. I. ElDiwani, *Int. J. Environ. Sci. Technol.*, 2008, **5**, 75–82.
57 M. P. Dorado, E. Ballesteros, M. Mittelbach and F. J. López, *Energy Fuels*, 2004, **18**, 1457–1462.
58 O. J. Alamu, S. O. Jekayinfa and T. A. Akintola, *Agric. Eng.*, 2007, **9**, 1–11.
59 K. H. Chung, J. Kim and K. Y. Lee, *Biomass Bioenergy*, 2009, **33**, 155–158.
60 S. K. Karmee and A. Chadha, *Bioresour. Technol.*, 2005, **96**, 1425–1429.
61 P. Felizardo, M. J. Neiva Correia, I. Raposo, J. F. Mendes, R. Berkemeier and J. M. Bordado, *Waste Manage.*, 2006, **26**, 487–494.
62 B. B. Uzun, M. Kiliç, N. Özbay, A. E. Pütün and E. Pütün, *Energy*, 2012, **44**, 347–351.
63 D. Y. C. Leung and Y. Guo, *Fuel Process. Technol.*, 2006, **87**, 883–890.
64 U. Rashid, F. Anwar, B. R. Moser and S. Ashraf, *Biomass Bioenergy*, 2008, **32**, 1202–1205.
65 Z. Ilham, *Malays. J. Biochem. Mol. Biol.*, 2009, **17**, 5–9.
66 S. T. Keera, S. M. El Sabagh and A. R. Taman, *Fuel*, 2011, **90**, 42–47.
67 U. Rashid, F. Anwar, T. M. Ansari, M. Arif and M. Ahmad, *J. Chem. Technol. Biotechnol.*, 2009, **84**, 1364–1370.
68 K. S. Chen, Y. C. Lin, K. H. Hsu and H. K. Wang, *Energy*, 2012, **38**, 151–156.
69 K. Jacobson, R. Gopinath, L. C. Meher and A. K. Dalai, *Appl. Catal., B*, 2008, **85**, 86–91.
70 Y. Wang, S. Ou, P. Liu, F. Xue and S. Tang, *J. Mol. Catal. A: Chem.*, 2006, **252**, 107–112.
71 M. Canakci and J. Van Gerpen, *Trans. ASAE*, 1999, **42**, 1203–1210.
72 X. Miao, R. Li and H. Yao, *Energy Convers. Manage.*, 2009, **50**, 2680–2684.
73 M. J. Nye, T. W. Williamson, W. Deshpande, J. H. Schrader, W. H. Snively, T. P. Yurkewich and C. L. French, *J. Am. Oil Chem. Soc.*, 1983, **60**, 1598–1601.
74 J. Zhang and L. Jiang, *Bioresour. Technol.*, 2008, **99**, 8995–8998.
75 V. B. Veljković, S. H. Lakićević, O. S. Stamenković, Z. B. Todorović and M. L. Lazić, *Fuel*, 2006, **85**, 2671–2675.
76 P. Dalvand and L. Mahdavian, *Biofuels*, 2018, **9**, 705–710.
77 Y. Ma, Q. Wang, X. Sun, C. Wu and Z. Gao, *Renewable Energy*, 2017, **107**, 522–530.
78 M. Farooq, A. Ramli and D. Subbarao, *J. Cleaner Prod.*, 2013, **59**, 131–140.
79 M. Zabeti, W. M. A. Wan Daud and M. K. Aroua, *Fuel Process. Technol.*, 2009, **90**, 770–777.
80 T. F. Dossin, M. F. Reyniers, R. J. Berger and G. B. Marin, *Appl. Catal., B*, 2006, **67**, 136–148.
81 M. C. Math, S. P. Kumar and S. V. Chetty, *Energy Sustainable Dev.*, 2010, **14**, 339–345.
82 M. Kouzu, S.-y. Yamanaka, J.-s. Hidaka and M. Tsunomori, *Appl. Catal., A*, 2009, **355**, 94–99.
83 M. L. Granados, M. D. Z. Poves, D. M. Alonso, R. Mariscal, F. C. Galisteo, R. Moreno-Tost, J. Santamaría and J. L. G. Fierro, *Appl. Catal., B*, 2007, **73**, 317–326.
84 A. Kawashima, K. Matsubara and K. Honda, *Bioresour. Technol.*, 2009, **100**, 696–700.
85 X. Liu, H. He, Y. Wang and S. Zhu, *Catal. Commun.*, 2007, **8**, 1107–1111.
86 H. Mootabadi, B. Salamatinia, S. Bhatia and A. Z. Abdullah, *Fuel*, 2010, **89**, 1818–1825.
87 J. Jitputti, B. Kitiyanan, P. Rangsunvigit, K. Bunyakiat, L. Attanatho and P. Jenvanitpanjakul, *Chem. Eng. J.*, 2006, **116**, 61–66.
88 M. Stöcker, *J. Mol. Catal.*, 1985, **29**, 371–377.
89 S. J. Yoo, H.-s. Lee, B. Veriansyah, J. Kim, J. D. Kim and Y. W. Lee, *Bioresour. Technol.*, 2010, **101**, 8686–8689.
90 R. B. da Silva, A. F. Lima Neto, L. S. Soares dos Santos, J. R. de Oliveira Lima, M. H. Chaves, J. R. dos Santos, G. M. de Lima, E. M. de Moura and C. V. R. de Moura, *Bioresour. Technol.*, 2008, **99**, 6793–6798.
91 G. Baskar, A. Gurugulladevi, T. Nishanthini, R. Aiswarya and K. Tamilarasan, *Renewable Energy*, 2017, **103**, 641–646.

92 S. Nakagaki, A. Bail, V. C. dos Santos, V. H. R. de Souza, H. Vrubel, F. S. Nunes and L. P. Ramos, *Appl. Catal., A*, 2008, **351**, 267–274.
93 M. Di Serio, M. Cozzolino, R. Tesser, P. Patrono, F. Pinzari, B. Bonelli and E. Santacesaria, *Appl. Catal., A*, 2007, **320**, 1–7.
94 B. Rongxian, T. Yisheng and H. Yizhuo, *Fuel Process. Technol.*, 2004, **86**, 293–301.
95 A. P. S. Chouhan and A. K. Sarma, *Renewable Sustainable Energy Rev.*, 2011, **15**, 4378–4399.
96 W. Xie, X. Huang and H. Li, *Bioresour. Technol.*, 2007, **98**, 936–939.
97 Q. Shu, B. Yang, H. Yuan, S. Qing and G. Zhu, *Catal. Commun.*, 2007, **8**, 2159–2165.
98 M. J. Ramos, A. Casas, L. Rodríguez, R. Romero and Á. Pérez, *Appl. Catal., A*, 2008, **346**, 79–85.
99 H. Wu, J. Zhang, Q. Wei, J. Zheng and J. Zhang, *Fuel Process. Technol.*, 2013, **109**, 13–18.
100 M. Feyzi and G. Khajavi, *Ind. Crops Prod.*, 2014, **58**, 298–304.
101 N. Narkhede and A. Patel, *Ind. Eng. Chem. Res.*, 2013, **52**, 13637–13644.
102 O. Babajide, N. Musyoka, L. Petrik and F. Ameer, *Catal. Today*, 2012, **190**, 54–60.
103 M. C. Manique, L. V. Lacerda, A. K. Alves and C. P. Bergmann, *Fuel*, 2017, **190**, 268–273.
104 N. Al-Jammal, Z. Al-Hamamre and M. Alnaief, *Renewable Energy*, 2016, **93**, 449–459.
105 L. Du, S. Ding, Z. Li, E. Lv, J. Lu and J. Ding, *Energy Convers. Manage.*, 2018, **173**, 728–734.
106 S. Semwal, A. K. Arora, R. P. Badoni and D. K. Tuli, *Bioresour. Technol.*, 2011, **102**, 2151–2161.
107 A. Bohlouli and L. Mahdavian, *Biofuels*, 2019, 1–14.
108 W. Xie and H. Li, *J. Mol. Catal. A: Chem.*, 2006, **255**, 1–9.
109 J. Paulo, A. Duarte, L. Di and A. Souza, *Renewable Sustainable Energy Rev.*, 2016, **59**, 887–894.
110 H. Ma, S. Li, B. Wang, R. Wang and S. Tian, *J. Am. Oil Chem. Soc.*, 2008, 263–270.
111 Y. Chen, Y. Huang, R. Lin, N. Shang and C. Chang, *J. Taiwan Inst. Chem. Eng.*, 2011, **42**, 937–944.
112 X. Zhang, Q. Ma, B. Cheng, J. Wang, J. Li and F. Nie, *J. Nat. Gas Chem.*, 2012, **21**, 774–779.
113 E. S. Umdu, M. Tuncer and E. Seker, *Bioresour. Technol.*, 2009, **100**, 2828–2831.
114 M. Zabeti, W. Mohd, A. Wan and M. K. Aroua, *Fuel Process. Technol.*, 2010, **91**, 243–248.
115 C. Samart, C. Chaiya and P. Reubroycharoen, *Energy Convers. Manage.*, 2010, **51**, 1428–1431.
116 T. Witoon, S. Bumrungsalee, P. Vathavanichkul and S. Palitsakun, *Bioresour. Technol.*, 2014, **156**, 329–334.
117 H. Wu, J. Zhang, Y. Liu, J. Zheng and Q. Wei, *Fuel Process. Technol.*, 2014, **119**, 114–120.
118 B. Narowska, M. Kułażyński, M. Łukaszewicz and E. Burchacka, *Renewable Energy*, 2019, **135**, 176–185.
119 A. Buasri, B. Ksapabutr, M. Panapoy and N. Chaiyut, *Korean J. Chem. Eng.*, 2012, **29**, 1708–1712.
120 L. J. Konwar, J. Boro and D. Deka, *Energy Sources, Part A*, 2018, **40**, 601–607.
121 B. H. Hameed, C. S. Goh and L. H. Chin, *Fuel Process. Technol.*, 2009, **90**, 1532–1537.
122 S. Baroutian, M. K. Aroua, A. Aziz, A. Raman, N. Meriam and N. Sulaiman, *Fuel Process. Technol.*, 2010, **91**, 1378–1385.
123 X. Li, Y. Zuo, Y. Zhang, Y. Fu and Q. Guo, *Fuel*, 2013, **113**, 435–442.
124 A. Buasri, N. Chaiyut, V. Loryuenyong and C. Rodklum, *ScienceAsia*, 2012, **38**, 283–288.
125 Z. Wan and B. H. Hameed, *Bioresour. Technol.*, 2011, **102**, 2659–2664.
126 A. B. Fadhil, A. M. Aziz and M. H. Altamer, *Fuel*, 2016, **170**, 130–140.
127 H. Liu, L. Su, Y. Shao and L. Zou, *Fuel*, 2012, **97**, 651–657.
128 I. B. Laskar, L. Rokhum, R. Gupta and S. Chatterjee, *Environ. Prog. Sustainable Energy*, 2019, **39**, 1–11.
129 Taslim, O. Bani, Iriany, N. Aryani and G. S. Kaban, *Key Eng. Mater.*, 2018, **777**, 262–267.
130 S. Abelló, F. Medina, D. Tichit, J. Pérez-Ramírez, J. C. Groen, J. E. Sueiras, P. Salagre and Y. Cesteros, *Chem.–Eur. J.*, 2005, **11**, 728–739.
131 D. P. Debecker, E. M. Gaigneaux and G. Busca, *Chem.–Eur. J.*, 2009, **15**, 3920–3935.
132 A. Navajas, I. Campo, A. Moral, J. Echave, O. Sanz, M. Montes, J. A. Odriozola, G. Arzamendi and L. M. Gandía, *Fuel*, 2018, **211**, 173–181.
133 H.-y. Zeng, Z. Feng, X. Deng and Y.-q. Li, *Fuel*, 2008, **87**, 3071–3076.
134 Y. Ma, Q. Wang, L. Zheng, Z. Gao, Q. Wang and Y. Ma, *Energy*, 2016, **107**, 523–531.
135 H. Y. Zeng, S. Xu, M. C. Liao, Z. Q. Zhang and C. Zhao, *Appl. Clay Sci.*, 2014, **91–92**, 16–24.
136 W. Trakarnpruk and S. Porntangjitlikit, *Renewable Energy*, 2008, **33**, 1558–1563.
137 Q. Liu, B. Wang, C. Wang, Z. Tian, W. Qu, H. Ma and R. Xu, *Green Chem.*, 2014, **16**, 2604–2613.
138 L. Gao, G. Teng, G. Xiao and R. Wei, *Biomass Bioenergy*, 2010, **34**, 1283–1288.
139 Y. Liu, E. Lotero, J. G. Goodwin and X. Mo, *Appl. Catal., A*, 2007, **331**, 138–148.
140 Z. Helwani, N. Aziz, M. Z. A. Bakar, H. Mukhtar, J. Kim and M. R. Othman, *Energy Convers. Manage.*, 2013, **73**, 128–134.
141 C. S. Cordeiro, G. G. C. Arizaga, L. P. Ramos and F. Wypych, *Catal. Commun.*, 2008, **9**, 2140–2143.
142 J. Tantirungrotechai, P. Chotmongkolsap and M. Pohmakotr, *Microporous Mesoporous Mater.*, 2010, **128**, 41–47.
143 H. Hattori, *Chem. Rev.*, 1995, **95**, 537–558.
144 A. Kawashima, K. Matsubara and K. Honda, *Bioresour. Technol.*, 2008, **99**, 3439–3443.
145 H. Sun, Y. Ding, J. Duan, Q. Zhang, Z. Wang, H. Lou and X. Zheng, *Bioresour. Technol.*, 2010, **101**, 953–958.
146 Z. Wen, X. Yu, S. T. Tu, J. Yan and E. Dahlquist, *Bioresour. Technol.*, 2010, **101**, 9570–9576.
147 C. L. Chen, C. C. Huang, D. T. Tran and J. S. Chang, *Bioresour. Technol.*, 2012, **113**, 8–13.

148 R. Madhuvilakku and S. Piraman, *Bioresour. Technol.*, 2013, **150**, 55–59.
149 S. Yan, S. O. Salley and K. Y. Simon Ng, *Appl. Catal., A*, 2009, **353**, 203–212.
150 C. Ngamcharussrivichai, P. Totarat and K. Bunyakiat, *Appl. Catal., A*, 2008, **341**, 77–85.
151 J. Su, Y. Li, H. Wang, X. Yan and D. Pan, *Chem. Phys. Lett.*, 2016, **663**, 61–65.
152 M. M. Ibrahim, H. R. Mahmoud and S. A. El-molla, *Catal. Commun.*, 2019, **122**, 10–15.
153 E. A. Faria, I. M. Dias, P. A. Z. Suarez and A. G. S. Prado, *J. Braz. Chem. Soc.*, 2009, **20**, 1732–1737.
154 M. C. G. Albuquerque, J. Santamaría-González, J. M. Mérida-Robles, R. Moreno-Tost, E. Rodríguez-Castellón, A. Jiménez-López, D. C. S. Azevedo, C. L. Cavalcante and P. Maireles-Torres, *Appl. Catal., A*, 2008, **347**, 162–168.
155 K. Rajkumari, D. Das, G. Pathak and L. Rokhum, *New J. Chem.*, 2019, **43**, 2134–2140.
156 E. Betiku, A. A. Okeleye, N. B. Ishola, A. S. Osunleke and T. V. Ojumu, *Catal. Lett.*, 2019, **149**, 1772–1787.
157 R. Shan, L. Lu, Y. Shi, H. Yuan and J. Shi, *Energy Convers. Manage.*, 2018, **178**, 277–289.
158 G. Pathak, K. Rajkumari and L. Rokhum, *Nanoscale Adv.*, 2019, **1**, 1013–1020.
159 B. Changmai, I. B. Laskar and L. Rokhum, *J. Taiwan Inst. Chem. Eng.*, 2019, **102**, 276–282.
160 C. Xu, M. Nasrollahzadeh, M. Sajjadi, M. Maham, R. Luque and A. R. Puente-Santiago, *Renewable Sustainable Energy Rev.*, 2019, **112**, 195–252.
161 Z. Wei, C. Xu and B. Li, *Bioresour. Technol.*, 2009, **100**, 2883–2885.
162 J. Goli and O. Sahu, *Renewable Energy*, 2018, **128**, 142–154.
163 A. A. Ayodeji, M. E. Ojewumi, B. Rasheed and J. M. Ayodele, *Data Brief*, 2018, **19**, 1466–1473.
164 G. Joshi, D. S. Rawat, B. Y. Lamba, K. K. Bisht, P. Kumar, N. Kumar and S. Kumar, *Energy Convers. Manage.*, 2015, **96**, 258–267.
165 Y. C. Sharma, B. Singh and J. Korstad, *Energy Fuels*, 2010, **24**, 3223–3231.
166 N. Tshizanga, E. F. Aransiola and O. Oyekola, *S. Afr. J. Chem. Eng.*, 2017, **23**, 145–156.
167 Y. H. Tan, M. O. Abdullah, C. Nolasco-Hipolito and N. S. Ahmad Zauzi, *Renewable Energy*, 2017, **114**, 437–447.
168 Y. C. Wong and R. X. Ang, *Open Chem.*, 2018, **16**, 1166–1175.
169 P. Suwannasom, R. Sriraksa, P. Tansupo and C. Ruangviriyachai, *Energy Sources, Part A*, 2016, **38**, 3221–3228.
170 G. Santya, T. Maheswaran and K. F. Yee, *SN Appl. Sci.*, 2019, **1**, 152–160.
171 P. Parthasarathy and S. K. Narayanan, *Environ. Prog. Sustainable Energy*, 2014, **33**, 676–680.
172 S. Niju, M. M. M. S. Begum and N. Anantharaman, *J. Saudi Chem. Soc.*, 2014, **18**, 702–706.
173 A. R. Gupta and V. K. Rathod, *Waste Manage.*, 2018, **79**, 169–178.
174 N. S. El-Gendy, S. F. Deriase, A. Hamdy and R. I. Abdallah, *Egypt. J. Pet.*, 2015, **24**, 37–48.
175 Y. P. Peng, K. T. T. Amesho, C. E. Chen, S. R. Jhang, F. C. Chou and Y. C. Lin, *Catalysts*, 2018, **8**, 81–91.
176 N. Viriya-Empikul, P. Krasae, W. Nualpaeng, B. Yoosuk and K. Faungnawakij, *Fuel*, 2012, **92**, 239–244.
177 P. Khemthong, C. Luadthong, W. Nualpaeng, P. Changsuwan, P. Tongprem, N. Viriya-Empikul and K. Faungnawakij, *Catal. Today*, 2012, **190**, 112–116.
178 N. Viriya-empikul, P. Krasae, B. Puttasawat, B. Yoosuk, N. Chollacoop and K. Faungnawakij, *Bioresour. Technol.*, 2010, **101**, 3765–3767.
179 A. Annam Renita, P. P. Chowdhury, P. Sultana, P. Phukan and A. Hannan, *Int. J. Pharm. Pharm. Sci.*, 2016, **8**, 143–146.
180 A. A. Jazie, H. Pramanik and A. S. K. Sinha, *Spec. Issue Int. J. Sustain. Dev. Green Econ.*, 2013, **2**, 2315–4721.
181 F. Yasar, *Fuel*, 2019, **255**, 115828.
182 K. Kara, F. Ouanji, M. El Mahi, E. M. Lotfi, M. Kacimi and Z. Mahfoud, *Biofuels*, 2019, **24**, 1–7.
183 E. Fayyazi, B. Ghobadian, H. H. Van De Bovenkamp, G. Najafi, B. Hosseinzadehsamani, H. J. Heeres and J. Yue, *Ind. Eng. Chem. Res.*, 2018, **38**, 12742–12755.
184 L. M. Correia, R. M. A. Saboya, N. de Sousa Campelo, J. A. Cecilia, E. Rodríguez-Castellón, C. L. Cavalcante and R. S. Vieira, *Bioresour. Technol.*, 2014, **151**, 207–213.
185 I. Reyero, F. Bimbela, A. Navajas, G. Arzamendi and L. M. Gandía, *Fuel*, 2015, **158**, 558–564.
186 S. B. Chavan, R. R. Kumbhar, D. Madhu, B. Singh and Y. C. Sharma, *RSC Adv.*, 2015, **5**, 63596–63604.
187 P. R. Pandit and M. H. Fulekar, *J. Environ. Manage.*, 2017, **198**, 319–329.
188 P. R. Pandit and M. H. Fulekar, *Renewable Energy*, 2019, **136**, 837–845.
189 P. R. Pandit and M. H. Fulekar, *Mater. Today: Proc.*, 2019, **10**, 75–86.
190 K. Kirubakaran and V. Arul Mozhi Selvan, *J. Environ. Chem. Eng.*, 2018, **6**, 4490–4503.
191 G. Santya, T. Maheswaran and K. F. Yee, *SN Appl. Sci.*, 2019, **1**, 152–160.
192 M. L. Savaliya, M. S. Bhakhar and B. Z. Dholakiya, *Catal. Lett.*, 2016, **146**, 2313–2323.
193 L. Da Silva Castro, A. G. Barañano, C. J. G. Pinheiro, L. Menini and P. F. Pinheiro, *Green Process. Synth.*, 2019, **8**, 235–244.
194 Y. Hangun-Balkir, *J. Chem.*, 2016, 1–10.
195 A. Ansori, S. A. Wibowo, H. S. Kusuma, D. S. Bhuana and M. Mahfud, *Open Chem.*, 2019, **17**, 1185–1197.
196 N. Mansir, S. Hwa Teo, M. Lokman Ibrahim and T. Y. Yun Hin, *Energy Convers. Manage.*, 2017, **151**, 216–226.
197 A. S. Yusuff, O. D. Adeniyi, M. A. Olutoye and U. G. Akpan, *Int. J. Technol.*, 2018, **1**, 1–11.
198 M. J. Borah, A. Das, V. Das, N. Bhuyan and D. Deka, *Fuel*, 2019, **242**, 345–354.
199 A. S. Oladipo, O. A. Ajayi, A. A. Oladipo, S. L. Azarmi, Y. Nurudeen, A. Y. Atta and S. S. Ogunyemi, *C. R. Chim.*, 2018, **21**, 684–695.

200 M. D. Putra, Y. Ristianingsih, R. Jelita, C. Irawan and I. F. Nata, *RSC Adv.*, 2017, **7**, 55547–55554.
201 N. Mansir, S. H. Teo, U. Rashid and Y. H. Taufiq-Yap, *Fuel*, 2018, **211**, 67–75.
202 S. H. Teo, A. Islam, H. R. F. Masoumi, Y. H. Taufiq-Yap, J. Janaun, E. S. Chan and M. A. khaleque, *Renewable Energy*, 2017, **111**, 892–905.
203 M. A. Olutoye, S. C. Lee and B. H. Hameed, *Bioresour. Technol.*, 2011, **102**, 10777–10783.
204 G. Chen, R. Shan, S. Li and J. Shi, *Fuel*, 2016, **143**, 110–117.
205 N. S. Lani, N. Ngadi, N. Y. Yahya and R. A. Rahman, *J. Cleaner Prod.*, 2018, **164**, 210–218.
206 G. Y. Chen, R. Shan, J. F. Shi and B. B. Yan, *Fuel Process. Technol.*, 2015, **133**, 8–13.
207 S. Sulaiman and N. I. F. Ruslan, *Energy Sources, Part A*, 2017, **39**, 154–159.
208 J. Boro, L. J. Konwar and D. Deka, *Fuel Process. Technol.*, 2014, **122**, 72–78.
209 W. U. Rahman, A. Fatima, A. H. Anwer, M. Athar, M. Z. Khan, N. A. Khan and G. Halder, *Process Saf. Environ. Prot.*, 2019, **122**, 313–319.
210 R. Chakraborty, S. Bepari and A. Banerjee, *Chem. Eng. J.*, 2010, **165**, 798–805.
211 D. Zeng, Q. Zhang, S. Chen, S. Liu, Y. Chen, Y. Tian and G. Wang, *J. Environ. Chem. Eng.*, 2015, **3**, 560–564.
212 S. Chowdhury, S. H. Dhawane, B. Jha, S. Pal, R. Sagar, A. Hossain and G. Halder, *Biomass Convers. Biorefin.*, 2019, 1–11.
213 G. Chen, R. Shan, J. Shi and B. Yan, *Bioresour. Technol.*, 2014, **171**, 428–432.
214 Y. B. Cho and G. Seo, *Bioresour. Technol.*, 2010, **22**, 8515–8519.
215 A. Buasri and V. Loryuenyong, *Mater. Today: Proc.*, 2017, **4**, 6051–6059.
216 J. Goli and O. Sahu, *Renewable Energy*, 2018, **128**, 142–154.
217 S. Niju, K. M. M. S. Begum and N. Anantharaman, *Environ. Prog. Sustainable Energy*, 2015, **34**, 248–254.
218 N. P. Asri, B. Podjojono, R. Fujiani and Nuraini, *IOP Conf. Ser. Earth Environ. Sci.*, 2017, **67**, 1–7.
219 L. M. Correia, R. M. A. Saboya, N. de Sousa Campelo, J. A. Cecilia, E. Rodríguez-Castellón, C. L. Cavalcante and R. S. Vieira, *Bioresour. Technol.*, 2014, **151**, 207–213.
220 S. Jairam, P. Kolar, R. Sharma-Shivappa Ratna, J. A. Osborne and J. P. Davis, *Bioresour. Technol.*, 2012, **104**, 329–335.
221 N. Nakatani, H. Takamori, K. Takeda and H. Sakugawa, *Bioresour. Technol.*, 2009, **100**, 1510–1513.
222 A. Buasri, T. Rattanapan, C. Boonrin, C. Wechayan and V. Loryuenyong, *J. Chem.*, 2015, 1–7.
223 S. Kaewdaeng, P. Sintuya and R. Nirunsin, *Energy Procedia*, 2017, **138**, 937–942.
224 W. Roschat, T. Siritanon, T. Kaewpuang, B. Yoosuk and V. Promarak, *Bioresour. Technol.*, 2016, **209**, 343–350.
225 X. Liu, H. Bai, D. Zhu and G. Cao, *Adv. Mater. Res.*, 2011, **148**, 794–798.
226 A. Birla, B. Singh, S. N. Upadhyay and Y. C. Sharma, *Bioresour. Technol.*, 2012, **106**, 95–100.
227 H. Liu, H. s. Guo, X. j. Wang, J. z. Jiang, H. Lin, S. Han and S. p. Pei, *Renewable Energy*, 2016, **93**, 648–657.
228 I. B. Laskar, K. Rajkumari, R. Gupta, S. Chatterjee, B. Paul and L. Rokhum, *RSC Adv.*, 2018, **8**, 20131–20142.
229 N. S. El-Gendy, S. F. Deriase and A. Hamdy, *Energy Sources, Part A*, 2014, **36**, 623–637.
230 J. Sani, S. Samir, I. I. Rikoto, A. D. Tambuwal, A. Sanda, S. M. Maishanu and M. M. Laden, *Innov. Energy Res.*, 2017, **6**, 1–4.
231 V. A. Fabiani, R. O. Asriza, A. R. Fabian and M. Kafillah, *IOP Conf. Ser. Earth Environ. Sci.*, 2019, **353**, 12012.
232 K. N. Krishnamurthy, S. N. Sridhara and C. S. Ananda Kumar, *Renewable Energy*, 2020, **146**, 280–296.
233 A. A. Otori, A. Mann, M. A. T. Suleiman and E. C. Egwimvol, *Niger. J. Chem. Res.*, 2011, **23**, 837–846.
234 A. Buasri, N. Chaiyut, V. Loryuenyong, P. Worawanitchaphong and S. Trongyong, *Sci. World J.*, 2013, 1–7.
235 H. Hadiyanto, A. H. Afianti, U. I. Navi'A, N. P. Adetya, W. Widayat and H. Sutanto, *J. Environ. Chem. Eng.*, 2017, **5**, 4559–4563.
236 S. Nurdin, N. A. Rosnan, N. S. Ghazali, J. Gimbun, A. H. Nour and S. F. Haron, *Energy Procedia*, 2015, **79**, 576–583.
237 R. Rezaei, M. Mohadesi and G. R. Moradi, *Fuel*, 2013, **109**, 534–541.
238 Y. Zhang, X. Shen, H. Bai and S. Liu, *World Automation Congress Proceedings*, 2012, pp. 1–4.
239 S. Hu, Y. Wang and H. Han, *Biomass Bioenergy*, 2011, **35**, 3627–3635.
240 A. Perea, T. Kelly and Y. Hangun-Balkir, *Green Chem. Lett. Rev.*, 2016, **9**, 27–32.
241 O. Nur Syazwani, U. Rashid and Y. H. Taufiq Yap, *Energy Convers. Manage.*, 2015, **101**, 749–756.
242 O. N. Syazwani, U. Rashid, M. S. Mastuli and Y. H. Taufiq-Yap, *Renewable Energy*, 2019, **131**, 187–196.
243 N. Asikin-Mijan, H. V. Lee and Y. H. Taufiq-Yap, *Chem. Eng. Res. Des.*, 2015, **102**, 368–377.
244 Y. Taufiq-Yap, H. Lee and P. Lau, *Energy Explor. Exploit.*, 2012, **30**, 853–866.
245 P. Nair, B. Singh, S. N. Upadhyay and Y. C. Sharma, *J. Cleaner Prod.*, 2012, **29**, 82–90.
246 N. Girish, S. P. Niju, K. M. Meera Sheriffa Begum and N. Anantharaman, *Fuel*, 2013, **111**, 653–658.
247 O. N. Syazwani, S. H. Teo, A. Islam and Y. H. Taufiq-Yap, *Process Saf. Environ. Prot.*, 2017, **105**, 303–315.
248 G. Y. Chen, R. Shan, B. B. Yan, J. F. Shi, S. Y. Li and C. Y. Liu, *Fuel Process. Technol.*, 2016, **143**, 110–117.
249 S. Boonyuen, S. M. Smith, M. Malaithong, A. Prokaew, B. Cherdhirunkorn and A. Luengnaruemitchai, *J. Cleaner Prod.*, 2018, **177**, 925–929.
250 W. Suryaputra, I. Winata, N. Indraswati and S. Ismadji, *Renewable Energy*, 2013, **50**, 795–799.
251 P. L. Boey, G. P. Maniam, S. A. Hamid and D. M. H. Ali, *Fuel*, 2011, **88**, 283–288.
252 S. L. Lee, Y. C. Wong, Y. P. Tan and S. Y. Yew, *Energy Convers. Manage.*, 2015, **93**, 282–288.

253 J. Xie, X. Zheng, A. Dong, Z. Xiao and J. Zhang, *Green Chem.*, 2009, **11**, 355–364.
254 J. Boro, A. J. Thakur and D. Deka, *Fuel Process. Technol.*, 2011, **92**, 2061–2067.
255 J. Boro, L. J. Konwar, A. J. Thakur and D. Deka, *Fuel*, 2014, **129**, 182–187.
256 H. Mazaheri, H. C. Ong, H. H. Masjuki, Z. Amini, M. D. Harrison, C. T. Wang, F. Kusumo and A. Alwi, *Energy*, 2018, **144**, 10–19.
257 L. Yang, A. Zhang and X. Zheng, *Energy Fuels*, 2009, **23**, 3859–3865.
258 R. Anr, A. A. Saleh, M. S. Islam, S. Hamdan and M. A. Maleque, *Energy Fuels*, 2016, **30**, 334–343.
259 P. Sivakumar, P. Sivakumar, K. Anbarasu, R. Mathiarasi and S. Renganathan, *Int. J. Green Energy*, 2014, **11**, 886–897.
260 V. Shankar and R. Jambulingam, *Sustainable Environ. Res.*, 2017, **27**, 273–278.
261 P. L. Boey, G. P. Maniam and S. A. Hamid, *Bioresour. Technol.*, 2011, **168**, 15–22.
262 D. Madhu, S. B. Chavan, V. Singh, B. Singh and Y. C. Sharma, *Bioresour. Technol.*, 2016, **214**, 210–217.
263 A. P. S. Chouhan and A. K. Sarma, *Biomass Bioenergy*, 2013, **55**, 386–389.
264 L. H. Chin, B. H. Hameed and A. L. Ahmad, *Energy Fuels*, 2009, **23**, 1040–1044.
265 P. L. Boey, S. Ganesan, S. X. Lim, S. L. Lim, G. P. Maniam and M. Khairuddean, *Energy*, 2011, **36**, 5791–5796.
266 E. Betiku and S. O. Ajala, *Ind. Crops Prod.*, 2014, **53**, 314–322.
267 A. O. Etim, E. Betiku, S. O. Ajala, P. J. Olaniyi and T. V. Ojumu, *Sustain*, 2018, **10**, 707–715.
268 V. Vadery, B. N. Narayanan, R. M. Ramakrishnan, S. K. Cherikkallinmel, S. Sugunan, D. P. Narayanan and S. Sasidharan, *Energy*, 2014, **70**, 588–594.
269 C. Ofori-Boateng and K. T. Lee, *Chem. Eng. J.*, 2013, **220**, 395–401.
270 D. C. Deka and S. Basumatary, *Biomass Bioenergy*, 2011, **35**, 1797–1803.
271 A. K. Sarma, P. Kumar, M. Aslam and A. P. S. Chouhan, *Catal. Lett.*, 2014, **144**, 1344–1353.
272 E. Betiku, A. M. Akintunde and T. V. Ojumu, *Energy*, 2016, **103**, 797–806.
273 S. E. Onoji, S. E. Iyuke, A. I. Igbafe and M. O. Daramola, *Energy Fuels*, 2017, **31**, 6109–6119.
274 M. Gohain, A. Devi and D. Deka, *Ind. Crops Prod.*, 2017, **109**, 8–18.
275 G. Pathak, D. Das, K. Rajkumari and L. Rokhum, *Green Chem.*, 2018, **20**, 2365–2373.
276 M. Sharma, A. A. Khan, S. K. Puri and D. K. Tuli, *Biomass Bioenergy*, 2012, **41**, 94–106.
277 B. K. Uprety, W. Chaiwong, C. Ewelike and S. K. Rakshit, *Energy Convers. Manage.*, 2016, **115**, 191–199.
278 M. Balajii and S. Niju, *Renewable Energy*, 2020, **146**, 2255–2269.
279 M. Balajii and S. Niju, *Energy Convers. Manage.*, 2019, **189**, 118–131.
280 I. M. Mendonça, F. L. Machado, C. C. Silva, S. Duvoisin Junior, M. L. Takeno, P. J. de Sousa Maia, L. Manzato and F. A. de Freitas, *Energy Convers. Manage.*, 2019, **200**, 112095.
281 B. Nath, B. Das, P. Kalita and S. Basumatary, *J. Cleaner Prod.*, 2019, **239**, 118112.
282 B. Changmai, P. Sudarsanam and L. Rokhum, *Ind. Crops Prod.*, 2019, **145**, 111911–111919.
283 B. Nath, P. Kalita, B. Das and S. Basumatary, *Renewable Energy*, 2020, **151**, 295–310.
284 I. M. Mendonça, O. A. R. L. Paes, P. J. S. Maia, M. P. Souza, R. A. Almeida, C. C. Silva, S. Duvoisin and F. A. de Freitas, *Renewable Energy*, 2019, **130**, 103–110.
285 M. Gohain, K. Laskar, H. Phukon, U. Bora, D. Kalita and D. Deka, *Waste Manage.*, 2020, **102**, 212–221.
286 E. Betiku, A. O. Etim, O. Pereao and T. V. Ojumu, *Energy Fuels*, 2017, **31**, 6182–6193.
287 M. R. Miladinović, M. V. Zdujić, D. N. Veljović, J. B. Krstić, I. B. Banković-Ilić, V. B. Veljković and O. S. Stamenković, *Renewable Energy*, 2020, **147**, 1033–1043.
288 H. H. Abdelhady, H. A. Elazab, E. M. Ewais, M. Saber and M. S. El-Deab, *Fuel*, 2020, **261**, 116481.
289 K. Rajkumari and L. Rokhum, *Biomass Convers. Biorefin.*, 2020, 1–10.
290 V. O. Odude, A. J. Adesina, O. O. Oyetunde, O. O. Adeyemi, N. B. Ishola, A. O. Etim and E. Betiku, *Waste Biomass Valorization*, 2019, **10**, 877–888.
291 M. Gohain, K. Laskar, A. K. Paul, N. Daimary, M. Maharana, I. K. Goswami, A. Hazarika, U. Bora and D. Deka, *Renewable Energy*, 2020, **147**, 541–555.
292 M. Aslam, P. Saxena and A. K. Sarma, *Energy Environ. Res.*, 2014, **4**, 1927-0569.
293 M. Di Serio, R. Tesser, L. Pengmei and E. Santacesaria, *Energy Fuels*, 2008, **22**, 207–217.
294 N. S. Talha and S. Sulaiman, *ARPN J. Eng. Appl. Sci.*, 2016, **11**, 439–442.
295 F. Allioux, B. J. Holland, L. Kong and L. F. Dumée, *Front. Mater.*, 2017, **4**, 1–10.
296 K. L. T. Rodrigues, V. M. D. Pasa and É. C. Cren, *J. Environ. Chem. Eng.*, 2018, **6**, 4531–4537.
297 L. Ma, Y. Han, K. Sun, J. Lu and J. Ding, *J. Energy Chem.*, 2015, 1–7.
298 S. Xia, X. Guo, D. Mao, Z. Shi, G. Wu and G. Lu, *RSC Adv.*, 2014, **4**, 51688–51695.
299 N. Shibasaki-kitakawa, K. Hiromori, T. Ihara, K. Nakashima and T. Yonemoto, *Fuel*, 2015, **139**, 11–17.
300 M. Banchero and G. Gojjelino, *Energies*, 2018, **11**, 1843–1851.
301 D. R. Radu and G. A. Kraus, *Heterogeneous Catalysis for Today's Challenges*, 2015, pp. 117–130.
302 N. Shibasaki-kitakawa, H. Honda, H. Kuribayashi and T. Toda, *Bioresour. Technol.*, 2007, **98**, 416–421.
303 Y. Ren, B. He, F. Yan, H. Wang, Y. Cheng, L. Lin, Y. Feng and J. Li, *Bioresour. Technol.*, 2012, **113**, 19–22.
304 T. M. Deboni, G. A. M. Hirata, G. G. Shimamoto, M. Tubino and A. J. A. Meirelles, *Chem. Eng. J.*, 2018, **333**, 686–696.
305 J. Kansedo, Y. X. Sim and K. T. Lee, *IOP Conf. Ser.: Mater. Sci. Eng.*, 2019, **495**, 012050–012060.

306 N. Jaya, B. K. Selvan and S. J. Vennison, *Ecotoxicol. Environ. Saf.*, 2015, **121**, 3–9.
307 A. Umar, A. Uba, M. L. Mohammed, M. N. Almustapha, C. Muhammad and J. Sani, *Nig. J. Basic Appl. Sci.*, 2019, **26**, 88.
308 J. Kansedo and K. T. Lee, *Energy Sci. Eng.*, 2014, **2**, 31–38.
309 O. Ilgen, A. N. Akin and N. Boz, *Turk. J. Chem.*, 2009, **33**, 289–294.
310 B. Vafakish and M. Barari, *Kem. Ind.*, 2017, **66**, 47–52.
311 R. Hartono, B. Mulia, M. Sahlan, T. S. Utami, A. Wijanarko and H. Hermansyah, *AIP Conf. Proc.*, 2017, **1826**, 020020.
312 N. Shibasaki-Kitakawa, T. Tsuji, M. Kubo and T. Yonemoto, *BioEnergy Res.*, 2011, **4**, 287–293.
313 N. Shibasaki-Kitakawa, T. Tsuji, K. Chida, M. Kubo and T. Yonemoto, *Energy Fuels*, 2010, **24**, 3634–3638.
314 Y. Feng, B. He, Y. Cao, J. Li, M. Liu, F. Yan and X. Liang, *Bioresour. Technol.*, 2010, **101**, 1518–1521.
315 N. Jalilnejad Falizi, T. Güngören Madenoğlu, M. Yüksel and N. Kabay, *Int. J. Energy Res.*, 2019, **43**, 2188–2199.
316 P. A. Alaba, Y. M. Sani, W. Mohd and A. Wan, *RSC Adv.*, 2016, **6**, 78351–78368.
317 Q. H. Xia, K. Hidajat and S. Kawi, *Chem. Commun.*, 2000, **22**, 2229–2230.
318 A. V. Ivanov, S. V. Lysenko, S. V. Baranova, A. V. Sungurov, T. N. Zangelov and E. A. Karakhanov, *Microporous Mesoporous Mater.*, 2006, **91**, 254–260.
319 S. H. I. Guo-liang, Y. U. Feng, Y. A. N. Xiao-liang and L. I. Rui-feng, *J. Fuel Chem. Technol.*, 2017, **45**, 311–316.
320 Q. H. Xia, K. Hidajat and S. Kawi, *J. Catal.*, 2002, **205**, 318–331.
321 H. Muthu, V. S. Selvabala, T. K. Varathachary, D. K. Selvaraj, J. Nandagopal and S. Subramanian, *Braz. J. Chem. Eng.*, 2010, **27**, 601–608.
322 M. K. Lam, K. T. Lee and A. R. Mohamed, *Appl. Catal., B*, 2009, **93**, 134–139.
323 C. O. Pereira, M. F. Portilho, C. A. Henriques and F. M. Z. Zotin, *J. Braz. Chem. Soc.*, 2014, **25**, 2409–2416.
324 G. Kafuku, K. T. Lee and M. Mbarawa, *Chem. Pap.*, 2010, **64**, 734–740.
325 X. Li and W. Huang, *Energy Sources, Part A*, 2009, **31**, 1666–1672.
326 M. L. Testa, V. La Parola, L. F. Liotta and A. M. Venezia, *J. Mol. Catal. A: Chem.*, 2013, **367**, 69–76.
327 M. L. Testa, V. La Parola and A. M. Venezia, *Catal. Today*, 2010, **158**, 109–113.
328 J. Gardy, A. Hassanpour, X. Lai and M. H. Ahmed, *Appl. Catal., A*, 2016, **527**, 81–95.
329 J. Gardy, A. Hassanpour, X. Lai, M. H. Ahmed and M. Rehan, *Appl. Catal., B*, 2017, **207**, 297–310.
330 T. Suzuta, M. Toba, Y. Abe and Y. Yoshimura, *J. Am. Oil Chem. Soc.*, 2012, **89**, 1981–1989.
331 K. Thirunavukkarasu, T. M. Sankaranarayanan, A. Pandurangan, R. Vijaya Shanthi and S. Sivasanker, *Catal. Sci. Technol.*, 2014, **4**, 851–860.
332 W. Xie, H. Wang and H. Li, *Ind. Eng. Chem. Res.*, 2012, **51**, 225–231.
333 F. H. Alhassan, U. Rashid and Y. H. Taufiq-Yap, *J. Oleo Sci.*, 2015, **64**, 505–514.
334 W. Xie and T. Wang, *Fuel Process. Technol.*, 2013, **109**, 150–155.
335 W. Xie and D. Yang, *Bioresour. Technol.*, 2012, **119**, 60–65.
336 H. Amani, Z. Ahmad, M. Asif and B. H. Hameed, *J. Ind. Eng. Chem.*, 2014, **20**, 4437–4442.
337 Q. Zhang, H. Li, X. Liu, W. Qin, Y. Zhang, W. Xue and S. Yang, *Energy Technol.*, 2013, **1**, 735–742.
338 F. H. Alhassan, U. Rashid and Y. H. Taufq-Yap, *J. Oleo Sci.*, 2015, **64**, 91–99.
339 A. Mahajan and P. Gupta, *Environ. Chem. Lett.*, 2020, **18**, 299–314.
340 M. Hara, T. Yoshida, A. Takagaki, T. Takata, J. N. Kondo, S. Hayashi and K. Domen, *Angew. Chem., Int. Ed.*, 2004, **43**, 2955–2958.
341 S. P. Adhikari, Z. D. Hood, S. Borchers and M. Wright, *ChemistrySelect*, 2020, **5**, 1534–1538.
342 R. A. Arancon, H. R. Barros, A. M. Balu, C. Vargas and R. Luque, *Green Chem.*, 2011, **13**, 3162–3167.
343 A. Sandouqa, Z. Al-Hamamre and J. Asfar, *Renewable Energy*, 2019, **132**, 667–682.
344 K. Malins, J. Brinks, V. Kampars and I. Malina, *Appl. Catal., A*, 2016, **519**, 99–106.
345 M. Kacem, G. Plantard, N. Wery and V. Goetz, *Chin. J. Catal.*, 2014, **35**, 1571–1577.
346 Q. Shu, J. Gao, Z. Nawaz, Y. Liao, D. Wang and J. Wang, *Appl. Energy*, 2010, **87**, 2589–2596.
347 M. Gonc̀alves, V. C. Souza, T. S. Galhardo, M. Mantovani, F. C. A. Figueiredo, D. Mandelli and W. A. Carvalho, *Ind. Eng. Chem. Res.*, 2013, **52**, 2832–2839.
348 Y. Zhong, Q. Deng, P. Zhang, J. Wang, R. Wang, Z. Zeng and S. Deng, *Fuel*, 2019, **240**, 270–277.
349 V. Trombettoni, D. Lanari, P. Prinsen, R. Luque, A. Marrocchi and L. Vaccaro, *Prog. Energy Combust. Sci.*, 2018, **65**, 136–162.
350 M. Otadi, A. Shahraki, M. Goharrokhi and F. Bandarchian, *Procedia Eng.*, 2011, **18**, 168–174.
351 K. Rajkumari, I. B. Laskar, A. Kumari, B. Kalita and L. Rokhum, *React. Funct. Polym.*, 2020, **149**, 104519.
352 P. P. Upare, J. M. Lee, D. W. Hwang, S. B. Halligudi, Y. K. Hwang and J. S. Chang, *J. Ind. Eng. Chem.*, 2011, **17**, 287–292.
353 K. Fukuhara, K. Nakajima, M. Kitano, S. Hayashic and M. Hara, *Phys. Chem. Chem. Phys.*, 2013, **15**, 9343.
354 T. S. Galhardo, N. Simone, M. Gonçalves, F. C. A. Figueiredo, D. Mandelli and W. A. Carvalho, *ACS Sustainable Chem. Eng.*, 2013, **1**, 1381–1389.
355 P. D. Rocha, L. S. Oliveira and A. S. Franca, *Renewable Energy*, 2019, **143**, 1710–1716.
356 M. Hara, *Energy Environ. Sci.*, 2010, **3**, 601–607.
357 L. J. Konwar, P. Mäki-Arvela and J. P. Mikkola, *Chem. Rev.*, 2019, **119**, 11576–11630.
358 I. B. Laskar, K. Rajkumari, R. Gupta and L. Rokhum, *Energy Fuels*, 2018, **32**, 12567–12576.
359 K. Rajkumari, I. B. Laskar, A. Kumari, B. Kalita and L. Rokhum, *React. Funct. Polym.*, 2020, **149**, 104519.

360 M. M. Alam, M. A. Hossain, M. D. Hossain, M. A. H. Johir, J. Hossen, M. S. Rahman, J. L. Zhou, A. T. M. K. Hasan, A. K. Karmakar and M. B. Ahmed, *Processes*, 2020, **8**, 203.
361 X. J. Zhang, Y. Y. Wang, Z. C. Jiang, P. T. Wu, Y. M. Jin and Y. Q. Hu, *New Carbon Mater.*, 2013, **28**, 484–488.
362 Q. Zhang, Y. Zhang, T. Deng, F. Wei, J. Jin and P. Ma, *Sustainable production of biodiesel over heterogeneous acid catalysts*, Elsevier B.V., 2020, pp. 407–432.
363 I. K. Mbaraka, D. R. Radu, V. S. Y. Lin and B. H. Shanks, *J. Catal.*, 2003, **219**, 329–336.
364 M. Toda, A. Takagaki, M. Okamura, J. N. Kondo, S. Hayashi, K. Domen and M. Hara, *Nature*, 2005, **438**, 178.
365 K. Nakajima, M. Hara, B. Hu, Q. Lu, Y.-t. Wu, Z.-x. Zhang, M.-s. Cui, D.-j. Liu, C.-q. Dong, Y.-p. Yang, V. Aniya, A. Kumari, D. De, D. Vidya, V. Swapna, P. K. Thella, B. Satyavathi, H. Zhang, X. Meng, C. Liu, Y. Wang and R. Xiao, *J. Anal. Appl. Pyrolysis*, 2018, **2**, 1296–1304.
366 K. Malins, V. Kampars, J. Brinks, I. Neibolte and R. Murnieks, *New Carbon Mater.*, 2015, **176**, 553–558.
367 S. Pandian, A. Sakthi Saravanan, P. Sivanandi, M. Santra and V. K. Booramurthy, *Refining Biomass Residues for Sustainable Energy and Bioproducts*. Academic Press, 2020. pp. 87–109.
368 M. Kitano, D. Yamaguchi, S. Suganuma, K. Nakajima, H. Kato, S. Hayashi and M. Hara, *Langmuir*, 2009, **25**, 5068–5075.
369 H. Yuan, B. L. Yang and G. L. Zhu, *Energy Fuels*, 2009, **23**, 548–552.
370 J. A. Melero, L. F. Bautista, G. Morales, J. Iglesias and D. Briones, *Energy Fuels*, 2009, **23**, 539–547.
371 D. Zuo, J. Lane, D. Culy, M. Schultz, A. Pullar and M. Waxman, *Appl. Catal., B*, 2013, **129**, 342–350.
372 K. A. Shah, J. K. Parikh and K. C. Maheria, *Res. Chem. Intermed.*, 2015, **41**, 1035–1051.
373 A. Varyambath, M. R. Kim and I. Kim, *New J. Chem.*, 2018, **42**, 12745–12753.
374 Shagufta, I. Ahmad and R. Dhar, *Catal. Surv. Asia*, 2017, **21**, 53–69.
375 H. Yu, S. Niu, C. Lu, J. Li and Y. Yang, *Fuel*, 2017, **208**, 101–110.
376 X. Tang and S. Niu, *J. Ind. Eng. Chem.*, 2019, **69**, 187–195.
377 S. Niu, Y. Ning, C. Lu, K. Han, H. Yu and Y. Zhou, *Energy Convers. Manage.*, 2018, **163**, 59–65.
378 I. F. Nata, M. D. Putra, C. Irawan and C. K. Lee, *J. Environ. Chem. Eng.*, 2017, **5**, 2171–2175.
379 Q. Guan, Y. Li, Y. Chen, Y. Shi, J. Gu, B. Li and R. Miao, *RSC Adv.*, 2017, **7**, 7250–7258.
380 I. M. Lokman, *Arabian J. Chem.*, 2016, **9**, 179–189.
381 I. Thushari and S. Babel, *Bioresour. Technol.*, 2018, **248**, 199–203.
382 Y. Wang, D. Wang, M. Tan, B. Jiang, J. Zheng, N. Tsubaki and M. Wu, *ACS Appl. Mater. Interfaces*, 2015, **7**, 26767–26775.
383 R. Liu, X. Wang, X. Zhao and P. Feng, *Carbon*, 2008, **46**, 1664–1669.
384 S. Dechakhumwat, P. Hongmanorom, C. Thunyaratchatanon, S. M. Smith, S. Boonyuen and A. Luengnaruemitchai, *Renewable Energy*, 2020, **148**, 897–906.
385 M. Mahdavi and A. H. Darab, *Preprints*, 2019, 2019090110, DOI: 10.20944/preprints201909.0110.v1.
386 M. Hara, *Top. Catal.*, 2010, **53**, 805–810.
387 T. T. V. Tran, S. Kaiprommarat, S. Kongparakul, P. Reubroycharoen, G. Guan, M. H. Nguyen and C. Samart, *Waste Manage.*, 2016, **52**, 367–374.
388 S. Hosseini, J. Janaun and T. S. Y. Choong, *Process Saf. Environ. Prot.*, 2015, **98**, 285–295.
389 L. J. Konwar, J. Wärnå, P. Mäki-Arvela, N. Kumar and J. P. Mikkola, *Fuel*, 2016, **166**, 1–11.
390 A. Endut, S. Hanis, Y. Sayid, N. Hanis, M. Hanapi, S. Hajar, A. Hamid, F. Lananan, M. Khairul, A. Kamarudin, R. Umar and H. Khatoon, *Int. Biodeterior. Biodegrad.*, 2017, **124**, 250–257.
391 F. Ezebor, M. Khairuddean, A. Z. Abdullah and P. L. Boey, *Energy Convers. Manage.*, 2014, **88**, 1143–1150.
392 T. Liu, Z. Li, W. Li, C. Shi and Y. Wang, *Bioresour. Technol.*, 2013, **133**, 618–621.
393 Y. Zhou, S. Niu and J. Li, *Energy Convers. Manage.*, 2016, **114**, 188–196.
394 H. H. Mardhiah, H. C. Ong, H. H. Masjuki, S. Lim and Y. L. Pang, *Energy Convers. Manage.*, 2017, **144**, 10–17.
395 B. L. A. Prabhavathi Devi, T. Vijai Kumar Reddy, K. Vijaya Lakshmi and R. B. N. Prasad, *Bioresour. Technol.*, 2014, **153**, 370–373.
396 B. L. A. P. Devi, K. N. Gangadhar, P. S. S. Prasad, B. Jagannadh and R. B. N. Prasad, *ChemSusChem*, 2009, **2**, 617–620.
397 X. Fu, D. Li, J. Chen, Y. Zhang, W. Huang, Y. Zhu, J. Yang and C. Zhang, *Bioresour. Technol.*, 2013, **146**, 767–770.
398 L. J. Konwar, R. Das, A. J. Thakur, E. Salminen, P. Mäki-Arvela, N. Kumar, J. P. Mikkola and D. Deka, *J. Mol. Catal. A: Chem.*, 2014, **388–389**, 167–176.
399 E. M. Santos, A. P. D. C. Teixeira, F. G. Da Silva, T. E. Cibaka, M. H. Araújo, W. X. C. Oliveira, F. Medeiros, A. N. Brasil, L. S. De Oliveira and R. M. Lago, *Fuel*, 2015, **150**, 408–414.
400 L. J. Konwar, P. Mäki-Arvela, E. Salminen, N. Kumar, A. J. Thakur, J. P. Mikkola and D. Deka, *Appl. Catal., B*, 2015, **176–177**, 20–35.
401 B. V. S. K. Rao, K. Chandra Mouli, N. Rambabu, A. K. Dalai and R. B. N. Prasad, *Catal. Commun.*, 2011, **14**, 20–26.
402 J. R. Kastner, J. Miller, D. P. Geller, J. Locklin, L. H. Keith and T. Johnson, *Catal. Today*, 2012, **190**, 122–132.
403 A. M. Dehkhoda, A. H. West and N. Ellis, *Appl. Catal., A*, 2010, **382**, 197–204.
404 A. M. Dehkhoda and N. Ellis, *Catal. Today*, 2013, **207**, 86–92.
405 L. Fjerbaek, K. V. Christensen and B. Norddahl, *Biotechnol. Bioeng.*, 2009, **102**, 1298–1315.
406 F. Moazeni, Y. C. Chen and G. Zhang, *J. Cleaner Prod.*, 2019, **216**, 117–128.
407 D. Kumar, T. Das, B. S. Giri, E. R. Rene and B. Verma, *Fuel*, 2019, **255**, 115801.
408 D. Kumar, T. Das, B. S. Giri and B. Verma, *New J. Chem.*, 2018, **42**, 15593–15602.

409 K. C. Badgujar, K. P. Dhake and B. M. Bhanage, *Process Biochem.*, 2013, **48**, 1335–1347.
410 N. R. Mohamad, N. H. C. Marzuki, N. A. Buang, F. Huyop and R. A. Wahab, *Biotechnol. Biotechnol. Equip.*, 2015, **29**, 205–220.
411 Z. Amini, Z. Ilham, H. C. Ong, H. Mazaheri and W. H. Chen, *Energy Convers. Manage.*, 2017, **141**, 339–353.
412 R. W. M. Mounguengui, C. Brunschwig, B. Baréa, P. Villeneuve and J. Blin, *Prog. Energy Combust. Sci.*, 2013, **39**, 441–456.
413 S. V. Ranganathan, S. L. Narasimhan and K. Muthukumar, *Bioresour. Technol.*, 2008, **99**, 3975–3981.
414 A. Gusniah, H. Veny and F. Hamzah, *Ind. Eng. Chem. Res.*, 2019, **58**, 581–589.
415 K. H. Kim, O. K. Lee and E. Y. Lee, *Catalysts*, 2018, **8**, 68.
416 J. Sebastian, C. Muraleedharan and A. Santhiagu, *Int. J. Green Energy*, 2017, **14**, 687–693.
417 J. H. C. Wancura, D. V. Rosset, M. V. Tres, J. V. Oliveira, M. A. Mazutti and S. L. Jahn, *Can. J. Chem. Eng.*, 2018, **96**, 2361–2368.
418 A. Arumugam and V. Ponnusami, *Heliyon*, 2017, **3**, 486.
419 R. Jambulingam, M. Shalma and V. Shankar, *J. Cleaner Prod.*, 2019, **215**, 245–258.
420 S. Rafiei, S. Tangestaninejad, P. Horcajada, M. Moghadam, V. Mirkhani, I. Mohammadpoor-Baltork, R. Kardanpour and F. Zadehahmadi, *Efficient biodiesel production using a lipase@ZIF-67 nanobioreactor*, 2018, vol. 334.
421 H. Taher, E. Nashef, N. Anvar and S. Al-Zuhair, *Biofuels*, 2019, **10**, 463–472.
422 R. S. Malani, S. B. Umriwad, K. Kumar, A. Goyal and V. S. Moholkar, *Energy Convers. Manage.*, 2019, **188**, 142–150.
423 J. Jayaraman, K. Alagu, P. Appavu, N. Joy, P. Jayaram and A. Mariadoss, *Renewable Energy*, 2020, **145**, 399–407.
424 M. Marín-Suárez, D. Méndez-Mateos, A. Guadix and E. M. Guadix, *Renewable Energy*, 2019, **140**, 1–8.
425 H. C. Nguyen, S. H. Liang, S. S. Chen, C. H. Su, J. H. Lin and C. C. Chien, *Energy Convers. Manage.*, 2018, **158**, 168–175.
426 C. G. Lopresto, S. Naccarato, L. Albo, M. G. De Paola, S. Chakraborty, S. Curcio and V. Calabrò, *Ecotoxicol. Environ. Saf.*, 2015, **121**, 229–235.
427 N. A. Kabbashi, N. I. Mohammed, M. Z. Alam and M. E. S. Mirghani, *J. Mol. Catal. B: Enzym.*, 2015, **116**, 95–100.
428 N. Choi, Y. Kim, J. S. Lee, J. Kwak, J. Lee and I. H. Kim, *J. Am. Oil Chem. Soc.*, 2016, **93**, 311–318.
429 P. Muanruksa and P. Kaewkannetra, *Renewable Energy*, 2020, **146**, 901–906.
430 N. Choi, D. S. No, H. Kim, B. H. Kim, J. Kwak, J. S. Lee and I. H. Kim, *Ind. Crops Prod.*, 2018, **120**, 140–146.
431 N. F. Sulaiman, W. Azelee, W. Abu, S. Toemen, N. M. Kamal and R. Nadarajan, *Renewable Energy*, 2019, **135**, 408–416.
432 M. Pirouzmand, M. Mahdavi and Z. Ghasemi, *Fuel*, 2018, **216**, 296–300.
433 A. Ramli and M. Farooq, *Malaysian J. Anal. Sci.*, 2015, **19**, 8–19.
434 M. E. Borges and A. Brito, *Int. J. Chem. React. Eng.*, 2011, **9**, 1–20.
435 W. Nor, N. Wan, N. Aishah and S. Amin, *Fuel Process. Technol.*, 2011, **92**, 2397–2405.
436 M. F. R. Nizah, Y. H. Taufiq-yap, U. Rashid, S. Hwa and Z. A. S. Nur, *Energy Convers. Manage.*, 2014, **88**, 3–8.
437 H. V. Lee, J. C. Juan and Y. H. Tau, *Renewable Energy*, 2015, **74**, 124–132.
438 F. Jamil, A. H. Al-muhatseb, M. Tay, Z. Myint, M. Al-hinai, L. Al-haj, M. Baawain, M. Al-abri, G. Kumar and A. E. Atabani, *Energy Convers. Manage.*, 2018, **155**, 128–137.
439 Y. Jeon, W. S. Chi, J. Hwang, D. H. Kim, J. H. Kim and Y. Shul, *Appl. Catal., B*, 2019, **242**, 51–59.
440 W. Liu, P. Yin, X. Liu and R. Qu, *Bioresour. Technol.*, 2014, **173**, 266–271.
441 O. Nur, U. Rashid and M. Sufri, *Renewable Energy*, 2019, **131**, 187–196.
442 F. Farzaneh and F. Moghzi, *React. Kinet., Mech. Catal.*, 2016, **118**, 509–521.
443 D. Salinas, S. Guerrero and P. Araya, *Catal. Commun.*, 2010, **11**, 773–777.
444 K. Srilatha, N. Lingaiah, B. L. A. P. Devi, R. B. N. Prasad, S. Venkateswar and P. S. S. Prasad, *Appl. Catal., A*, 2009, **365**, 28–33.
445 C. M. R. Prado and N. R. Antoniosi Filho, *J. Anal. Appl. Pyrolysis*, 2009, **86**, 338–347.
446 A. Wisniewski, V. R. Wiggers, E. L. Simionatto, H. F. Meier, A. A. C. Barros and L. A. S. Madureira, *Fuel*, 2010, **89**, 563–568.
447 J. Van Gerpen, *Fuel Process. Technol.*, 2005, **86**, 1097–1107.
448 S. H. Y. S. Abdullah, N. H. M. Hanapi, A. Azid, R. Umar, H. Juahir, H. Khatoon and A. Endut, *Renewable Sustainable Energy Rev.*, 2017, **70**, 1040–1051.